UNIVERSITY OF CALIFORNIA, SAN DIEGO

Responses of mesopelagic fish assemblages to environmental disturbance: ocean deoxygenation and oceanic fronts

A dissertation submitted in partial satisfaction of the requirements for the degree Doctor of Philosophy

in

Oceanography

by

Amanda Nicole Netburn

Committee in charge:

Mark D. Ohman, Chair
Jules Jaffe
J. Anthony Koslow
Lisa A. Levin
Frank Powell
Martin Tresguerres

2016

The dissertation of Amanda Nicole Netburn is approved, and it is acceptable in quality and form for publication on microfilm and electronically:

Chair

University of California, San Diego

2016

TABLE OF CONTENTS

LIST OF FIGURES

LIST OF TABLES

ACKNOWLEDGEMENTS

Chapter 2, in full, is a reprint of the material as it appears in Deep-Sea Research I, 2015, Netburn, A.N., and J.A. Koslow, Elsevier Press, 2015. The dissertation author was the primary investigator and author of this paper.

Chapter 3 is currently submitted for publication for publication in Marine Ecology Progress Series. Netburn, A.N., Tresguerres, M., and M.D. Ohman. Inter-Research Science Center, 2016. The dissertation author was the primary investigator and author of the paper.

VITA

2003	Bachelor of Science in Biological Sciences, Stanford University
2010	Master of Advanced Studies in Marine Biodiversity and Conservation, University of California, San Diego
2016	Doctor of Philosophy in Oceanography, University of California, San Diego

PUBLICATIONS

Netburn AN, Koslow JA (2015) Dissolved oxygen as a constraint on daytime deep scattering layer depth in the southern California current ecosystem. Deep Sea Res Part I Oceanogr Res Pap 104:149–158

Abbriano R, Carranza M, Hogle S, Levin R, **Netburn A**, Seto K, Snyder S, SIO280, Franks P (2011) Deep Water Horizon Oil Spill A review of the Planktonic response. Oceanography 24:294–301

ABSTRACT OF THE DISSERTATION

Responses of mesopelagic fish assemblages to environmental disturbance: ocean deoxygenation and oceanic fronts

by

Amanda Nicole Netburn

Doctor of Philosophy in Oceanography

University of California, San Diego, 2016

Professor Mark D. Ohman, Chair

Throughout the global ocean, there is an abundant and diverse assemblage of fishes aggregated at mesopelagic (200-1000 m) depths. These fishes are critical to pelagic food webs and carbon transport. In the southern California Current Ecosystem, with naturally hypoxic mesopelagic waters, mesopelagic fishes may be vulnerable to predicted ocean deoxygenation. Additionally, water property discontinuities at oceanic fronts can disproportionately affect abundance, compositions, and reproduction of marine

animals. In this dissertation, I investigate responses of mesopelagic fishes to ocean deoxygenation and fronts.

First, I correlated acoustically-detected Deep-Scattering Layers (DSL) of mesopelagic fishes with midwater oxygen, irradiance, and temperature, and found that the lower DSL boundary correlates most with oxygen. The upper boundary correlates with both oxygen and irradiance. Assuming current deoxygenation rates, I predicted both lower and upper boundaries will shoal. Next, I measured activities of the aerobic enzymes Citrate Synthase and Malate Dehydrogenase, and the anaerobic enzyme Lactate Dehydrogenase to test for changes in metabolic activities of mesopelagic fish in response to dissolved oxygen. There was an apparent suppression of activity at low oxygen concentrations for all species combined. There was no increased reliance on anaerobic activity at depressed oxygen concentrations. Although there is evidence that some mesopelagic fishes may have a rare alternate anaerobic pathway catalyzed in part by Alcohol Dehydrogenase, I did not detect any Alcohol Dehydrogenase activity for 16 species studied.

Finally, I compared responses of mesopelagic fish assemblages at three frontal systems. I found no abundance changes across fronts, except for larvae which were elevated at the most stable system. Non-vertically migratory assemblages were uniform across frontal gradients, while migratory and larval fish assemblages were typically altered across fronts. Changes in population growth potential were detected across the two more stable frontal systems for migrators and larvae, though not for non-migrators.

These results suggest that deoxygenation may cause habitat compression and metabolic suppression, while changes to frontal frequency could impact the structure and

population growth of mesopelagic fish assemblages. Ongoing monitoring of these populations using existing and novel technologies will allow further understanding of mesopelagic fish responses to these and other environmental changes.

CHAPTER 1

INTRODUCTION

1.1 Overview

The mesopelagic region (i.e., "the twilight zone," 200-1000m) is one of the largest ecosystems on earth, and the resident fauna is both diverse and abundant (Robinson et al. 2010). Deep-dwelling mesopelagic animals are important to global marine food webs, fisheries, conservation, and biogeochemistry (Robinson et al. 2010), yet remain understudied due to inaccessibility and the inadequacy of traditional sampling tools (Robison 2009). Anthropogenic disturbances have only recently been recognized to have effects on deep-sea environments (Devine et al. 2006, Robison 2009, Ramirez-Llodra et al. 2011, Levin & Le Bris 2015, Quintana-Rizzo et al. 2015). Scientists and conservationists are responding with demands to implement management of deep-sea environments (Mengerink et al. 2014). For example, off the west coast of the United States, the Pacific Fisheries Management Council has responded in part by pre-emptively closing fisheries for many mesopelagic fish species, given the lack of available information to access whether such a fishery could be sustainable (PFMC 2015). In addition, climate change has been linked to disturbances in the pelagic environment that include ocean deoxygenation (Stramma, et al. 2010a) and changes to frequency and persistence of epipelagic fronts (Kahru et al. 2012). Little is known about how these disturbances will affect mesopelagic communities. The indirect stressors of human activity, including acidification, warming, and deoxygenation (Mora et al. 2013, Levin & Le Bris 2015), combined with direct impacts from fishing, oil and gas extraction, mining and pollution (Mengerink et al. 2014) could intensify pressures on the ongoing survival of mesopelagic species. With many mesopelagic fishes performing a diel vertical migration (DVM) into epipelagic waters (<200 m) (Pearcy et al. 1977), they are now

known to be important contributors to carbon transfer between the epipelagic and mesopelagic realms, especially in more oligotrophic regions of the NE Pacific (Robinson et al. 2010, Davison et al. 2013). Little is known about many aspects of their ecology (Robison 2009), and in particular, how populations respond to perturbations to their environment. With the predicted (Shaffer et al. 2009, Keeling et al. 2010) and observed global expansion of oxygen minimum zones (OMZs; Stramma et al. 2008, 2010b, Bograd et al. 2008) and observed changes in the frequency of oceanic fronts (Kahru et al. 2012), the mesopelagic fauna may undergo changes in abundance and composition that, given the current state of knowledge, could go mostly unnoticed by scientists, marine managers, and conservation biologists.

1.2 Mesopelagic Fishes

Mesopelagic fishes include the vertebrate taxa with the highest biomass (the family Myctophidae) and that with the greatest abundance (Genus *Cyclothone*, in the family Gonostomatidae) (Gjosaeter & Kawaguchi 1980) on earth. Other dominant mesopelagic families include the Bathylagidae, Stomiidae, Sternoptychidae and Phosichthyidae (Brodeur & Yamamura 2005). With little sunlight reaching the mesopelagic, there is no photosynthetic primary production at these depths, hence food resources and density of animals are low in the mesopelagic zone compared with surface layers. Still, due to the large ocean volume that they occupy, mesopelagic fish biomass integrated over surface area is equal to or exceeds the biomass of the well-studied epipelagic clupeid fish species (e.g., sardines, anchovies) (Davison et al. 2015). Global mesopelagic fish abundance has been estimated at 10^9 tons (Gjosaeter & Kawaguchi

1980, Lam & Pauly 2005), however this estimate is based primarily on net trawls, which generally underestimate abundance by an order of magnitude (Koslow et al. 1997, Kaartvedt et al. 2012, Irigoien et al. 2014), so the actual value is likely higher. Biomass is usually estimated as a static value. There are few studies that actually enumerate trends in adult and juvenile abundance or biomass over time of any of the mesopelagic fishes (but note Watanabe & Kawaguchi 2003). Mesopelagic ichthyoplankton have been used as proxy measures of adult abundances in the California Current System, revealing temporal changes in population stability (Moser et al. 1987, Moser & Smith 1993, Hsieh et al. 2009), spawning locations (Moser 1996), variations in relation to dissolved oxygen (Koslow et al. 2011), and multi-decadal changes in phenology (Asch 2015).

The biomass of mesopelagic fish correlates positively with surface productivity at basin and global scales (Davison et al. 2013, Irigoien et al. 2014). The mesopelagic fishes are significant consumers of global marine plankton production, as evidenced by stomach content analysis and energetic modeling (Williams et al. 2001, Field & Francis 2006, Davison et al. 2013), and are themselves key prey to higher predators, including commercially-exploited fishes such as tunas and billfishes (Bertrand et al. 2002, Potier et al. 2007), squids (Field et al. 2007), marine mammals (Pauly et al. 1998, Guinet et al. 2014), and seabirds (Thompson et al. 1998, Bost et al. 2002).

The fishes that inhabit the mesopelagic have specialized adaptations to life in this environment. Many, though not all, mesopelagic fishes perform a diel vertical migration (DVM), migrating into shallower waters at night to forage (Pearcy et al. 1977). The primary adaptive value of this behavior is thought to be predator avoidance: that is, the animals trade off daytime occupancy at depths with low food availability in the midwater

environment in order to avoid detection by visually-oriented predators (Lampert 1993, De Meester et al. 1999). Mesopelagic fishes have been described as "lillipution" (Murray & Hjort 1912), because they are small compared with most epipelagic fishes. The largest myctophids are rarely larger than ~15 cm (Catul et al. 2010), and many of the *Cyclothone* are even paedomorphic, with reproductively mature individuals resembling larvae in size and form (Miya & Nishida 1996). In general, shallower dwellers and vertical migrators are blue-green to silver in color, while the non-migrators are brown to black (Badcock 1970, Catul et al. 2010), shading which acts as camouflage within the ambient light regimes. Many mesopelagic fish are bioluminescent, with rows of photophores on their ventral surface (e.g., most Myctophidae, Gonostomatidae, Sternoptychidae), or lures that harbor bioluminescent bacteria (e.g., Lophiiformes (anglerfish), *Idiacanthus* sp.) (Davis et al. 2014). Deeper-dwelling fishes within the same genus tend to be larger in size (Miya & Nishida 1996) and have larger mouths, which Childress & Nygaard (1973) attribute to adaptation to feed on calorically-rich migratory fishes, while those which forage in epipelagic environments tend to feed on zooplankton. In general, non-migrators have higher water content, lower carbon and nitrogen content, and lower metabolic rates than their migrating counterparts (Childress & Nygaard 1973, Torres et al. 1979).

The mesopelagic fish fauna of the southern CCE is diverse, with approximately 100 species identified in CalCOFI tows conducted between 2010 and 2012 (Davison et al. 2015 and unpublished data). **Figure 1.1** shows the number of specimens of the most common of these species. **Tables 1.1** & **1.2** list some of the most common fishes collected in the southern CCE, and summarizes key traits such as migratory behavior, diet, and vertical range. Some of the most common vertical migrators include the

Myctophidae *Triphotorus mexicanus*, *Diaphus theta* and *Nannobrachium ritteri* and the Bathylagidae *Leuroglossus stilbius*, and *Lipolagus ochotensis*. The common myctophid *Stenobrachius leucopsarus* has migratory and non-migratory members, although it is unknown whether individuals consistently either migrate or stay at depth each night or whether different individuals migrate on different days (Pearcy et al. 1977, Watanabe et al. 1999). Common non-migrating fishes include the members of the genus *Cylcothone* and all of the Sternoptychidae. Due to their dominance in mesopelagic assemblages in the eastern North Pacific, more studies have focused on *S. leucopsarus* than other mesopelagic fishes in the region (Brodeur & Yamamura 2005).

1.3 Bioacoustics

Sonar has proven to be a useful method for remotely sensing organisms in the ocean. In active acoustics, a pressure wave is generated and propagated in the direction of interest (in the case of ship-mounted echosounders, this is generally directly downward or laterally). The sound wave is reflected and scattered by any object that has a different acoustic impedance than the surrounding water. Using the speed of sound in the water, and the time difference between emission and detection of the reflected sound, the range of the target is calculated. Echosounders were originally developed to detect the seafloor, but their utility for studying water column and benthic organisms was soon realized, and numerous studies over the last several decades have made use of bioacoustics for surveying populations of marine animals. A scientific echosounder can be operated throughout an oceanographic cruise without interfering with other scientific activities.

Acoustics are therefore a convenient and relatively low-cost method for surveying the midwater community at high spatial and temporal resolutions (Koslow 2009).

The "holy grail" of fisheries acoustics continues to be what is called the inverse scattering problem: that is, appropriately identifying targets that are detected acoustically. There remains a great deal of uncertainty in identifying targets because target strength is affected by the presence, size and shape of gas-filled swimbladders in many fishes, tissue composition, size and life stage of the organisms, and orientation relative to the sound source (i.e., tilt angle and rotation; Misund 1997).

Benoit-Bird (2009) summarizes well the three ways that multifrequency data are used: 1) In the forward approach, the volume backscatter of animals collected by the net (or other seatruthing method) is estimated based on models and then compared to the measured acoustic return. 2) In the Inverse approach, samples are used to calculate relative densities and sizes of scattering types, and to determine relevant acoustic-backscattering cross sections, and a data-fitting approach is used to find the best combination of the number of scatterers of each type and size to produce the observed measurements of volume backscatter at each frequency. However, the inverse approach requires that the frequencies used span the transition from Rayleigh to geometric scattering, which is not the case for many fishes. 3) dB-differencing compares scattering at multiple frequencies. Because different types of scatterers have a characteristic Target Strength (TS)frequency spectra (e.g., Stanton et al. 1998, **Figure 1.2**), changes in TS at different frequencies can be used to identify acoustic groups of animals with similar frequency responses (Korneliussen & Ona 2002). Subtracting or dividing two frequencies can be used to infer which acoustic group is present. Although seatruthing

with other types of observations (usually nets, but visual observations with cameras prove informative as well) are required in order to interpret taxonomic information from echograms (McClatchie et al. 2000), acoustic backscatter data can sometimes be used to identify and study DSL distributions without the need for co-located trawl data (Tont 1975, Urmy et al. 2012, Bianchi et al. 2013). Herein, I use acoustic detections to detect the mostly fish-derived component of the DSL.

1.4 Oxygen Minimum Zones and Ocean Deoxygenation

In some parts of the ocean there exists a permanent subsurface hypoxic layer, called the oxygen minimum zone (OMZ), which arises due to the combination of limited surface ventilation, respiratory oxygen consumption, and ocean circulation (Sverdrup 1938, Wyrtki 1962, Karstensen et al. 2008). OMZs are typically defined by a concentration of oxygen less than or equal to 0.5 ml l^{-1} (equivalent to 22 μM kg^{-1}). A variety of different units and different thresholds are used to characterize oxygen in different studies, such as μM kg^{-1}, % saturation, ml l^{-1}, mg l^{-1}, and kPa (Levin 2003, Seibel 2011). The most developed OMZs are in the tropical ocean and in eastern boundary currents (**Figure 1.3**; Hofmann et al. 2011).

In the southern CCE, the pelagic OMZ depths (defined here by 0.5 ml l^{-1}) vary from approximately 300 m to over 500 m (**Figure 3.2**). There are seasonal, interannual, and spatial variations in the depths of the upper and lower boundaries of the OMZ .

Increased ocean stratification and changes to global circulation patterns are predicted to accompany global climate change, resulting in decreased dissolved oxygen content and expansion of OMZs (Deutsch et al. 2006, 2011a, Shaffer et al. 2009, Keeling

et al. 2010). Such expansions have already been observed in the southern CCE (**Figure 1.4**) (Bograd et al. 2008, McClatchie et al. 2010), across the northern North Pacific (Crawford & Peña 2013, Watanabe 2003, Whitney et al. 2007), and in the tropics (Stramma et al. 2008). For example, in the southern CCE, the upper boundary of the hypoxic boundary (60 μmol kg^{-1}) has shoaled by as much as 80 m (Bograd et al. 2008). In the southern CCE, oxygen concentrations have been associated with the strengthening of the California Undercurrent (Bograd et al. 2014), and there is evidence that OMZs could contract again in the future as a result of weakening tropical trade winds (Deutsch et al. 2014a). Ocean acidification has a compounding effect on organisms in hypoxic waters because reduced pH reduces the affinity of proteins such as hemoglobin for O_2 (Seibel & Walsh 2001). As oxygen concentration and pH covary (Alin et al. 2012), this may be especially problematic for organisms already living at the limits of their pH and oxygen tolerances. Further, the effects of climate change on metabolic demands can vary as well. Hypoxia-adapted species may decrease their metabolic levels due to metabolic suppression in low oxygen conditions (Seibel 2011a, Stewart et al. 2014), but metabolic activity is increased in higher temperatures (Portner 2010, Gilly et al. 2013).

In the benthic environment, where sessile organisms are not able to simply swim away from hypoxic water, dissolved oxygen has been observed to play a significant role in shaping the resident communities. Low diversity and high species dominance are common in OMZs, and significant zonation accompanies gradients in oxygen concentration (Levin 2003), due to wide variation in hypoxia tolerance of different benthic taxa (Vaquer-Sunyer & Duarte 2008, Seibel 2011a). Increases in upwelling events of hypoxic waters fatal to some animals in shallow nearshore environments off the

coast of Oregon has received significant attention from the public due to the effects of severe hypoxia on commercial oyster farms and wild fisheries (Chan et al. 2008, Grantham et al. 2004).

In the pelagic environment, biological impacts of OMZs and their expansion can be harder to document, due to the ability of pelagic organisms to move throughout their environment compared with sedentary benthic organisms. The term *hypoxic boundary* (HB) has been used to describe an oxygen concentration that acts as an apparent boundary to distributions of pelagic and benthic organisms (Bograd et al. 2008, Friedman et al. 2012). There are several examples of specific oxygen concentrations acting as a HB for pelagic animals. Strong zonation of pelagic plankton is coincident with gradients of oxygen concentration in both the Arabian Sea and the eastern tropical Pacific OMZs (Saltzman & Wishner 1997, Wishner et al. 2008). The deeper diving behavior of western Atlantic istiophorid billfishes (e.g., marlins, sailfish) compared with their eastern Pacific counterparts has been attributed to the lack of an OMZ in the western Atlantic (Prince & Goodyear 2006, Stramma et al. 2011). The maximum depth range of the epipelagic fish community off Peru, dominated by Peruvian anchovy (*Engraulis ringens*), is highly correlated with a dissolved oxygen concentration of 0.80 ml l^{-1} regardless of the time of day, distance from shore or depth of that oxygen level (Bertrand et al. 2010). At their open ocean aggregation sites in the central north Pacific, the diving depths of great white sharks (*Carcharodon carcharias*) appears to be limited by the 1.5 ml l^{-1} O_2 isopleth (Nasby-Lucas et al. 2009).

Using larval abundance as a proxy for adult abundance, Koslow et al. (2011) inferred that populations of mesopelagic fish in the southern CCE were reduced by over

60% in years with relatively low midwater (200-400m) oxygen concentrations. Koslow et al. (2011) postulate that the OMZ acts as a boundary to the mesopelagic fish fauna, and the shoaling OMZ therefore forces the animals into shallower waters where irradiance is higher, making the fishes vulnerable to predation by visually-oriented predators.

1.5 Deep Scattering Layers and the OMZ

Mesopelagic organisms are usually aggregated into one or more layers in the ocean. These layers are referred to as deep scattering layers (DSL), due to the high acoustic reflectance observed using sonar systems. Light is classically considered to be a primary determinant of DSL depths (Kampa & Boden 1954, Tont 1975, Frank & Widder 2002). However, previous analyses have been conducted either in places that lack an OMZ (e.g., Frank & Widder 2002), or have only considered the top of the DSL (e.g., Tont 1975), which is less likely to abut a hypoxic boundary than the bottom of the DSL. Boden & Kampa (1965) suggested that hypoxia in a fjord may act as a bottom boundary for euphausiids, but did not explicitly test this hypothesis. A study within the northern CCE found that the bottom of the DSL over a stationary upward facing echosounder descended from ~400m in the spring to over 700 m in September and August (Urmy et al. 2012). The authors suggest that the change in depth is consistent with displacement of the upper edge of the OMZ in the region, however they did not conduct a statistical analysis or present the environmental measurements to support this hypothesis.

Different organisms display a wide range of tolerances to hypoxia (e.g., Seibel 2011), and Deutsch et al. (2015) predict range shifts of marine ectotherms based on the metabolic constraints of increasing temperature and decreasing oxygen. In parts of the

ocean, such as the Humboldt Current, DSLs have been observed within the OMZ (Cornejo & Koppelmann 2006). The bulk of the acoustic backscatter observed by Cornejo & Koppelmann (2006) came from *Vinciguerria lucetia,* which seem to be especially tolerant of hypoxic conditions. With hypoxic conditions rising to very shallow depths in that region, these fishes may be trading off exposure to hypoxia in order to decrease predation risk. This tradeoff may not be necessary in the CCE due to the deeper depth of hypoxic waters, accompanied by decreased predation risk. *Triphoturus mexicanus* has been collected well within the OMZ in Gulf of California, at O_2 concentrations as low as 0.17 ml l^{-1} (Holton 1969). The range expansion of hypoxia-tolerant Humboldt squid (*Doscidicus gigas*) observed in recent years has been attributed to the expansion of the OMZ throughout the CCE (Field et al. 2007), although anecdotal evidence suggests their range has subsequently contracted. Active populations of the copepods are found at oxygen concentrations below 0.1 ml l^{-1} in the Eastern Tropical Pacific and Arabian Sea (Wishner et al. 2000), and mesopelagic fishes of the Arabian Sea are commonly captured within the OMZ (Luo et al. 2000, Karuppasamy et al. 2010). Due to the relatively deep depth of the upper boundary of the OMZ in the southern CCE (300 to >500 m, **Fig. 3.2**), pelagic fishes may not be adapted to living regularly within the OMZ in this region.

Bianchi et al. (2013) analyzed 38-150 kHz ADCP data collected across the globe, and found that the depth of the DSL is correlated with the oxygen concentration in the upper mesopelagic (150-500m, **Figure 1.5**). Their findings corroborate the hypothesis that the DSL depth is limited by climatological oxygen concentrations.

1.6 Respiratory Physiology

Physiological stress could explain the association of DSL boundaries with oxygen concentrations. For most mesopelagic fishes, tissue water content increases with the depth at which the fish lives, while carbon and nitrogen content and respiration rates generally decrease with increasing habitat depth (Childress & Nygaard 1973, Torres et al. 1979). Two percent of the decline in respiration rates observed by Torres et al. (1979) could be accounted for by the concurrent decrease in temperature with depth, and 30% accounted for by the increased water content of fishes, so some other property must be causing these declines. Because similar patterns of decline in respiration rates with depth have been observed for the sighted crustaceans and cephalopods, but not for chaetognaths, cnidarians, polychaetes and pteropods (Childress 1995), it is though that this pattern is related to vision. The *visual interactions hypothesis* (Childress 1995, Seibel & Drazen 2007) maintains that the metabolic rates of visual pelagic organisms decreases with depth, but that of non-visual organisms does not because of the reduced reaction distance of predator-prey interactions (due to reduced irradiance) for visual predators and visual prey (Childress 1995). As visual pursuit and evasion are reduced in the mesopelagic due to low light levels, locomotory capacity is decreased along with metabolic capacity (Seibel & Drazen 2007).

A number of studies have used activity of respiratory pathway enzymes to study the relative contributions of aerobic and anaerobic pathways to respiration (Childress & Somero 1979, Vetter et al. 1994). Typically Citrate Synthase (CS) and/or Malate Dehydrogenase (MDH) activities are used as proxies for aerobic respiration, and Pyruvate Kinase and/or Lactate Dehydrogenase (LDH) as proxies for anaerobic capacity.

However, there are alternative anaerobic pathways to lactate production available to some taxa (Hochachka & Somero 2002). Childress & Seibel (1998) concluded that OMZ inhabitants in the CCE do not rely much on anaerobic respiration, but are instead adapted to residence in the hypoxic zone through mechanisms to increase removal of O_2 from the environment, such as enhanced gill surface area, short diffusion distances from the water to the blood, and heme-containing respiratory proteins with a very high affinity for O_2. However, recent work by Torres et al. (2012) measured the activity of the enzyme Alcohol Dehydrognase (ADH), which reduces pyruvate to ethanol, an alternative pathway to the reduction of pyruvate to lactate (catalyzed by LDH). The ADH pathway was elevated in multiple species of myctophids in areas with OMZs, the Arabian Sea and Gulf of Mexico, compared with related species from the Gulf of Mexico and the Antarctic that lack an OMZ. The only vertebrates previously known to utilize the ADH pathway are in the family Cyprinidae (i.e, goldfish and carp) (Shoubridge & Hochachka 1980, Johnston & Bernard 1983, Vornanen et al. 2009). The discovery of the ADH pathway in response to hypoxia in the lanternfishes implies that this pathway may be more common than previously believed.

1.7 Fronts

Fronts are places in the ocean where two water masses meet. They are characterized by strong horizontal gradients in physical properties such as temperature, salinity and density. The physical dynamics at a front may lead to aggregations of organisms, and frontal regions are often accompanied by elevated primary production (Chekalyuk et al. 2012, Taylor et al. 2012), zooplankton (Ohman et al. 2012, Powell &

Ohman 2015a), and abundance of higher trophic levels (Hoefer 2000, Polovina et al. 2001, Doniol-Valcroze et al. 2007). Powell & Ohman (2015b) found that fronts in the CCE exhibit changes in extent of diel vertical migrations and changes in size distribution of zooplankton. Although the physical gradients at a front are often strongest in epipelagic waters, biological impacts may extend into deeper strata. At a front off the continental shelf of Northern Norway, Kaartvedt et al. (1996) found that the depth distribution of populations of the mesopelagic fish *Maurolicus muelleri* and the euphausiid *Trisopterus esmarkii* varied by ~100 m between the two sides of the front. The authors attribute this range shift to a steep change in deep light concentrations resulting from shading by photosynthetic organisms on the nearshore side of the front. McClatchie et al. (2012) similarly found elevated fluorescence (an indicator of phytoplankton biomass) and zooplankton and micronekton biomass at a front across a filament extending from the Ensenada Front near San Nicolas Island, CA. They found that mesopelagic fish were most abundant in oceanic waters to the west of the front, and market squid, krill and decapods most abundant in the front.

In October 2008, the CCE-LTER program conducted intensive sampling of multiple trophic levels across a front called the "A-Front". Primary production, and zooplankton and fish biomass were enhanced at the front itself. The biomass of acoustically inferred krill and fish were elevated at the cold (north) side of the front, with higher number of species in the south (Ohman et al. 2012, Landry, Ohman et al. 2012). From direct sampling with a midwater trawl, Lara-Lopez et al. (2012) found significant differences in the community composition and biomass of mesopelagic fishes on either

side of the front for fishes that undergo DVM, but not for the non-migrating component of the community.

Another study in the CCE region found that the frequency of detectable fronts in the southern sector of the California Current System may be increasing (Kahru et al. 2012)**.** This finding has strong implications for the mesopelagic fish assemblage, warranting further study of the dynamics that may lead to the aggregations of mesopelagic fishes at fronts. Through the CCE-LTER program, two additional front studies have taken place, in 2011 (C-front) and 2012 (E-front), during which data and samples were collected for the present research.

1.8 Mesopelagic Sampling Programs- CalCOFI & LTER

The CalCOFI program began collecting fish larvae at its inception in 1949, providing a long-term record of abundance and composition within the larval assemblage (Moser 1996). Using this dataset, Moser & Smith (1993) discerned two major biogeographical assemblages of larval fishes, the Subarctic-Transition Zone province and the Eastern Tropical Pacific/Central Water province. However, larval abundance of taxa from both provinces have been found to correlate strongly with oxygen concentrations (Koslow et al. 2011). In 2009, the CalCOFI program augmented its already extensive data collection program with continuous collection of acoustic backscatter data across the core stations with a 5-frequency Simrad EK-60 echosounder accompanied by midwater trawl collections with a Matsuda-Oozeki-Hui Trawl (MOHT) (Oozeki et al. 2004). These systems have also been used on the quasi-Lagrangian CCE-LTER process cruises, and

these data are the core of my investigations on mesopelagic fish response to environmental variability in the CCE.

1.9 Overview of Dissertation

Global climate change effects on deep-sea environments remain largely unknown (Levin & Le Bris 2015), as do responses of adult mesopelagic fishes to existing perturbations in their environment. Mesopelagic fish populations have rarely been systematically sampled over time in any one location or region. Because ocean deoxygenation disproportionally affects mesopelagic waters in the CCE (Gilly et al. 2013), I identified deoxygenation as a process likely to affect the mesopelagic fish assemblage. I similarly identified fronts as a secondary area of inquiry, because they are often areas of disproportionately high primary and secondary productivity, with potential influences on mesopelagic animals.

I have completed three related studies to understand the effects of oxygen variability and fronts on mesopelagic fish assemblages in the southern CCE:

<u>Chapter 2:</u> Dissolved oxygen as a constraint on daytime deep scattering layer depth in the southern California Current Ecosystem

In this chapter I investigate the effects that variable midwater oxygen concentrations have on the vertical distributions of mesopelagic fishes. I specifically test whether oxygen, irradiance, or temperature correlate with depths of Deep Scattering Layers (DSLs). To do this, I use acoustic backscatter data to remotely sense the DSL, and develop an algorithm to detect its upper and lower boundaries. By sampling

throughout the southern CCE on a series of CalCOFI cruises in different seasons, I am able to analyze changes in DSL depths across a range of hypoxic boundary depths. I assess the determinants of both the upper and lower DSL boundaries and predict future DSL changes if OMZ shoaling continues in the future. These results were published in the peer-reviewed journal, Deep Sea Research I (Netburn & Koslow 2015), and the manuscript presented herein.

Chapter 3: Survival in a deoxygenating ocean: Evidence of reduced metabolic activity in mesopelagic fishes in an oxygen minimum zone

In this chapter, I investigate the physiological adaptations of a suite of a mesopelagic fishes to natural variability in midwater oxygen concentrations to test whether ambient oxygen concentrations affect total metabolic activity, and to assess the relative contributions of aerobic and anaerobic respiration. I further explore the relationships of DVM behavior, phylogeny, and tissue content as explanatory variables to variation in metabolic activities. I collected fish throughout the southern CCE on both CalCOFI and CCE-LTER process cruises at stations with a wide range in midwater oxygen concentrations. I measured activities of the aerobic enzymes Citrate Synthase and Malate Dehydrogenase, and the anaerobic enzyme Lactate Dehydrogenase. I also measured activities of Alcohol Dehydrogenase to test for activity of an ethanol-production anaerobic pathway that is thought, but not proven, to occur in myctophids.

Chapter 4: Mesopelagic fish assemblages across across oceanic fronts: a comparison of three frontal systems in the southern California Current Ecosystem

For this chapter, I compare the responses of mesopelagic fish abundance, assemblage composition, and population growth potential to frontal gradients across three different frontal systems in the southern CCE. I conduct separate analyses for non-migratory, migratory, and larval fishes because they live at different depth strata. I also relate my results to expected changes in frontal frequency in the CCE region.

Chapter 5: **Summary and Conclusions**

Finally, in my concluding chapter I summarize the key findings of Chapters 2-4, synthesize the results, and suggest future directions for this area of research.

1.10 Figures

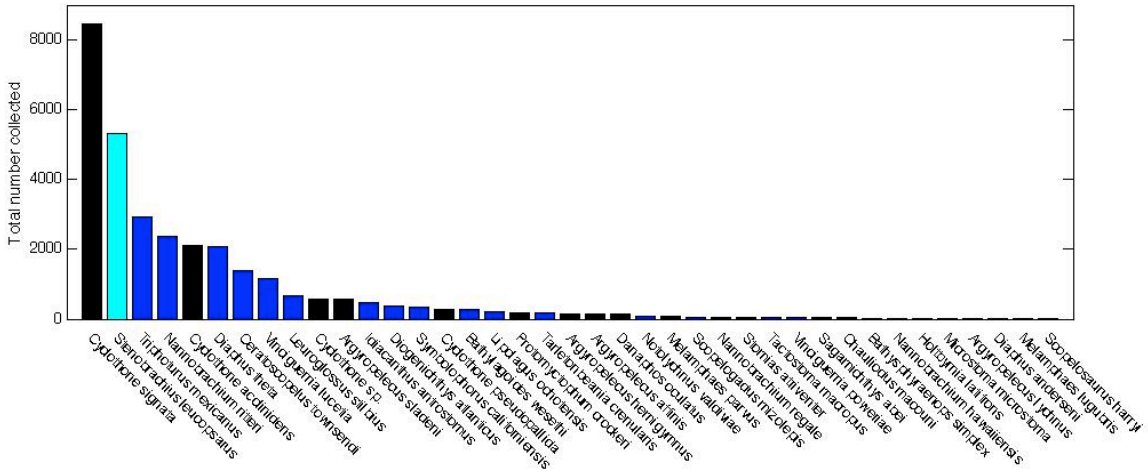

Figure 1.1. Total counts of mesopelagic fishes captured in daytime and nighttime MOHT tows on CalCOFI cruises Winter 2010, Summer 2010, Fall 2010, Winter 2011, Summer 2011, Fall 2011, and Winter 2012. Only those species with >20 total specimens collected are shown. Black bars indicate non-migratory species, cyan are species known to have both migratory and non-migratory components, and the blue are migratory (Davison 2015, and unpublished data).

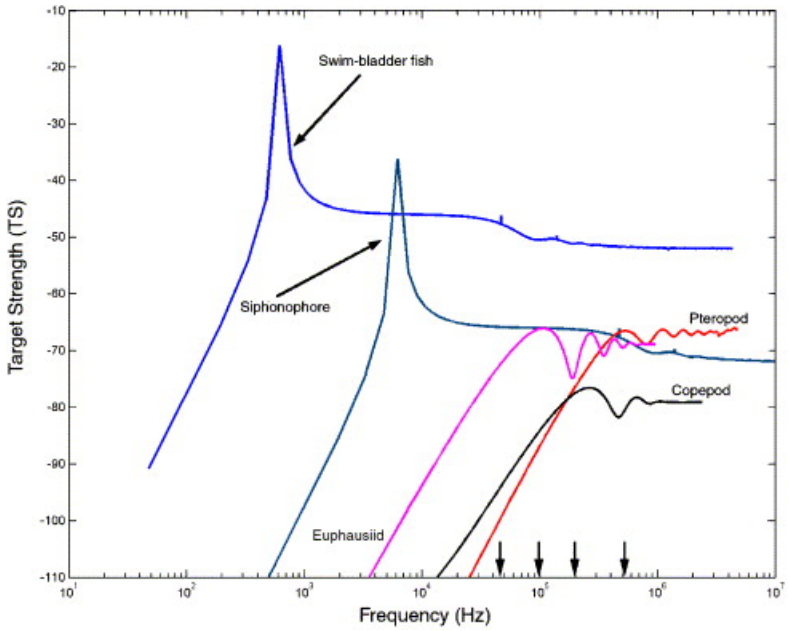

Figure 1.2. Plot of theoretical target strengths at different frequencies for fishes and some zooplankton groups (6 mm long copepod, 2 mm diameter shelled pteropod, 2.5 cm long euphausiids). These curves are based on the scattering models of Stanton et al. (1998), where pteropods are modeled as deformed elastic-shelled spheres, euphausiids and copepods as deformed fluid-filled cylinders, and siphonophores and fishes as bubbles with tissue. Arrows mark the location of 38, 120, 200, and 420kHz on the x-axis. (Sutor et al. 2005)

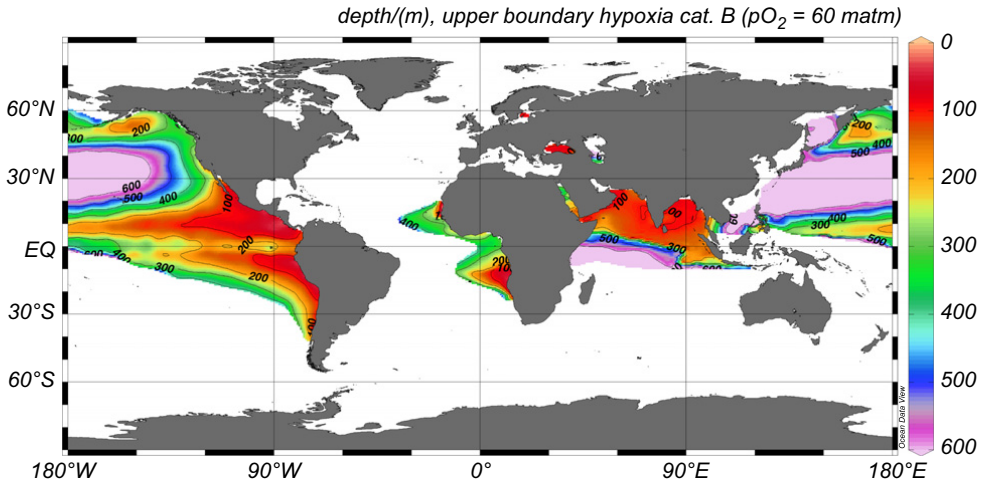

Figure 1.3. The world's OMZs (Hofmann et al. 2011). Colors indicate the depth in meters of the upper boundary of the OMZ (defined by pO_2 = 60 matm).

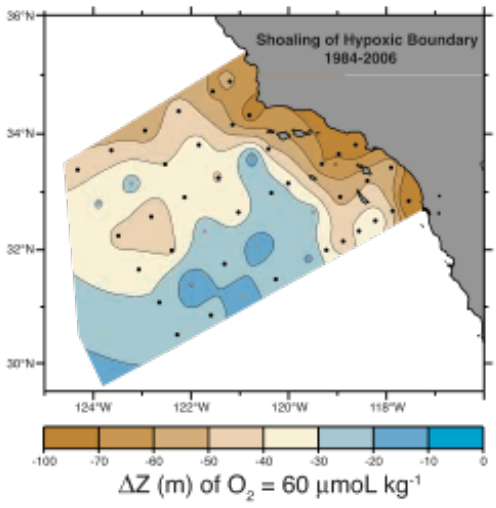

Figure 1.4. Shoaling of the hypoxic boundary in the southern California current system. Total change in the depth (m) of the O_2 = 60 µmol/kg surface on the CalCOFI survey grid over the period 1984-2006. Stations with significant linear regressions ($p<0.05$) are marked black. (Bograd et al. 2008)

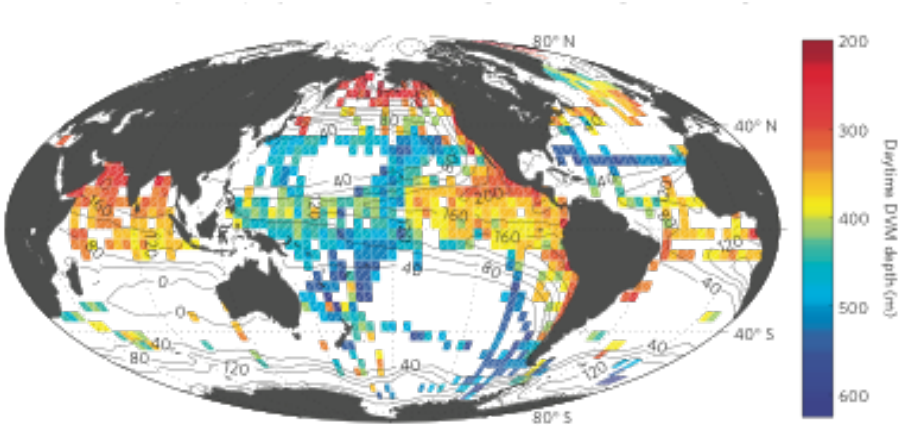

Figure 1.5. Daytime Deep Scattering Layer (DSL) depths are correlated with mesopelagic oxygen concentrations (Bianchi et al. 2013).

1.11 Tables

Table 1.1. Common vertically-migrating mesopelagic fish species of the CCE, together with swimbladder type, depth distributions, and prey items identified in stomach contents. Fishes were classified as migrating versus non-migrating based on classifications by Lara-Lopez et al. (2012), although there is not consensus in the literature for many species. Swimbladder type was categorized based on Davison (2011): (I) both small and large individuals have gas-filled swimbladders, (II) small individuals documented with gas-filled bladders, but not large individuals, (III) no gas-filled swimbladder. Boldface in the prey column indicates dominant prey items based on numerical abundance.

*Specimens collected in waters with only 600 m bottom depth

**No day/night differences provided.

Species (swimbladder type)	Daytime depth (m)	Nighttime depth (m)	Prey
Myctophidae (lanternfish)			
Diaphus theta *I*	300-500[a] 300-600 [b]	20-200[a] 0-200 [b]	**euphausiids, copepods, amphipods** salps, appendicularean**s**[c,d,e]
Triphoturus mexicanus *II*	250-800 (peak 450-550)[f]	0 to 750 (peak 50-150)[f,g]	**euphasiids, copepods,** fish[d,h]
Stenobrachius leucopsarus *II*	300-600 (peak)[a] 200-600[i] <800[j]	0-50 and 300-600 (peak)[a] 0-200 (peak)[i]	**euphausiids, copepods, amphipods, ostracods,** fish eggs, zoea, chaetognaths, fish larvae, siphonophores, salps, appendicularean**s**,[c,d,e,i]
Symbolophorus californiensis I	300-500[a] 200-600[i]	20-100[a] 0-600[i]	copepods and euphausiids[d]
Nannobrachium ritteri *II*	220-1000 m[r] (d/n not provided)		**chaetognaths**, **fishes, copepods, euphausiids**[r]
Ceratoscopelus townsendi *II*	>700 m[k]	<150 m[k]	crustaceans[d]
Tarletonbeania crenularis *I*	200-800[b]	0-200 m[b]	**euphausiids, copepods, amphipods,** other crustaceans, salps, appendicularean**s** [c,d,e]
Bathylagidae (deep sea smelts)			
Bathylagoides wesethi *III*	40-1100[s,**]		
Lipolagus ochotensis *III*	40 m (minimum depth)[s]	to 800 m[r] 1000m[s]	Appendicularians, coelenterates, copepod, euphausiids, amphipods, ctenophores[u]
Leuroglossus stilbius *III*	200-600[i]* 400-800[i]	0-200[i]	**larvaceans, salps**, ostracods, copepods, euphausiids[i]

Table 1.1. Common vertically-migrating mesopelagic fish species of the CCE, Continued.

Species (swimbladder type)	Daytime depth (m)	Nighttime depth (m)	Prey
Melamphaidae			
Scopelogadus mizolepis *II*	130-1600 m[s,**]		crustaceans[d] larvaceans, euphausiids, ostracods, amphipods, decapods[t]
Phosichthyidae (lightfishes)			
Vinciguerria nimbaria *I*	>400 (at least to 1600)[l]	0-200[l]	**copepods**, **ostracods**, euphasiid, pteropod, amphiipod, fish[l]
Stomiidae (barbeled dragonfishes)			
Tactostoma macropus *III*	300-600[b] <650[j]	0-200 (peak at surface)[b]	
Idiacanthus antrostomus *III*	150 m (minimum depth)[w]	1100 m (as reported in fishbase.org)	Small fishes and crustaceans[m]

Table 1.2. Common non-vertically-migrating mesopelagic fish species of the CCE, together with depth distributions and prey items identified in stomach contents.

Species	Daytime depth (m)	Prey
Gonostomatidae (bristlemouths)		
Cyclothone signata	300-500[n]	**copepods**, ostracods[v]
I	<800[j]	
Cyclothone acclinidens	<800[k]	fish, amphipod, copepods[d,o]
III	500-1000[n]	
	650-1000[j]	
Cyclothone pseudopallida	400-700[n]	copepods, euphausiids[o]
I	< 650[j]	
Mcytophidae		
Protomyctophum crockeri	to 530 m[r]	empty[d]
I		
Platytrochidae (Tubeshoulder)		
Sagamichthys abei	200-900 m[r]	small crustaceans[r]
III		
Sternoptychidae (hatchetfishes)		
Argyropelecus sladeni	100-700 m[r]	copepods, euphausiids and
I		ostracods[o]
Argyropelecus affinis I	110-800m[r]	-
Argyropelecus hemigymnus I	450-650 (night 300-450)[k]	**copepods, ostracods**, **amphipods**,
	350-500 (night 300-400)[p]	chaetognaths, egg case, polchaete,
		pteropod, euphausiids[q,p]
Stomiidae		
Chauliodus macouni	300-600[b]	Chaetognaths, crustaceans
III	<800[j]	fishes, squids[m,r]
	<1600 m[r]	

(a) (Watanabe et al. 1999), western north Pacific **(b)** (Pearcy et al. 1977), Oregon **(c)** (Tyler & Pearcy 1975), Oregon **(d)** (Collard 1970), Eastern Pacific **(e)** (Suntsov & Brodeur 2008), northern CC **(f)** (Rainwater 1975), southern CC (**g)** (Paxton 1967), southern CC **(h)** (Imsand 1981), southern CC and Gulf of California **(i)** (Cailliet & Ebeling 1990), southern CC (**j)** (Willis & Pearcy 1982), Oregon, Note: < 500 m was not sampled **(k)** (Badcock 1970), Canary Islands (Atlantic) **(l)** (Ozawa et al. 1977), Japan **(m)** (Fitch & Lavenberg 1968) **(n)** (Miya & Nishida 1996), worldwide **(o)** (Hopkins et al. 1996), Gulf of Mexico **(p)** (Hopkins & Baird 1985), Gulf of Mexico **(q)** (Merrett & Roe 1974), **(r)** (Hart 1973) **(s)** (Miller & Lea 1976) **(t)** (Bartow 2010) **(u)** (Beamish et al. 1999) **(v)** Dewitt & Cailliet **(w)** (Childress & Nygaard 1973)

1.12 References

Alin SR, Feely RA, Dickson AG, Hernández-Ayón JM, Juranek LW, Ohman MD, Goericke R (2012) Robust empirical relationships for estimating the carbonate system in the southern California Current System and application to CalCOFI hydrographic cruise data (2005–2011). J Geophys Res 117:C05033

Asch RG (2015) Climate change and decadal shifts in the phenology of larval fishes in the California Current ecosystem. Proc Natl Acad Sci:201421946

Badcock J (1970) The vertical distribution of mesopelagic fishes collected on the SOND cruise. J Mar Biol Assoc UK 50:1001–1044

Benoit-Bird KJ (2009) The effects of scattering-layer composition, animal size, and numerical density on the frequency response of volume backscatter. ICES J Mar Sci 66:582–593

Bertrand A, Ballón M, Chaigneau A (2010) Acoustic observation of living organisms reveals the upper limit of the oxygen minimum zone. PLoS One 5:e10330

Bertrand A, Bard F-X, Josse E (2002) Tuna food habits related to the micronekton distribution in French Polynesia. Mar Biol 140:1023–1037

Bianchi D, Galbraith ED, Carozza DA, Mislan K, Stock CA (2013) Intensification of open-ocean oxygen depletion by vertically migrating animals. Nat Geosci 6:545–548

Boden BP, Kampa EM (1965) An aspect of euphausiid ecology revealed by echo-sounding in a fjord. Crustaceana 9:155–173

Bograd SJ, Buil MP, Lorenzo E Di, Castro CG, Schroeder ID, Goericke R, Anderson CR, Benitez-Nelson C, Whitney FA (2014) Changes in source waters to the Southern California Bight. Deep Sea Res Part II Top Stud Oceanogr:1–11

Bograd SJ, Castro CG, Lorenzo E Di, Palacios DM, Bailey H, Gilly W, Chavez FP (2008) Oxygen declines and the shoaling of the hypoxic boundary in the California Current. Geophys Res Lett 35:1–6

Bost C, Zorn T, Maho Y Le, Duhamel G (2002) Feeding of diving predators and diel vertical migration of prey: King penguin diet versus trawl sampling at Kerguelen Islands. Mar Ecol Prog Ser 227:51–61

Brodeur R, Yamamura O (2005) Micronekton of the North Pacific. Sidney, BC Canada

Catul V, Gauns M, Karuppasamy PK (2010) A review on mesopelagic fishes belonging to family Myctophidae. Rev Fish Biol Fish 21:339–354

Chekalyuk AM, Landry MR, Goericke R, Taylor AG, Hafez MA (2012) Laser fluorescence analysis of phytoplankton across a frontal zone in the California Current ecosystem. J Plankton Res 34:761–777

Childress JJ (1995) Are there physiological and biochemical adaptations of metabolism in deep-sea animals? Trends Ecol Evol 10:30–36

Childress JJ, Nygaard MH (1973) The chemical composition of midwater fishes as a function of depth of occurrence off southern California. Deep Sea Res 20:1093–1109

Childress J, Seibel B (1998) Life at stable low oxygen levels: adaptations of animals to oceanic oxygen minimum layers. J Exp Biol 201:1223–32

Childress JJ, Somero GN (1979) Depth-related enzymic activities in muscle, brain and heart of deep-living pelagic marine teleosts. Mar Biol 52:273–283

Collard SB (1970) Forage of some eastern Pacific midwater fishes. Copeia 1970:348–354

Cornejo R, Koppelmann R (2006) Distribution patterns of mesopelagic fishes with special reference to Vinciguerria lucetia Garman 1899 (Phosichthyidae: Pisces) in the Humboldt Current Region off Peru. Mar Biol 149:1519–1537

Council PFM (2015) Pacific Fishery Management Council Recommendations on Comprehensive Ecosystem- Based Amendment 1: Protecting Unfished and Unmanaged Forage Fish Species.

Crawford WR, Peña MA (2013) Declining oxygen on the British Columbia continental shelf. Atmosphere-Ocean 51:88–105

Davis MP, Holcroft NI, Wiley EO, Sparks JS, Leo Smith W (2014) Species-specific bioluminescence facilitates speciation in the deep sea. Mar Biol 161:1139–1148

Davison PC, Checkley DM, Koslow JA, Barlow J (2013) Carbon export mediated by mesopelagic fishes in the northeast Pacific Ocean. Prog Oceanogr 116:14–30

Davison P, Lara-Lopez A, Anthony Koslow J (2015) Mesopelagic fish biomass in the southern California current ecosystem. Deep Sea Res Part II Top Stud Oceanogr 112:129–142

Deutsch C, Berelson W, Thunell R, Weber T, Tems C, McManus J, Crusius J, Ito T, Baumgartner T, Ferreira V, Mey J, Geen a. van (2014) Centennial changes in North Pacific anoxia linked to tropical trade winds. Science (80-) 345:665–668

Deutsch C, Brix H, Ito T, Frenzel H, Thompson L (2011) Climate-Forced Variability of Ocean Hypoxia. Science (80-) 333:336–339

Deutsch C, Emerson S, Thompson L (2006) Physical-biological interactions in North Pacific oxygen variability. J Geophys Res 111:1–16

Deutsch C, Ferrel A, Seibel BA, Pörtner H-O, Huey RB (2015) Climate change tightens a metabolic constraint on marine habitats. Science (80-) 348:1132–1135

Devine JA, Baker KD, Haedrich RL (2006) Deep-sea fishes qualify as endangered. Nature 439:29–29

Doniol-Valcroze T, Berteaux D, Larouche P, Sears R (2007) Influence of thermal fronts on habitat selection by four rorqual whale species in the Gulf of St. Lawrence. Mar Ecol Prog Ser 335:207–216

Field J, Francis R (2006) Considering ecosystem-based fisheries management in the California Current. Mar Policy 30:552–569

Field JC, Phillips A, Baltz K, Walker WA (2007) Range expansion and trophic interactions of the jumbo squid, Dosidicus gigas, in the California Current. CalCOFI Reports 48:131–146

Fitch JE, Lavenberg RJ (1968) Deep-water teleostean fishes of California. University of California Press, Berkeleley and Los Angeles

Frank T, Widder E (2002) Effects of a decrease in downwelling irradiance on the daytime vertical distribution patterns of zooplankton and micronekton. Mar Biol 140:1181–1193

Friedman JR, Condon NE, Drazen JC (2012) Gill surface area and metabolic enzyme activities of demersal fishes associated with the oxygen minimum zone off California. Limnol Oceanogr 57:1701–1710

Gilly WF, Beman JM, Litvin SY, Robison BH (2013) Oceanographic and Biological Effects of Shoaling of the Oxygen Minimum Zone. Ann Rev Mar Sci:1–28

Gjosaeter J, Kawaguchi K (1980) A review of the world resources of mesopelagic fish, FAO Fisher. Rome

Guinet C, Vacquié-Garcia J, Picard B, Bessigneul G, Lebras Y, Dragon A, Viviant M, Arnould J, Bailleul F (2014) Southern elephant seal foraging success in relation to temperature and light conditions: insight into prey distribution. Mar Ecol Prog Ser 499:285–301

Hochachka PW, Somero GN (2002) Biochemical adaptation: mechanism and process in physiological evolution. Oxford University Press, New York

Hoefer CJ (2000) Marine bird attraction to thermal fronts in the California Current System. Condor 102:423

Hofmann AF, Peltzer ET, Walz PM, Brewer PG (2011) Hypoxia by degrees: Establishing definitions for a changing ocean. Deep Sea Res Part I Oceanogr Res Pap 58:1212–1226

Holton AA (1969) Feeding behavior of a vertically migrating lanternfish. Pacific Sci 23:325–331

Hopkins TL, Baird RC (1985) Feeding ecology of four hatchetfishes (Sternoptychidae) in the eastern Gulf of Mexico. Bull Mar Sci 36:260–277

Hopkins TL, Sutton TT, Lancraft TM (1996) The trophic structure and predation impact of a low latitude midwater fish assemblage. Prog Oceanogr 38:205–239

Hsieh CH, Kim HJ, Watson W, Lorenzo E Di, Sugihara G (2009) Climate-driven changes in abundance and distribution of larvae of oceanic fishes in the southern California region. Glob Chang Biol 15:2137–2152

Imsand S (1981) Comparison of the food of Triphoturus mexicanus and T. nigrescens, two lanternfishes of the Pacific ocean. Mar Biol 63:87–100

Irigoien X, Klevjer TA, Røstad A, Martinez U, Boyra G, Acuña JL, Bode A, Echevarria F, Gonzalez-Gordillo JI, Hernandez-Leon S, Agusti S, Aksnes DL, Duarte CM, Kaartvedt S (2014) Large mesopelagic fishes biomass and trophic efficiency in the open ocean. Nat Commun 5

Johnston IA, Bernard LM (1983) Utilization of the ethanol pathway in carp following exposure to anoxia. J Exp Biol 104:73–78

Kaartvedt S, Staby A, Aksnes D (2012) Efficient trawl avoidance by mesopelagic fishes causes large underestimation of their biomass. Mar Ecol Prog Ser 456:1–6

Kaartvedt S, Webjorn M, Knutsen T, Skjoldal HR (1996) Vertical distribution of fish and krill beneath water of varying optical properties. Mar Ecol Prog Ser 136:51–58

Kahru M, DiLorenzo E, Manzano-Sarabia M, Mitchell BG (2012) Spatial and temporal statistics of sea surface temperature and chlorophyll fronts in the California Current. J Plankton Res 34:749–760

Kampa EM, Boden BP (1954) Submarine illumination and the twilight movements of a sonic scattering layer. Nature 174:869–871

Karstensen J, Stramma L, Visbeck M (2008) Oxygen minimum zones in the eastern tropical Atlantic and Pacific oceans. Prog Oceanogr 77:331–350

Karuppasamy PK, Muraleedharan KR, Dineshkumar PK, Nair M (2010) Distribution of mesopelagic micronekton in the Arabian Sea during the winter monsoon. Indian J Mar Sci 39:227–237

Keeling RF, Körtzinger A, Gruber N (2010) Ocean deoxygenation in a warming world. Ann Rev Mar Sci 2:199–229

Korneliussen R, Ona E (2002) An operational system for processing and visualizing multi-frequency acoustic data. ICES J Mar Sci 59:293–313

Koslow JA (2009) The role of acoustics in ecosystem-based fishery management. ICES J Mar Sci 66:966–973

Koslow J, Goericke R, Lara-Lopez A, Watson W (2011) Impact of declining intermediate-water oxygen on deepwater fishes in the California Current. Mar Ecol Prog Ser 436:207–218

Koslow J, Kloser R, Williams A (1997) Pelagic biomass and community structure over the mid-continental slope off southeastern Australia based upon acoustic and midwater trawl sampling. Mar Ecol Prog Ser 146:21–35

Lampert W (1993) Ultimate causes of diel vertical migration of zooplankton: new evidence for the predator avoidance hypothesis. Arch Hydrobiol/BeihErgebLimnol

39:79–88

Landry MR, Ohman MD, Goericke R, Stukel MR, Barbeau, K.A.Bundy R, Kahru M (2012) Pelagic community responses to a deep-water front in the California Current Ecosystem: overview of the A-front study. J Plankton Res 34:739–748

Lara-Lopez AL, Davison P, Koslow JA (2012) Abundance and community composition of micronekton across a front off Southern California. J Plankton Res 34:828–848

Levin LA (2003) Oxygen minimum zone benthos: adaptation and community response to hypoxia. Oceanogr Mar Biol an Annu Rev 41:1–45

Levin LA, Bris N Le (2015) The deep ocean under climate change. Sci 350 :766–768

Luo J, Ortner PB, Forcucci D, Cummings SR (2000) Diel vertical migration of zooplankton and mesopelagic fish in the Arabian Sea. Deep Sea Res II 47:1451–1473

McClatchie S, Cowen R, Nieto K, Greer A, Luo JY, Guigand C, Demer D, Griffith D, Rudnick D (2012) Resolution of fine biological structure including small narcomedusae across a front in the Southern California Bight. J Geophys Res 117:1–18

McClatchie S, Goericke R, Cosgrove R, Auad G, Vetter R (2010) Oxygen in the Southern California Bight: Multidecadal trends and implications for demersal fisheries. Geophys Res Lett 37:1–5

McClatchie S, Thorne RE, Grimes P, Hanchet S (2000) Ground truth and target identification for fisheries acoustics. Fish Res 47:173–191

Meester L De, Dawidowics P, Gool E, Loos C (1999) Ecology and evolution of predator behavior in zooplankton: depth selection behavior and diel vertical migration. In: Tollrian R, Harvell C (eds) The ecology and evolution of inducible defenses. Princeton University Press, Princeton, p 160

Mengerink KJ, Dover CL Van, Ardron J, Baker M, Escobar-Briones E, Gjerde K, Koslow JA, Ramirez-Llodra E, Lara-Lopez A, Squires D, Sutton T, Sweetman AK, Levin L a (2014) A call for deep-ocean stewardship. Science 344:696–8

Merrett NR, Roe HSJ (1974) Patterns and selectivity in the feeding of certain mesopelagic fishes. Mar Biol 28:115–126

Misund O a (1997) Underwater acoustics in marine fisheries and fisheries research. Rev Fish Biol Fish 7:1–34

Miya M, Nishida M (1996) Molecular phylogenetic perspective on the evolution of the deep-sea fish genus Cyclothone. Ichthyol Res 43:375–398

Mora C, Wei C-L, Rollo A, Amaro T, Baco AR, Billett D, Bopp L, Chen Q, Collier M, Danovaro R, Gooday AJ, Grupe BM, Halloran PR, Ingels J, Jones DOB, Levin L a, Nakano H, Norling K, Ramirez-Llodra E, Rex M, Ruhl H a, Smith CR, Sweetman AK, Thurber AR, Tjiputra JF, Usseglio P, Watling L, Wu T, Yasuhara M (2013) Biotic and human vulnerability to projected changes in ocean biogeochemistry over the 21st century. PLoS Biol 11:e1001682

Moser H (1996) The early stages of fishes in the California Current region.

Moser G, Smith P (1993) Larval fish assemblages of the California Current region and their horizontal and vertical distributions across a front. Bull Mar Sci 53:645–691

Moser H, Smith P, Eber L (1987) Larval Fish Assemblages in the California Current Region, 1954-1960, a Period of Dynamic Environmental Change. CalCOFI Reports 18:97–127

Murray J, Hjort J (1912) The Depths of the Ocean. MacMillan, London

Nasby-Lucas N, Dewar H, Lam CH, Goldman KJ, Domeier ML (2009) White shark offshore habitat: a behavioral and environmental characterization of the eastern Pacific shared offshore foraging area. PLoS One 4:e8163

Netburn AN, Koslow JA (2015) Dissolved oxygen as a constraint on daytime deep scattering layer depth in the southern California current ecosystem. Deep Sea Res Part I Oceanogr Res Pap 104:149–158

Ohman MD, Powell JR, Picheral M, Jensen DW (2012) Mesozooplankton and particulate matter responses to a deep-water frontal system in the southern California Current System. J Plankton Res 34:815–827

Oozeki Y, Hu F, Kubota H, Sugisaki H, Kimura R (2004) Newly designed quantitative frame trawl for sampling larval and juvenile pelagic fish. Fish Sci 70:223–232

Ozawa T, Fujii K, Kawaguchi K (1977) Feeding chronology of the vertically migrating gonostomatid fish,Vinciguerria nimbaria (Jordan and Williams), off southern Japan. J Oceanogr Soc Japan 33:320–327

Pauly D, Trites AW, Capuli E, Christensen V (1998) Diet composition and trophic levels of marine mammals. ICES J Mar Sci 55:467–481

Paxton JR (1967) A distributional analysis for the lanternfishes (Family Myctophidae) of the San Pedro Basin, California. 1967:422–440

Pearcy WG, Krygier EE, Mesecar R, Ramsey F (1977) Vertical distribution and migration of oceanic micronekton off Oregon. Deep Sea Res 24:223–245

Polovina JJ, Howell E, Kobayashi DR, Seki MP (2001) The transition zone chlorophyll front, a dynamic global feature defining migration and forage habitat for marine resources. Prog Oceanogr 49:469–483

Portner H-O (2010) Oxygen- and capacity-limitation of thermal tolerance: a matrix for integrating climate-related stressor effects in marine ecosystems. J Exp Biol 213:881–893

Potier M, Marsac F, Cherel Y, Lucas V, Sabatie R, Maury O, Menard F (2007) Forage fauna in the diet of three large pelagic fishes (lancetfish, swordfish and yellowfin tuna) in the western equatorial Indian Ocean. Fish Res 83:60–72

Powell JR, Ohman MD (2015a) Changes in zooplankton habitat, behavior, and acoustic scattering characteristics across glider-resolved fronts in the Southern California Current System. Prog Oceanogr 134:77–92

Powell JR, Ohman MD (2015b) Covariability of zooplankton gradients with glider-detected density fronts in the Southern California Current System. Deep Res Part II Top Stud Oceanogr 112:79–90

Prince ED, Goodyear CP (2006) Hypoxia-based habitat compression of tropical pelagic fishes. Fish Oceanogr 15:451–464

Quintana-Rizzo E, Torres JJ, Ross SW, Romero I, Watson K, Goddard E, Hollander D (2015) δ13C and δ15N in deep-living fishes and shrimps after the Deepwater Horizon oil spill, Gulf of Mexico. Mar Pollut Bull

Rainwater C (1975) An ecological study of midwater fishes in Santa Catalina Basin off southern California, using cluster analysis (Dissertation)

Ramirez-Llodra E, Tyler PA, Baker MC, Bergstad OA, Clark MR, Escobar E, Levin LA, Menot L, Rowden AA, Smith CR, Dover CL Van (2011) Man and the last great wilderness: human impact on the deep sea (P Roopnarine, Ed.). PLoS One 6:e22588

Robinson C, Steinberg DK, Anderson TR, Arístegui J, Carlson CA, Frost JR, Ghiglione J-F, Hernández-León S, Jackson GA, Koppelmann R (2010) Mesopelagic zone ecology and biogeochemistry – a synthesis. Deep Sea Res Part II Top Stud Oceanogr 57:1504–1518

Robison BH (2009) Conservation of deep pelagic biodiversity. Conserv Biol 23:847–58

Saltzman J, Wishner KF (1997) Zooplankton ecology in the eastern tropical Pacific oxygen minimum zone above a seamount: 2. Vertical distribution of copepods. Deep Sea Res I 44:931–954

Seibel BA (2011) Critical oxygen levels and metabolic suppression in oceanic oxygen minimum zones. J Exp Biol 214:326–336

Seibel BA, Drazen JC (2007) The rate of metabolism in marine animals: environmental constraints, ecological demands and energetic opportunities. Philos Trans R Soc London Ser B 362:2061–78

Seibel BA, Walsh PJ (2001) Carbon cycle. Potential impacts of CO2 injection on deep-sea biota. Science 294:319–20

Shaffer G, Olsen SM, Pedersen JOP (2009) Long-term ocean oxygen depletion in response to carbon dioxide emissions from fossil fuels. Nat Geosci 2:105–109

Shoubridge EA, Hochachka PW (1980) Ethanol: a novel end product of vertebrate anaerobic metabolism. Science (80-) 209:308–309

Stanton TK, Chu D, Wiebe PH (1998) Sound scattering by several zooplankton groups. II. Scattering models. J Acoust Soc Am 103:236–53

Stewart JS, Hazen EL, Bograd SJ, Byrnes JEK, Foley DG, Gilly WF, Robison BH, Field JC (2014) Combined climate- and prey-mediated range expansion of Humboldt squid (Dosidicus gigas), a large marine predator in the California Current System. Glob Chang Biol 20:1832–43

Stramma L, Johnson GC, Firing E, Schmidtko S (2010) Eastern Pacific oxygen minimum zones: Supply paths and multidecadal changes. J Geophys Res 115:C09011

Stramma L, Johnson GC, Sprintall J, Mohrholz V (2008) Expanding oxygen-minimum zones in the tropical oceans. Science 320:655–8

Stramma L, Prince ED, Schmidtko S, Luo J, Hoolihan JP, Visbeck M, Wallace DWR,

Brandt P, Körtzinger A (2011) Expansion of oxygen minimum zones may reduce available habitat for tropical pelagic fishes. Nat Clim Chang:1–5

Stramma L, Schmidtko S, Levin LA, Johnson GC (2010) Ocean oxygen minima expansions and their biological impacts. Deep Sea Res Part I Oceanogr Res Pap 57:587–595

Suntsov A V, Brodeur RD (2008) Trophic ecology of three dominant myctophid species in the northern California Current region. 373:81–96

Sutor MM, Cowles TJ, Peterson WT, Pierce SD (2005) Acoustic observations of finescale zooplankton distributions in the Oregon upwelling region. Deep Sea Res Part II Top Stud Oceanogr 52:109–121

Sverdrup HU (1938) On the explanation of the oxygen minima and maxima in the oceans. ICES J Mar Sci 13:163–172

Taylor AG, Goericke R, Landry MR, Selph KE, Wick DA, Roadman MJ (2012) Sharp gradients in phytoplankton community structure across a frontal zone in the California Current Ecosystem. J Plankton Res 34:778–789

Thompson DR, Furness RW, Monteiro LR (1998) Seabirds as biomonitors of mercury inputs to epipelagic and mesopelagic marine food chains. Sci Total Environ 213:299–305

Tont SA (1975) Deep scattering layers: patterns. CalCOFI Reports 18:112–117

Torres JJ, Belmanf BW, Childress JJ (1979) Oxygen consumption rates of midwater fishes as a function of depth of occurrence. Deep Sea Res 26:185–197

Torres JJ, Grigsby MD, Clarke ME (2012) Aerobic and anaerobic metabolism in oxygen minimum layer fishes: the role of alcohol dehydrogenase. J Exp Biol 215:1905–14

Tyler HR, Pearcy WG (1975) The feeding habits of three species of lanternfishes (family Myctophidae) off Oregon, USA. Mar Biol 32:7–11

Urmy SS, Horne JK, Barbee DH (2012) Measuring the vertical distributional variability of pelagic fauna in Monterey Bay. ICES J Mar Sci 69:184–196

Vaquer-Sunyer R, Duarte CM (2008) Thresholds of hypoxia for marine biodiversity. Proc Natl Acad Sci U S A 105:15452–7

Vetter R, Lynn E, Garza M, Costa A (1994) Depth zonation and metabolic adaptation in Dover sole, Microstomus pacificus, and other deep-living flatfishes: factors that affect the sole. Mar Biol 120:145–159

Vornanen M, Steyk J, Nilsoon G (2009) The anoxia-tolerant crucian carp (Carassius carassius L.). In: Richards J, Farrell A, Brauner C (eds) Fish Physiology, Vol. 27: Hypoxia. Academic Press, Amsterdam, p 398–443

Watanabe H, Kawaguchi K (2003) Decadal change in abundance of surface migratory myctophid fishes in the Kuroshio region from 1957 to 1994. Fish Oceanogr 12:100–111

Watanabe H, Moku M, Kawaguchi K, Ishimaru K, Ohno A (1999) Diel vertical migration of myctophid fishes (Family Myctophidae) in the transitional waters of the western North Pacific. Fish Oceanogr 8:115–127

Watanabe YW, Wakita M, Maeda N (2003) Synchronous bidecadal periodic changes of oxygen, phosphate and temperature between the Japan Sea deep water and the North Pacific intermediate water. Geophys Res Lett 30

Whitney FA, Freeland HJ, Robert M (2007) Persistently declining oxygen levels in the interior waters of the eastern subarctic Pacific. Prog Oceanogr 75:179–199

Williams A, Koslow JA, Terauds A, Haskard K (2001) Feeding ecology of five fishes from the mid-slope micronekton community off southern Tasmania, Australia. Mar Biol 139:1177–1192

Willis JM, Pearcy WG (1982) Vertical distribution and migration of fishes of the lower mesopelagic zone off Oregon. Mar Biol 70:87–98

Wishner KF, Gelfman C, Gowing MM, Outram DM, Rapien M, Williams RL (2008) Vertical zonation and distributions of calanoid copepods through the lower oxycline of the Arabian Sea oxygen minimum zone. Prog Oceanogr 78:163–191

Wishner KF, Gowing MM, Gelfman C (2000) Living in suboxia: Ecology of an Arabian Sea oxygen minimum zone copepod. Limnol Oceanogr 45:1576–1593

Wyrtki K (1962) The oxygen minima in relation to ocean circulation. Deep Sea Res Oceanogr Abstr 9:11–23

CHAPTER 2

DISSOLVED OXYGEN AS A CONSTRAINT ON DAYTIME DEEP SCATTERING LAYER DEPTH IN THE SOUTHERN CALIFORNIA CURRENT ECOSYSTEM

Deep-Sea Research I 104 (2015) 149–158

Contents lists available at ScienceDirect

Deep-Sea Research I

journal homepage: www.elsevier.com/locate/dsri

Dissolved oxygen as a constraint on daytime deep scattering layer depth in the southern California current ecosystem

Amanda N. Netburn*, J. Anthony Koslow

Scripps Institution of Oceanography (UCSD), University of California, San Diego, La Jolla, CA 92093-0208, USA

ARTICLE INFO

Article history:
Received 19 December 2014
Received in revised form
10 June 2015
Accepted 13 June 2015
Available online 23 June 2015

Keywords:
Deep scattering layer
Oxygen minimum zone
Hypoxia
Irradiance
Mesopelagic fish
Climate change

ABSTRACT

Climate change-induced ocean deoxygenation is expected to exacerbate hypoxic conditions in mesopelagic waters off the coast of southern California, with potentially deleterious effects for the resident fauna. In order to understand the possible impacts that the oxygen minimum zone expansion will have on these animals, we investigated the response of the depth of the deep scattering layer (i.e., upper and lower boundaries) to natural variations in midwater oxygen concentrations, light levels, and temperature over time and space in the southern California Current Ecosystem. We found that the depth of the lower boundary of the deep scattering layer (DSL) is most strongly correlated with dissolved oxygen concentration, and irradiance and oxygen concentration are the key variables determining the upper boundary. Based on our correlations and published estimates of annual rates of change to irradiance level and hypoxic boundary, we estimated the corresponding annual rate of change of DSL depths. If past trends continue, the upper boundary is expected to shoal at a faster rate than the lower boundary, effectively widening the DSL under climate change scenarios. These results have important implications for the future of pelagic ecosystems, as a change to the distribution of mesopelagic animals could affect pelagic food webs as well as biogeochemical cycles.

1. Introduction

In some parts of the ocean there exists a permanent subsurface hypoxic layer, called the oxygen minimum zone (OMZ), which arises due to the combination of limited surface ventilation, respiratory oxygen consumption, and ocean circulation (Sverdrup 1938; Wyrtki 1962; Karstensen et al., 2008). OMZs are commonly defined by oxygen concentrations of less than 0.5 ml l^{-1} (Gilly et al., 2013; Helly & Levin 2004; Paulmier & Ruiz-Pino, 2009), however hypoxia tolerances vary greatly by species and environment (Levin 2003; Seibel 2011). The most developed OMZs are in tropical and subtropical oceans and eastern boundary currents, including the California Current off the west coast of the United States.

Increased ocean stratification and changes to global circulation patterns are predicted to accompany global climate change, resulting in decreased dissolved oxygen content, particularly at depths of 200–700 m, and expansion of OMZs (Deutsch et al., 2006, 2011; Shaffer et al., 2009; Keeling et al., 2010). Such expansions have already been observed in tropical and subtropical regions (Stramma et al., 2008, 2010), across the northern North Pacific (Watanabe et al., 2003; Whitney et al., 2007; Crawford and Peña, 2013), and in the southern California Current Ecosytem (CCE) (Bograd et al., 2008; McClatchie et al., 2010) where deoxygenation has been linked to intensification of the California Undercurrent (Bograd et al., 2014). Deleterious effects of ocean deoxygenation have been observed for shallow-dwelling and coastal organisms exposed to extreme hypoxic events such as the summertime "dead zone" appearance in the Gulf of Mexico (Rabalais et al., 2002), entrapment of epipelagic fishes in California harbors (Stauffer et al., 2012), and strong upwelling events along the Oregon coast (Grantham et al., 2004; Chan et al., 2008).

The mesopelagic zone is one of the largest ecosystems on earth, and the resident fauna is both diverse and abundant (Robison, 2009). Many mesopelagic organisms are aggregated into one or more layers in the ocean, referred to as deep scattering layers (DSLs) due to the high acoustic reflectance observed using sonar systems. The animals comprising the DSL are important to global marine food webs, fisheries, conservation, and biogeochemistry (Robinson et al., 2010), yet remain understudied due to inaccessibility and the inadequacy of traditional sampling tools (Robison, 2009; Davison et al., 2013). Anthropogenic disturbances have only recently been recognized to have effects on deep-sea environments (Devine et al., 2006; Robison, 2009; Ramirez-Llodra et al., 2011). With few long-term studies on mesopelagic populations, it is not well understood how these communities respond to perturbations to their environment. The organisms that live in

* Corresponding author.

http://dx.doi.org/10.1016/j.dsr.2015.06.006
0967-0637/

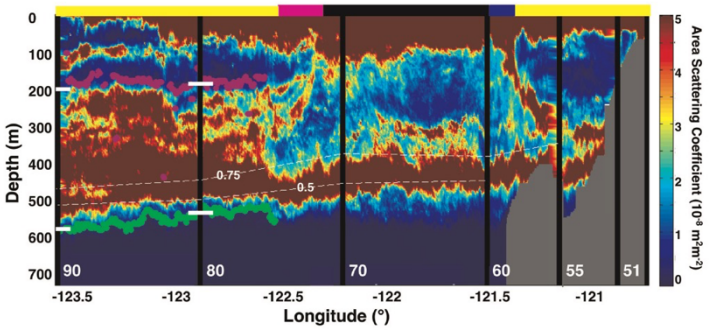

Fig. 1. A representative echogram illustrating the scattering coefficient at 38 kHz along CalCOFI line 76.7. The transect was conducted from nearshore (east) to offshore (west), from 10:00 PDT on 15 May to 12:30 PDT on 16 May, 2010. The pink and green points indicate the upper and lower boundaries of the deep scattering layer (DSL), respectively. Black vertical bars indicate the location of each CalCOFI station, with station number labeled toward the bottom of the plot. White horizontal bars indicate DSL lower and upper boundaries averaged within 2.75 km of the CalCOFI station. The dashed lines are the 0.75 and 0.5 ml l^{-1} oxygen isopleths. (Bar at top of the plot: yellow = daytime, blue = dusk, black = night, pink = dawn).

already hypoxic mesopelagic depths (200–1000 m) of the CCE are living at the limits of their hypoxia tolerance (Childress and Seibel, 1998), and are thus especially vulnerable to declining oxygen levels in their environment. With the predicted and observed global expansion of midwater OMZs, the mesopelagic fauna could undergo changes in abundance and composition that, given the current state of knowledge, may go mostly unnoticed by scientists, marine resource managers and conservation biologists.

Using larval abundance as a proxy for adult abundance, Koslow et al. (2011) inferred that populations of mesopelagic fish in the southern CCE were reduced by over 60% in years with relatively low midwater (200–400 m) oxygen concentrations. The authors hypothesized that the underlying mechanism leading to this decline is that a hypoxic boundary (HB) limits the maximum depth available as suitable habitat for the mesopelagic fauna. In years of low midwater oxygen concentrations, the HB shoals, thereby forcing animals into shallower waters with higher irradiance, where the fishes are more vulnerable to predation by visually-oriented predators. A number of fish species are known to be bound by HBs, including Peruvian anchovy (*Engraulis ringens*, Bertrand et al., 2010), great white sharks (*Carcharodon carcharias*, Nasby-Lucas et al., 2009), and istiophorid billfishes (e.g., marlins, sailfish) (Prince and Goodyear, 2006; Stramma et al., 2011).

Irradiance has consistently been found to be a primary determinant of DSL depths (Kampa and Boden, 1954; Tont, 1975; Frank and Widder, 2002). This effect is attributed to DSL animals taking refuge from visually-oriented predators in darker waters (Lampert, 1993; De Meester et al., 1999). While some studies have considered the role of oxygen content and other variables in constraining DSL depths, many earlier analyses have been conducted either in places that lack an OMZ (e.g., Frank and Widder, 2002), or have only considered a single depth to describe the "DSL depth" (e.g., Tont, 1975; Bianchi et al., 2013). Given that the DSL width can span several hundred meters, it is likely that different environmental factors limit the top and bottom boundaries. The responses of each of these boundaries could be differentially affected by a changing climate.

Several recent studies have suggested a relationship between DSL depths and hypoxia. A global analysis of 38–150 kHz Shipboard Acoustic Doppler Current Profiler (ADCP) data concluded that the depth of the DSL is correlated with the oxygen concentration in the upper mesopelagic (150–500 m) (Bianchi et al., 2013). Their findings indicate that the DSL depth on large scales is limited by climatological oxygen concentrations. Another study within the central CCE attributed a ~300 m change in DSL depth between seasons to potential changes in OMZ depth (Urmy et al., 2012). Neither study collected simultaneous environmental measurements with the acoustic data.

The purpose of the present study is to explore the effects that the predicted decline of oxygen in the southern CCE may have on habitat use by the mesopelagic fish assemblage. Because it is not possible to isolate variation in oxygen concentrations from other natural variability in the environment, we further explore how the DSL responds to light and temperature. The DSL top and bottom boundaries were detected with echosounder-collected acoustic backscatter data, and the relationships between their depths to changes in the different variables were tested using linear regression and general additive models. We tested the following hypotheses:

(1) There is a positive relationship between ***predation risk*** (using midwater irradiance as a proxy) and DSL depths. We expect this response to be stronger at the DSL upper boundary because predation risk is strongest at the shallower depths.
(2) There is a positive relationship between ***oxygen concentration*** and DSL depth. We expect this relationship to be strongest at the bottom boundary of the DSL, because this is in closest contact to the most hypoxic waters.
(3) There is a positive relationship between ***temperature*** and DSL depth, because there is likely an optimal thermal range for basal metabolic and other activities.

To test these hypotheses, we developed an algorithm to detect DSL depths from continuously-collected acoustic backscatter data across the core California Cooperative Oceanic Fisheries Investigations (CalCOFI) stations, accompanied by midwater trawls to characterize the mesopelagic fish fauna on a subset of cruises and stations (Fig. 1). With midwater oxygen levels varying spatially, seasonally, and annually, and concurrent station measurements of environmental variables including temperature, dissolved oxygen, and irradiance, these data allowed us to probe for the mechanisms that lead to the abundance declines observed by Koslow et al. (2011).

After determining the important variables for constraining each of the top and bottom boundaries, we explored how potential climate change impacts may shift the vertical range of the DSL. The

expectation is that either the entire vertical range will shift into better illuminated waters, or that habitat compression will result from shoaling at the lower boundary alone.

2. Methods

2.1. Acoustic backscatter

Acoustic backscatter data were collected on twelve California Cooperative Oceanic Fisheries Investigations (CalCOFI) cruises from 2009 to 2012 and in all 4 seasons with a 5-frequency (18, 38, 70, 120 and 200 kHz) Simrad EK-60 echosounder. Three cruises were omitted from the analysis, because of missing backscatter data. Only the 38 kHz data were used in the determination of DSL depth, as this frequency penetrates to the requisite depths while avoiding some of the resonance effects of air-bladdered fishes at 18 kHz (Kloser et al., 2002; Godø et al., 2009; Davison et al., 2015a). While most small zooplankton do not scatter strongly at 38 kHz (Lavery et al., 2007), the detected DSL layer likely includes some invertebrate taxa, such as squid, decapods, and siphonophores, in addition to fish. In particular, physonect siphonophores have strong backscatter at this frequency due to the inclusion of a gas-fill pneumatophore (Warren, 2001; Benfield et al., 2003; Lavery et al., 2007), and the DSL that we detected at this frequency likely includes both fishes and siphonophores. Siphonophores are not typically well preserved in net catches and were not enumerated for this analysis. However, a detailed comparison of the acoustic and trawl data for these cruises indicates that fish likely dominated the acoustic signal except during the August 2010 cruise in the region around the Channel Islands (Davison et al., 2015b). The cruises for which data were used for this study are presented in Table 1. Transducers were calibrated using a tungsten carbide reference sphere suspended beneath the research vessel either at the start or end of each cruise (Foote et al., 1987).

All bioacoustic data were cleaned using EchoView software. The cleaning process involves removal of ship noise, acoustic reflections from the CTD during casts, background noise and false bottoms (i.e, acoustic reflections from the seafloor), and filling in areas of removed data with interpolated nearby data. The volume backscatter data were binned into 5 m vertical by 500 m horizontal bins to resolve horizontal and vertical gradients in the backscatter at a scale that can be compared to measurements of water column properties, such as oxygen concentration and temperature, over the CalCOFI sampling region. Backscatter data were converted from nautical area scattering coefficient (NASC, m^2 nmi^{-2}) to area scattering coefficient (s_a, in $m^2\ m^{-2}$).

Table 1
California Cooperative Oceanic Fisheries Investigations (CalCOFI) sampling cruises on which bioacoustic data were collected for this analysis, and availability of concurrently collected animals with a Matsuda Oozeki Hui Trawl (MOHT). All cruises were conducted on the RV New Horizon, except for CalCOFI 1004, which took place on the NOAA RV Miller Freeman.

Cruise name	Dates	500 m MOHT trawls
CalCOFI 0911	6–23 Nov, 2009	
CalCOFI 1001	12 Jan–4 Feb, 2010	
CalCOFI 1004	27 Apr–17 May, 2010	
CalCOFI 1008	30 Jul–17 Aug, 2010	✓
CalCOFI 1011	28 Oct–12 Nov, 2011	✓
CalCOFI 1101	12 Jan–4 Feb, 2011	
CalCOFI 1108	27 Jul–12 Aug, 2011	✓
CalCOFI 1202	27 Jan–13 Feb, 2012	✓
CalCOFI 1210	19 Oct–5 Nov, 2012	✓

2.2. Deep scattering layer depth detection algorithm

A layer detection algorithm was developed (in Matlab v. 2012a) to detect the top and bottom boundaries of the deepest detected DSL at each station using the 38 kHz acoustic backscatter data. The 3 depth bin vertical running mean of the s_a was first calculated to smooth the data. The algorithm then searched from the bottom up, starting at the maximum depth for which backscatter data were recorded (750–800 m). A DSL bottom was detected when the following conditions were met: (1) $s_a \geq a$ threshold value (4×10^{-9} $m^2\ m^{-2}$ was chosen based on agreement with visual inference), (2) the change in s_a from the next deepest bin was positive, and (3) the positive gradient persisted for at least 3 depth bins (i.e., 15 m). The top of the layer was similarly defined as the upper-most bin where s_a was $\geq$ the cutoff value and the gradient was negative for at least 3 depth bins. In order to compare acoustic backscatter with station-based water column variables, the mean DSL upper and lower boundary depths were calculated for each CalCOFI CTD station from data within 2.75 km on either side of the station (Fig. 1). We only analyzed daytime DSL depth distributions.

Seamounts and continental shelves have an aggregating effect on many organisms. The behavior of the layers near these features was different than in the open ocean region, with high backscatter from the surface to the seafloor in many cases. Therefore the layer detection algorithm for the offshore was not appropriate for waters at nearshore and seamount-associated stations. Data were thus excluded from within 20 km of any region with bottom depths shallower than 600 m. Additional filters were applied to remove detections of anomalous speckle (noise and detections of large individuals that were outside of the core layer) and to ensure that a small gap in the layer did not cause a detected layer to be split into two. In limited cases the algorithm failed to identify the appropriate top or bottom due to anomalous backscatter near the station. In these cases, the DSL top or bottom depth was identified visually.

2.3. Fish assemblages

On five of the cruises in this analysis, there was concurrent daytime oblique trawl sampling to 500 m with a 1.6 mm mesh Matsuda-Oozeki-Hu trawl (MOHT) with a 5-m^2 mouth opening (Oozeki et al., 2004) and TSK flowmeter (Table 1) at a subset of stations. Although avoidance behavior and escapement lead to undersampling with any net system, the MOHT has recently been found to outperform other systems in its capture efficiency (Pakhomov and Yamamura, 2010). No net collections took place at dawn and dusk to avoid sampling during the diel vertical migrations. Efforts were made to allocate the tows evenly across the full CalCOFI grid, and all trawls were conducted using the same approximate ship speed, wire speed, and wire paid out. The collected fish were preserved in 10% sodium tetraborate-buffered formalin and later identified to lowest taxonomic unit possible in the lab. Cluster analysis based on Bray–Curtis dissimilarities of $\log_{10}(x+1)$ transformed data has revealed two distinct assemblages based on geographical region: (1) a nearshore/core California Current assemblage (inshore of and including station 80), and (2) an offshore-associated group (beyond station 80 (X. Rojas-Rocha, pers. comm). Because the number of concurrent fish trawls and acoustic backscatter stations was limited, all CalCOFI stations were assigned a region, with stations ≤ 80 designated the nearshore region and ≥ 90 assigned to the offshore region (Fig. 2). Regressions were fit independently for data collected at each of the two regions.

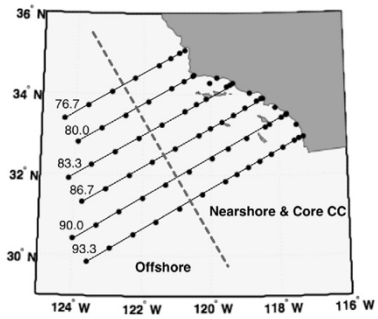

Fig. 2. CalCOFI core hydrographic stations. Acoustic sampling occurred along the CalCOFI transect lines (76.7–93.3) for each cruise included in this analysis. All stations west of the broken grey line (stations >80) were assigned as offshore stations, and those inshore of the grey line ($<=80$) were assigned as nearshore/core California Current stations.

2.4. Environmental variables

Given previous work done on the subject, irradiance, dissolved oxygen, and temperature were considered as likely explanatory variables for predicting the lower and upper DSL boundary layer depths.

2.4.1. Light level estimates: irradiance index

Due to the inherent difficulties of measuring or estimating light levels at mesopelagic depths, an index of irradiance was calculated based on light attenuation near the surface where most of the light is attenuated, with the assumption that irradiance at depth is proportional to irradiance in the upper water column (Li et al., 2014). The Irradiance Index (II) is: $II = PAR * e^{-k_{490}} * 30$, where PAR is photosynthetically available radiation at the surface ($E\,m^{-2}\,d^{-1}$) and k_{490} is the diffuse attenuation coefficient at 490 nm light (blue) in the surface mixed layer, which is approximated as 30 m. This index is appropriate as most of the light attenuation per unit depth occurs in the upper 30 m, and satellites are unable to sense below this level. Surface PAR and k_{490} were derived from satellite measurements (SeaWiFS, MODIS-Terra and MODIS-Aqua) as per Kahru et al. (2014), using the methods of Frouin et al. (2003) to derive PAR and the standard NASA KD2 algorithm for k_{490} (http://oceancolor.gsfc.nasa.gov/REPROCESSING/R2009/kdv4/). Data were recorded at the pixel closest in time and space to each CalCOFI CTD station as possible.

2.4.2. Oxygen

Dissolved oxygen concentrations were measured to ~500 m at each station using a CTD equipped with dual SBE43 oxygen sensors, and corrected with Winkler titration measurements on discrete depth bottle samples at each station. Visual inspection of the DSL indicates a possible hypoxic boundary at ~0.5 ml l^{-1} (Fig. 4 in Koslow et al. (2011)), although the oxygen at the bottom boundary for the present dataset varied from 0.15 to 0.71 ml l^{-1} O_2 during the day. Because the bottom of the DSL was often detected deeper than 500 m, the 0.75 ml l^{-1} isopleth was chosen as an appropriate predictor variable due to the availability of data to calculate this metric at all stations. The depth of the 0.75 ml l^{-1} isopleth is strongly correlated with the depth of the 0.5 ml l^{-1} isopleth ($r^2=0.803$, $p<0.001$) as well as with other deep oxygen isopleths, thus serving as a reasonable proxy for the threshold oxygen concentration. Oxygen concentrations at the upper boundary of the DSL spanned a much greater range than at the bottom boundary, with concentrations ranging from 0.57 to 3.7 ml l^{-1}. In order to choose the best oxygen variable to use for the models, we ran regressions for a number of different oxygen isopleths (results not shown). The 2.0 ml l^{-1} isopleth was chosen for the models as it had the strongest correlation with the depth of the upper DSL boundary, and is also near the mean value for oxygen concentration at the top of the DSL (2.16 ml l^{-1}).

2.4.3. Temperature

Temperature was measured with dual SBE3plus fast response temperature sensors to ~500 m at each station. Various isotherms were considered, and those with the highest predictive power for each of the top and bottom of the DSL used for the analysis: the 7.5° and 8.5 °C isotherm for the bottom and top, respectively.

2.4.4. Statistical analyses

Because there is variability in measurements for both the independent and dependent variables, we fitted the data using Model II regressions (Ricker, 1973). Testing for a difference from zero slope of a Model II regression is uncertain, so we first tested for a significant relationship using Pearson product-moment correlation analysis. Where fits were significant ($p<0.05$) for both inshore and offshore faunistic regions, we then tested for a significant difference between the slopes of the two lines using the method of Clarke (1980) to determine whether the two characteristic assemblages respond differently to the environmental variables. Both regression equations are presented where the slopes are significantly different between the two regions. If the slopes are not different ($p>0.05$), we instead fit the entire data set using the Model II regression. Co-variation between variables was

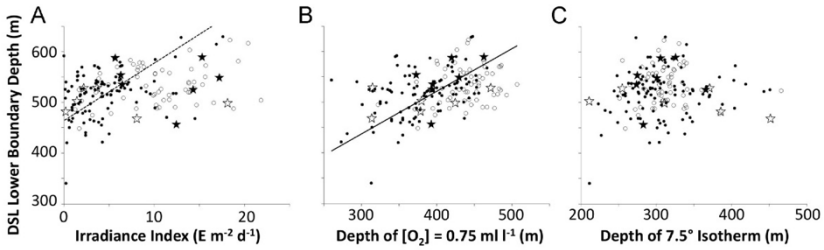

Fig. 3. Relationships between the depth of the lower boundary of the deep scattering layer (DSL) and each of the four predictor variables. Irradiance is a continuous measurement, while the oxygen and temperature variables are discrete depths. Closed circles represent nearshore and core California Current stations and open circles represent offshore-associated stations. Stars indicate locations where deep (~500 m) MOHT trawls were conducted, with open and closed indicating the two characteristic species assemblages. Black broken lines are fitted to nearshore/CC stations, and the grey broken lines are fitted to the offshore stations. Solid black lines are fitted to the full dataset. (A) Irradiance Index (Nearshore/CC: $y=11.37x+452.6$, $r^2=0.11$, Offshore: NS), (B) Depth of $[O_2]=0.75$ ml l^{-1} isopleth: ($y=0.842x+184.2$, $r^2=0.18$), and (C) Depth of the 7.5° isotherm (NS).

initially examined with a loess smoother and found to be adequately approximated by a linear fit in most cases.

In order to explore additive effects, a stepwise general additive model (GAM), incorporating all variables, was performed for both the bottom and top of the DSL. The stepwise GAM runs forward and backward at each step. Starting from the null model, the term with the lowest p-value is introduced, and then any terms with a p-value beyond a threshold are removed, before considering the next term.

3. Results

3.1. Lower DSL boundary

Results from the single variable regression analyses for lower boundary depth are illustrated in Fig. 3. The DSL lower boundary depth exhibited a significant positive correlation with the irradiance index for only the nearshore region ($p < 0.01$). The lower boundary depth was significantly correlated with the depth of 0.75 ml l^{-1} oxygen concentration for both regions (Nearshore/CC: $p < 0.001$, Offshore, $p < 0.05$), with no difference in the slopes. The 7.5 °C isotherm was not significantly correlated with the lower boundary depth ($p > 0.10$). The results of the stepwise General Additive Model (GAM) were slightly incongruent with the single variable outcome, with oxygen ($p < 0.001$) and, to a lesser extent, temperature ($p < 0.05$) contributing significantly to the response variable, but not light (Table 2a).

3.2. Upper boundary

Single variable regression analyses for upper boundary depth are illustrated in Fig. 4. The DSL upper boundary depth exhibited significant positive correlation with both the irradiance index (no significant difference between the two regions) and the depth of the 2.0 ml l^{-1} oxygen isopleths ($p < 0.001$ for both regions), with different fits for the offshore and nearshore regions. The upper boundary depth exhibited a significant correlation with the 8.5 °C isotherm only for the offshore region ($p < 0.01$), where it explained only 16% of the variance. Results of the GAM were in agreement with the single variable results, with oxygen ($p < 0.001$), irradiance index ($p < 0.001$), and to a lesser extent, temperature ($p < 0.05$) contributing significantly to predicting the depth of the DSL upper boundary (Table 2b).

Table 2
Results of Stepwise General Additive Model explaining: (A) lower boundary depth as a function of the three explanatory variables (model: $y = 1 + x2 + x3$, $n = 169$, $r^2 = 0.21$, $F = 21.4$, $p < 0.001$), and (B) upper boundary depth as a function of three explanatory variables (model: $y = 1 + x1 + x2 + x3$, $n = 130$, $r^2 = 0.56$, $F = 54.2$, $p < 0.001$). (SE = standard error, $t = t$-statistic, $p = p$-value).

(A)	Estimate	SE	t	p
Intercept	324.93			
Irradiance Index (E m^{-2} d^{-1})	1.177	0.658	1.79	> 0.05
Depth of 0.75 ml l^{-1} [O_2] isopleth	0.377	0.059	6.41	< 0.001
Depth of 7.5 °C isotherm	0.151	0.069	2.17	< 0.05
(B)				
Intercept	20.85			
Irradiance Index (E m^{-2} d^{-1})	4.019	0.924	4.350	< 0.001
Depth of 2.0 ml l^{-1} [O_2] isopleth	0.556	0.095	5.940	< 0.001
Depth of 8.5 °C isotherm	0.222	0.104	2.135	< 0.05

4. Discussion

Our algorithm allowed us to define the boundaries of the DSL at a much higher resolution than permissible by depth-stratified trawl sampling, providing insights into the sensitivity of the community to relatively small changes in their environment.

4.1. Bottom boundary

The occurrence of a distinct lower DSL boundary in the southern California Current Ecosystem at depths shallower than in regions that lack an OMZ (Chapman and Marshall, 1966; Williams and Koslow, 1997; Bianchi et al., 2013) suggests that most of the southern California mesopelagic community is bounded by an ecological threshold in the environment. Although a diverse group of metazoans has been found to reside within OMZ cores, this occurs primarily in regions with very shallow OMZs (e.g. the Arabian Sea, eastern tropical Pacific, Humboldt Current, etc.) (Holton, 1969; Childress and Nygaard, 1973; Luo et al., 2000; Cornejo and Koppelmann, 2006; Seibel and Drazen, 2007; Wishner et al., 2008; Karuppasamy et al., 2010; Maas et al., 2014), where diel vertical migrations to mesopelagic depths to avoid visually-orienting predators is only possible by migrating into the OMZ and entering a state of metabolic suppression in the day and re-oxygenating in near-surface waters at night (Seibel et al., 2012, 2014; Maas et al., 2012). Our results suggest that the majority of the pelagic fish biomass in the CCE, where the core of the OMZ is

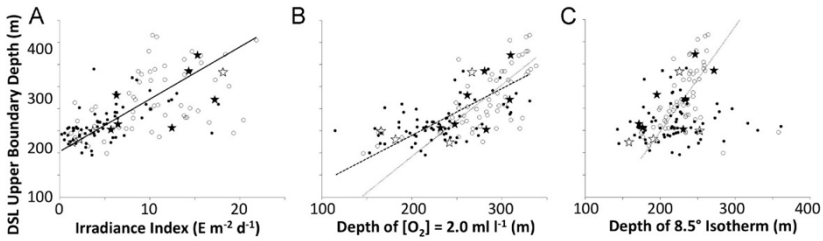

Fig. 4. Relationships between the depth of the upper boundary of the DSL and each of the four predictor variables. Irradiance is a continuous measurement, while the oxygen and temperature variables are discrete depths. Closed circles represent nearshore and core California Current stations and open circles represent offshore-associated stations. Stars indicate locations where deep (~500 m) MOHT trawls were conducted, with open and closed indicating the two characteristic species assemblages. Black broken lines are fitted to nearshore/CC stations, and the grey broken lines are fitted to the offshore stations. Solid black lines are fitted to the full dataset. (A) Irradiance Index ($y = 11.83x + 152.9$, $r^2 = 0.39$), (B) Depth of [O_2] = 2.0 ml l^{-1} isopleth (Nearshore/CC: $y = 1.058x - 22.1$, $r^2 = 0.29$, Offshore: $y = 1.623x - 183.9$, $r^2 = 0.48$), and (C) Depth of the 8.5° isotherm (Nearshore/CC: NS, Offshore: $y = 2.372x - 277.9$, $r^2 = 0.16$).

at ~600–800 m depth, is constrained primarily by a minimum oxygen threshold.

4.2. Upper boundary

Irradiance and oxygen concentration (depth of the 2.0 ml l^{-1} isopleth) were strong predictors of the upper boundary of the DSL for both the single variable regressions and the GAM, and there was a weaker relationship with temperature. A light threshold as predictor of DSL depths is consistent with the view that the animals of the DSL are taking refuge in dark water (Lampert, 1993; De Meester et al., 1999). A relationship between light and the DSL depth has been observed in previous studies (e.g., Tont, 1975), but the relatively strong predictive power of an oxygen threshold as an upper boundary to the DSL was somewhat unexpected. There is no obvious physiological explanation for why the community would need to remain below a given oxygen concentration, although entering a state of metabolic suppression for periods of time may be an adaptive strategy to confer significant energy savings (Seibel et al., 2014). It is likely that the mesopelagic fishes are taking refuge not only in the darkness of mesopelagic waters, but in areas with low oxygen concentrations, such as the CCE, midwater depths are also too hypoxic for their more active predators (as proposed by Bianchi et al., 2013). Supporting this interpretation, the oxygen concentrations at the upper DSL are slightly below levels tolerable to epipelagic visually-oriented predators, such as sharks (1.7 ml l^{-1}, Nasby-Lucas et al., 2009), billfishes (<3.5 ml l^{-1}, Prince and Goodyear, 2006) and skipjack and yellowfin tunas (<3.5 ml l^{-1}, Ingham et al., 1977; Cayré, 1991).

For many of the environmental variables, the DSLs of the offshore and nearshore assemblages responded similarly. However the relationships between the DSL upper boundary depths and both oxygen and temperature were significantly different between nearshore and offshore regions, with temperature only acting as a significant predictor for the DSL upper depth offshore. Given that the upper boundary likely experiences more frequent environmental variability in the nearshore region than offshore (Bograd et al., 2008; Send and Nam, 2012), the DSL may be better adapted there to this variability. Ongoing collection of acoustic backscatter data in both nearshore and offshore regions over multiple years and seasons would help to resolve the mechanism leading to these observed regional differences.

Our study suggests that vertical distributions of DSL organisms in the CCE are limited by midwater oxygen concentrations. This is in agreement with some previous work in the CCE (Urmy et al., 2012), French Polynesia (Bertrand et al., 1999, 2002), and globally (Bianchi et al., 2013), and there is evidence that midwater hypoxia limits distributions of many fish taxa, such as larval fish in the Benguela current (Ekau and Verheye, 2005), Peruvian anchovetta (Bertrand et al., 2010), and billfishes and tuna in the Eastern Tropical Pacific (Stramma et al., 2011). Yet DSLs have been detected acoustically within the OMZ cores of the Arabian Sea (Kinzer et al., 1993; Karuppasamy et al., 2010), and myctophids and other midwater fishes have been collected within OMZs of the Arabian Sea (Karuppasamy et al., 2010), Eastern Tropical Pacific (Maas et al., 2014), and Humboldt Current (Cornejo and Koppelmann, 2006), regions where the OMZ is shallower than in the CCE (on the order of 100 m). Mesopelagic taxa in those areas appear to have adapted to a shallow OMZ by evolving the ability to enter the OMZ during the diel period, undergoing marked metabolic suppression, and migrating at night into near-surface waters to feed and re-oxygenate (Seibel, 2011).

Thin biomass peaks of zooplankton at specific oxygen levels of oxyclines have been revealed by depth-stratified net sampling (Wishner et al., 2008, 2013), and likely result from an advantage of occupying waters at the edge of a species' hypoxia tolerance. There may be similar zonation of fishes within the CCE DSL that we were unable to detect with our methods. Assemblage-level biomass peaks could potentially be distinguished through more sophisticated algorithms (Cade and Benoit-Bird, 2014), and taxon-specific peaks revealed through depth-stratified trawl sampling. The Eastern Tropical Pacific and Arabian Sea OMZs span a greater depth range, are shallower, and have lower minimum oxygen concentrations than the CCE OMZ, which may lead to different dynamics in habitat utilization of inhabitant organisms. The OMZ in the CCE may be deep enough that mesopelagic fish can simultaneously avoid both predation risk and hypoxia, but in other areas must make a trade-off to avoid predation at the expense of oxygen availability. Paired trawl and acoustic sampling over a range of OMZ depths would shed some light on the discrepancies between our findings and other studies.

Ocean acidification is a compounding stressor on organisms in hypoxic waters because reduced pH decreases the affinity of proteins such as hemoglobin for oxygen (Seibel and Walsh, 2001). As oxygen concentration and pH covary (Alin et al., 2012), this may be especially problematic for organisms already living at the limits of their pH and oxygen tolerances. While we acknowledge that the shift in DSL depths attributed here to oxygen variability may in part be a response to changes in pH, it is not possible to decouple the oxygen and pH variability, so we rely on evidence that mobile fishes are not as susceptible to low pH as to changes in oxygen availability (Melzner et al., 2009; Kroeker et al., 2013) to assume that they are responding primarily to respiratory demands.

4.3. Predicting changes to DSL upper and lower boundary depths due to ocean deoxygenation and increased light attenuation

Oxygen concentrations and irradiance levels are the strongest predictors of the DSL depth in our study region. Dissolved oxygen levels in the ocean have been declining globally (Helm et al., 2011). The North Pacific region is experiencing some of the greatest change in oxygen concentrations, at least some of which is due to decadal-scale climate variability (McClatchie et al., 2010; Deutsch, 2005; Duetsch et al., 2011, 2014). The average decline in oxygen concentration in the southern CCE from the mid-1980s to present was 21% (Bograd et al., 2008, 2014), and global climate models predict a further decline in midwater oxygen concentration of ~20–40% over the coming century or so due to climate change (Sarmiento et al., 1998; Matear and Hirst, 2003; Shaffer et al., 2009). By extrapolating from a linear relationship between the two variables, Koslow et al. (2013) find that midwater fish biomass would approach zero with a further ~30% decline in midwater oxygen concentrations. This implies that midwater fishes will either have to modify their behavior (i.e. descend into the OMZ during the daytime and undergo metabolic suppression) or they will be replaced by a fauna that does. Light attenuation in the CCE has increased over the last half century (Aksnes and Ohman, 2009). Although DSL depths have been found to respond to midwater irradiance levels (e.g., Tont, 1975), no studies have explored the effects of the decreased irradiance on distributions of mesopelagic fauna.

In order to explore how the vertical range of the DSL may be altered by continued deoxygenation and changes to light attenuation, we used estimates of annual rates of change in the variables that had the highest predictive power for DSL upper and lower boundary depths, and substituted these values into equations determined by the present study that relate DSL upper and lower boundary depths to the same environmental variables. For these projections we consider only the variables with the strongest and most consistent effects on the bottom boundary (dissolved oxygen) and upper boundary (dissolved oxygen and irradiance).

Bottom

The maximum shoaling rate of the 0.75 ml l^{-1} oxygen concentration depth in the southern CCE from 1984 to 2013 (calculated as per Bograd et al., 2008) is

$$\frac{\Delta Z_{0.75}}{\Delta t} = 2.74 \text{ m y}^{-1}$$

(This excludes one anomalously high rate of 4.46 m y^{-1} in the Santa Barbara basin). The slope relating DSL bottom depth and the 0.75 ml l^{-1} oxygen isopleths (see Fig. 3b legend) is

$$\frac{\Delta Z_{DSL\_Bot}}{\Delta Z_{0.75}} = 0.84 \text{ m m}^{-1}$$

We multiply these terms to arrive at a maximum shoaling of the bottom of the DSL

$$\frac{\Delta Z_{DSL\_Bot}}{\Delta t} = \frac{\Delta Z_{0.75}}{\Delta t} * \frac{\Delta Z_{DSL\_Bot}}{\Delta Z_{0.75}} = 2.74 \text{ m y}^{-1} * 0.84 \text{ m m}^{-1} = 2.3 \text{ m y}^{-1}$$

Top

Since oxygen and irradiance are the primary drivers of the upper boundary depth, we explore the effects of each in isolation in order to determine how each may shift the depth of the upper DSL boundary. The maximum shoaling rate of the 2.0 ml l^{-1} oxygen concentration depth in the southern CCE from 1984 to 2013 (calculated as per Bograd et al., 2008) is

$$\frac{\Delta Z_{2.0}}{\Delta t} = 3.98 \text{ m y}^{-1}$$

The slope relating DSL upper depth and the 2.0 ml l^{-1} oxygen isopleths (see Fig. 4b legend) is

$$\frac{\Delta Z_{DSL\_Top}}{\Delta Z_{2.0}} = 1.06 \text{ m m}^{-1}$$

We multiply these terms to arrive at a maximum shoaling of the top of the DSL

$$\frac{\Delta Z_{DSL\_Top}}{\Delta t} = \frac{\Delta Z_{2.0}}{\Delta t} * \frac{\Delta Z_{DSL\_Top}}{\Delta Z_{2.0}} = 3.98 \text{ m y}^{-1} * 1.06 \text{ m m}^{-1} = 4.2 \text{ m y}^{-1}$$

Note that we used the regression derived for the nearshore region in this calculation, as the maximum shoaling rates of hypoxic waters is in the nearshore region.

To estimate the potential shift in upper DSL boundary depth due to changes in irradiance, we first rearrange the II equation (Section 2.4.1).

$$k_{490} = \frac{-\ln(II / PAR)}{30}$$

For simplicity, we assume that variation in II is due only to changes in k_{490}, and use a constant PAR value for the calculations

$PAR = 100\ E\ \text{m}^{-2}\ \text{d}^{-1}$

Given the range of the Irradiance Index values in our dataset, $1.118 \times 10^{-6}\ E\ \text{m}^{-1}\ \text{d}^{-1}$ at DSL upper depth of 348 m to 21.852 $E\ \text{m}^{-1}\ \text{d}^{-1}$ at 187 m, we calculate a concurrent k_{490} range

$$min\ k_{490} = \frac{-\ln(II / PAR)}{30} = \frac{-\ln(1.118 \times 10^{-6}\ E\ \text{m}^{-1}\ \text{d}^{-1} / 100\ E\ \text{m}^{-2}\ \text{d}^{-1})}{30} = 0.0507 \text{ m}^{-1}$$

$$max\ k_{490} = \frac{-\ln(II / PAR)}{30} = \frac{-\ln(21.852\ E\ \text{m}^{-1}\ \text{d}^{-1} / 100\ E\ \text{m}^{-2}\ \text{d}^{-1})}{30} = 0.610 \text{ m}^{-1}$$

We then calculate the change in DSL upper depth per unit of k_{490}

$$\frac{\Delta Z_{DSL\_Top}}{\Delta k_{490}} = \frac{348 \text{ m} - 187 \text{ m}}{0.0507 \text{ m}^{-1} - 0.610 \text{ m}^{-1}} = -288 \text{ m}^2$$

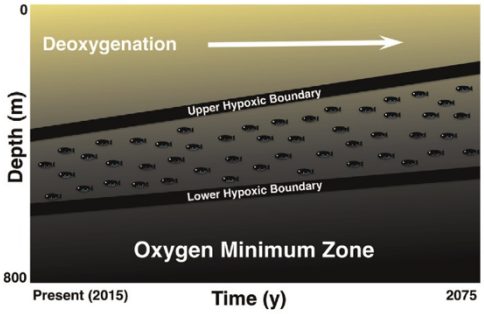

Fig. 5. Schematic of changes to deep scattering layer depths under conditions of continued ocean deoxygenation and increased light attenuation over the next 50 years. We assume that the current rates of change in oxygen concentration and irradiance and the response rates of the DSL upper and lower boundaries to these variables are constant over the time period. Relative light levels are represented by the yellow to black gradient, and exhibit a slight shoaling. The hypoxic boundaries represented are approximately 0.5 ml l^{-1} (lower) and 2.0 ml l^{-1} (upper). The upper boundary is predicted to shoal at a rate faster than the lower boundary, effectively expanding the width of the deep scattering layer. (For interpretation of the references to color in this figure legend, the reader is referred to the web version of this article.)

From 1949 to 2007, the light attenuation coefficient increased by an estimated $9.84 \times 10^{-4}\ \text{m}^{-1}\ \text{y}^{-1}$ (Aksnes and Ohman, 2009, Table 4), consistent with increases in nutrients and chlorophyll concentrations (Bograd et al., 2014). To obtain the annual shoaling rate of the DSL upper boundary due to changes in light attenuation, we multiply these terms together:

$$\frac{\Delta Z_{DSL\_Top}}{k_{490}} * \frac{\Delta k_{490}}{\Delta t} = -288 \text{ m}^2 * 9.84 \times 10^{-4}\ \text{m}^{-1}\ \text{y}^{-1} = 0.274 \text{ m y}^{-1}$$

This value implies that the effect on the upper boundary due to changing irradiance is considerably smaller than the effect due to changing dissolved oxygen, and is therefore unlikely to contribute much to long-term changes in the upper boundary depth.

According to these calculations, the bottom oxygen boundary of the DSL is expected to shoal with continued ocean deoxygenation, consistent with our expectation. Still, the upper boundary will shoal faster than the lower boundary due to changes in the dissolved oxygen concentration, suggesting that there will be expansion of the daytime vertical habitat available to mesopelagic fishes (Fig. 5). However, different types of predators may be differentially limited by either hypoxia or irradiance, and further studies on trophic linkages and predator behavior and habitat use is needed to be certain how the varying effects of shoaling hypoxia and shoaling darkness will ultimately affect the mesopelagic fauna.

Our irradiance index is a relatively coarse proxy for mesopelagic light levels at each station. Neither the effects of differential shading due to plankton patchiness nor midwater bioluminescence heave been considered here. The ability to determine the DSL response to light levels would be enhanced by direct in situ light measurements (e.g., Haag et al., 2014). Furthermore, there were some segments of the backscatter data where the algorithm failed to detect an upper DSL boundary due to heightened backscatter throughout the upper water column. If we instead consider the sea surface as the absolute limit for upper boundary of habitat available to mesopelagic fishes, we find that the shoaling of the hypoxic boundary does in fact lead to a decline in total available habitat. With a significant portion of the mesopelagic community

moving into shallower waters, carbon transport to the deep sea will likely be impacted.

Our predictions for future changes in DSL depth and breadth may be biased by assumptions made in order to estimate these responses. We assumed that recent trends in changes to HB and euphotic zone depths will continue in the same direction and at the same rates. However, McClatchie et al. (2010) showed that the direction of change in HB depth has reversed before, although global climate models generally predict continued deoxygenation into the foreseeable future (Matear and Hirst, 2003; Shaffer et al., 2009). Further, the mechanism leading to the changes in euphotic depth is not well understood (Asknes and Ohman, 2009), so it is unclear whether the observed shoaling trend from 1949 to 2007 will continue. Upwelling rates are expected to continue to increase (Sydeman et al., 2014), which would bring more nutrients and lower oxygen into the surface waters, initially decreasing both oxygen levels and irradiance.

There is no obvious seasonal pattern in the depths of the oxygen variables for the time period of this study, however there was a lot of variation in the depths of both the 0.75 (260–513 m) and 2.0 ml l^{-1} (115–350 m) isopleths throughout the full dataset, as well as within any given station. For example, at a northern nearshore station, 80.55, the 0.75 ml l^{-1} oxygen depth ranged from 362 to 448 m and the 2.0 ml l^{-1} depth from 123 to 184 m. At the southern offshore corner of the CalCOFI grid, station 93.120, the 0.75 ml l^{-1} isopleth ranged from 424 to 471 m, and the 2.0 ml l^{-1} level from 288 to 319 m. Given that this within-station variation is greater than that predicted with long-term climatological change, we expect there to be shifts in use of the vertical habitat on seasonal time scales, and even on hourly to daily time scales such as are documented by permanently-mounted echosounders (Urmy et al., 2012). Long-term monitoring with higher temporal sampling (e.g., a bottom-mounted echosounder) would resolve the response time of the DSL fish habitat use to changes in oxygen profiles.

Our results have implications for the availability of suitable habitat for mesopelagic animals as the oxygen levels in the ocean decline. This study was limited to the southern California Current region, however the questions of how habitats of mesopelagic fishes are affected by environmental change over time and space should be further explored throughout the ocean in order to better understand what these changes will mean for mesopelagic communities in other regions. Over the range of the CalCOFI sampling region there is a relatively large range of light levels from oligotrophic gyre water to the very productive nearshore upwelling region (Aksnes and Ohman, 2009). In contrast, while there is variation in the range of OMZ depths, the range in the CalCOFI region is only a subset of the range of OMZ depths that exist throughout the global ocean (Stramma et al., 2011). The responses of the DSL should be determined in regions with both shallower and deeper OMZs as well as in areas that lack an OMZ entirely.

This is the first study that we know to investigate the differential responses of the upper and lower boundaries of the DSL to key environmental variables. Tont (1975) found a correlation between light and mean DSL depth, Bianchi et al. (2013) used the location of peak backscatter to identify as DVM depth, and Hazen and Johnston (2010) detected a relationship between integrated water column backscatter and the depth of the oxycline and thermocline. Powell and Ohman (2015) identified a positive relationship between the amplitude of diel vertical migration and euphotic zone depth. The high spatial and temporal sampling provided by the CalCOFI surveys and the overlap of CTD stations with bioacoustic sampling has provided a unique opportunity to explore the responses of the DSL to environmental variability. However, with only three years of bioacoustic data available, we could not resolve responses of the DSL depth over time, and instead had to rely on a space for time exchange, using the natural variation in environmental properties over space as a proxy for future climate change.

Ongoing sampling by the methods outlined here is necessary in order to access how DSL depth and vertical ranges change with natural and human-induced climatic changes. Further refinements to these methods that would assist in better resolving the response of the DSL distribution to environmental variability include obtaining real-time measurements of mesopelagic light levels, collecting CTD data to at least the bottom depth of the DSL, and conducting depth-stratified sampling to ascertain the differential responses of various taxa of fishes that constitute the DSL.

Acknowledgements

The Gordon and Betty Moore Foundation provided funding for the EK60 and MOHT. CalCOFI shiptime for midwater trawling and acoustic calibration was provided by the NSF-funded California Current Ecosystem LTER program. We thank the captains, crew, and CalCOFI science parties of the R/V New Horizon. J. Liu operated and maintained the EK60 acoustic system and cleaned the acoustic data. P. Davison, A. Lara-Lopez, C. Allen, K. Blincow, J. Liu, and L. Shiosaka collected fishes. T. Au, K. Blincow, T. Castellano, B. DeWes, A. Miller, X. Rojas-Rocha, J. Xie and J. Chang assisted with the identification and measurement of the trawl catches. M. Kahru provided irradiance data, and G. Mitchell advised us on the irradiance estimations. S. Bograd assisted with calculating changes in oxygen depths. We especially thank M.D. Ohman for guidance on data analysis and manuscript preparation.

Appendix A. Supporting information

Supplementary data associated with this article can be found in the online version at http://dx.doi.org/10.1016/j.dsr.2015.06.006. These data include Google maps of the most important areas described in this article.

References

Alin, S.R., Feely, R.A., Dickson, A.G., Hernández-Ayón, J.M., Juranek, L.W., Ohman, M. D., Goericke, R., 2012. Robust empirical relationships for estimating the carbonate system in the southern California Current System and application to CalCOFI hydrographic cruise data (2005-2011). J. Geophys. Res. 117, C05033. doi:10.1029/2011JC007511.

Aksnes, D.L., Ohman, M.D., 2009. Multi-decadal shoaling of the euphotic zone in the southern sector of the California current system. Limnol. Oceanogr. 54, 1272–1281.

Benfield, M.C., Lavery, A.C., Wiebe, P.H., Greene, C.H., Stanton, T.K., Copley, N.J., 2003. Distributions of physonect siphonulae in the Gulf of Maine and their potential as important sources of acoustic scattering. Can. J. Fish. Aquat. Sci. 60, 759–772.

Bertrand, A., Ballón, M., Chaigneau, A., 2010. Acoustic observation of living organisms reveals the upper limit of the oxygen minimum zone. PLoS One 5, e10330.

Bertrand, A., Bard, F.-X., Josse, E., 2002. Tuna food habits related to the micronekton distribution in French Polynesia. Mar. Biol. 140, 1023–1037.

Bertrand, A., LeBorgne, R., Josse, E., 1999. Acoustic characterization of micronekton distribution in French Polynesia. Mar. Ecol. Prog. Ser 191, 127–140.

Bianchi, D., Galbraith, E.D., Carozza, D.A., Mislan, K., Stock, C.A., 2013. Intensification of open-ocean oxygen depletion by vertically migrating animals. Nat. Geosci. 6, 545–548.

Bograd, S.J., Buil, M.P., Lorenzo, E., Di, Castro, C.G., Schroeder, I.D., Goericke, R., Anderson, C.R., Benitez-Nelson, C., Whitney, F.A., 2014. Changes in source waters to the Southern California Bight. Deep Sea Res. Part II Top. Stud. Oceanogr.

Bograd, S.J., Castro, C.G., Lorenzo, E., Di, Palacios, D.M., Bailey, H., Gilly, W., Chavez, F. P., 2008. Oxygen declines and the shoaling of the hypoxic boundary in the California current. Geophys. Res. Lett. 35, 1–6.

Cade, D., Benoit-Bird, K., 2014. An automatic and quantitative approach to the detection and tracking of acoustic scattering layers. Limnol. Oceanogr. Methods 12, 742–756.

Cayré, P., 1991. Behaviour of yellowfin tuna (Thunnus albacares) and skipjack tuna

(Katsuwonus pelamis) around fish aggregating devices (FADs) in the Comoros Islands as determined by ultrasonic tagging. Aquat. Living Resour. 4, 1–12.
Chan, F., Barth, J., Lubchenco, J., Kirincich, A., Weeks, H., Peterson, W., Menge, B., 2008. Emergence of anoxia in the California current large marine ecosystem. Science 319, 920.
Chapman, R., Marshall, J., 1966. Reverberation from deep scattering layers in the Western North Atlantic. J. Acoust. Soc. Am. 40, 405–411.
Childress, J.J., Nygaard, M.H., 1973. The chemical composition of midwater fishes as a function of depth of occurrence off southern California. Deep Sea Res. 20, 1093–1109.
Childress, J., Seibel, B., 1998. Life at stable low oxygen levels: adaptations of animals to oceanic oxygen minimum layers. J. Exp. Biol. 201, 1223–1232.
Clarke, M.R.B., 1980. Biometrika 67 (2), 441–446.
Cornejo, R., Koppelmann, R., 2006. Distribution patterns of mesopelagic fishes with special reference to Vinciguerria lucetia Garman 1899 (Phosichthyidae: Pisces) in the Humboldt Current Region off Peru. Mar. Biol. 149, 1519–1537.
Crawford, W.R., Peña, M.A., 2013. Declining oxygen on the British Columbia continental shelf. Atmos.–Ocean 51, 88–105.
Davison, P.C., Koslow, J.A., Kloser, R.J., 2015a. Acoustic biomass estimation of mesopelagic fish: backscattering from individuals, populations, and communities. ICES J. Mar. Sci.
Davison, P., Lara-Lopez, A., Koslow, J.A., 2015b. Mesopelagic fish biomass in the southern California current ecosystem. Deep Sea Res. II 112, 129–142.
Davison, P.C., Checkley, D.M., Koslow, J.A., Barlow, J., 2013. Carbon export mediated by mesopelagic fishes in the northeast Pacific Ocean. Prog. Oceanogr. 116, 14–30.
De Meester, L., Dawidowics, P., Gool, E., Loos, C., 1999. Tollrian, R., Harvell, C. (Eds.), In: The ecology and evolution of inducible defenses. Princeton University Press, Princeton, p. 160.
Deutsch, C., 2005. Fingerprints of climate change in North Pacific oxygen. Geophys. Res. Lett. 32, L16604.
Deutsch, C., Emerson, S., Thompson, L., 2006. Physical–biological interactions in North Pacific oxygen variability. J. Geophys. Res. 111, 1–16.
Deutsch, C., Berelson, W., Thunell, R., Weber, T., Tems, C., McManus, J., Crusius, J., Ito, T., Baumgartner, T., Ferreira, V., Mey, J., Geen, A. van, 2014. Oceanography: centennial changes in North Pacific anoxia linked to tropical trade winds. Science 345, 665–668.
Deutsch, C., Brix, H., Ito, T., Frenzel, H., Thompson, L., 2011. Climate-Forced Variability of Ocean Hypoxia. Science 333, 336–339, doi:10.1126/science.1202422.
Devine, J.A., Baker, K.D., Haedrich, R.L., 2006. Deep-sea fishes qualify as endangered. Nature 439 29.
Foote, G., Knudsen, P., Vestnes, G., MacLennan, D., Simmonds, E., 1987. Calibration of acoustic instruments for fish density estimation: a practical guide, ICES Cooperative Research Report. Copenhagen.
Ekau, W., Verheye, H., 2005. Influence of oceanographic fronts and low oxygen on the distribution of ichthyoplankton in the Benguela and southern Angola currents. African J. Mar. Sci. 27, 629–639.
Frank, T., Widder, E., 2002. Effects of a decrease in downwelling irradiance on the daytime vertical distribution patterns of zooplankton and micronekton. Mar. Biol. 140, 1181–1193.
Frouin, R., Franz, B.A., Werdell, P.J., 2003. The SeaWiFS PAR product. In: Hooker, S.B., Firestone, E.R., Algorithm Updates for the Fourth SeaWiFS Data Reprocessing. NASA/TM-2003-206892, 22 p.
Gilly, W.F., Beman, J.M., Litvin, S.Y., Robison, B.H., 2013. Oceanographic and biological effects of shoaling of the Oxygen Minimum Zone. Ann. Rev. Mar. Sci., 1–28.
Godø, O., Patel, R., Pedersen, G., 2009. Diel migration and swimbladder resonance of small fish: some implications for analyses of multifrequency echo data. ICES J. Mar. Sci. 66, 1143–1148.
Grantham, B.A., Chan, F., Nielsen, K.J., Fox, D.S., Barth, J.A., Huyer, A., Lubchenco, J., Menge, B.A., 2004. Upwelling-driven nearshore hypoxia signals ecosystem and oceanographic changes. Nature 429, 749–754.
Haag, J.M., Roberts, P.L.D., Papen, G.C., Jaffe, J.S., Li, L., Stramski, D., 2014. Deep-sea low-light radiometer system. Opt. Express 22, 30074–30091.
Hazen, E.L., Johnston, D.W., 2010. Meridional patterns in the deep scattering layers and top predator distribution in the central equatorial Pacific. Fish. Oceanogr. 19, 427–433.
Helly, J., Levin, L., 2004. Global distribution of naturally occurring marine hypoxia on continental margins. Deep Sea Res. Part I Oceanogr. Res. Pap. 51, 1159–1168.
Helm, K.P., Bindoff, N.L., Church, J.A., 2011. Observed decreases in oxygen content of the global ocean. Geophys. Res. Lett. 38.
Holton, A.A., 1969. Feeding behavior of a vertically migrating lanternfish. Pac. Sci. 23, 325–331.
Ingham, M.C., Cook, S.K., Hausknecht, K.A., 1977. Oxycline characteristics and skipjack tuna distribution in the southeastern tropical Atlantic. Fish. Bull., 75.
Kahru, M., Jacox, M.G., Lee, Z., Kudela, R.M., Manzano-Sarabia, M., Mitchell, B.G., 2014. Optimized multi-satellite merger of primary production estimates in the California Current using inherent optical properties. J. Mar. Syst.
Kampa, E.M., Boden, B.P., 1954. Submarine illumination and the twilight movements of a sonic scattering layer. Nature 174, 869–871.
Karstensen, J., Stramma, L., Visbeck, M., 2008. Oxygen minimum zones in the eastern tropical Atlantic and Pacific oceans. Prog. Oceanogr. 77, 331–350.
Karuppasamy, P.K., Muraleedharan, K.R., Dineshkumar, P.K., Nair, M., 2010. Distribution of mesopelagic micronekton in the Arabian Sea during the winter monsoon. Indian J. Mar. Sci. 39, 227–237.
Keeling, R.F., Körtzinger, A., Gruber, N., 2010. Ocean deoxygenation in a warming world. Ann. Rev. Mar. Sci. 2, 199–229.
Kinzer, J., Böttger-Schnack, R., Schulz, K., 1993. Aspects of horizontal distribution and diet of myctophid fish in the Arabian Sea with reference to the deep water oxygen deficiency. Deep Sea Res. Part II Top. Stud. Oceanogr. 40, 783–800.
Koslow, J.A., Goericke, R., Watson, W., 2013. Fish assemblages in the Southern California Current: relationships with climate, 1951-2008. Fish. Oceanogr. 22, 207–219.
Kloser, R.J., Ryan, T., Sakov, P., Williams, A., Koslow, J.A., 2002. Species identification in deep water using multiple acoustic frequencies. Can. J. Fish. Aquat. Sci. 59, 1065–1077.
Koslow, J., Goericke, R., Lara-Lopez, A., Watson, W., 2011. Impact of declining intermediate-water oxygen on deepwater fishes in the California current. Mar. Ecol. Prog. Ser. 436, 207–218.
Kroeker, K.J., Kordas, R.L., Crim, R., Hendriks, I.E., Ramajo, L., Singh, G.S., Duarte, C. M., Gattuso, J.-P., 2013. Impacts of ocean acidification on marine organisms: quantifying sensitivities and interaction with warming. Glob. Chang Biol. 19, 1884–1896.
Lampert, W., 1993. Ultimate causes of diel vertical migration of zooplankton: new evidence for the predator avoidance hypothesis. Arch. Hydrobiol./Beih Ergeb Limnol. 39, 79–88.
Lavery, A.C., Wiebe, P.H., Stanton, T.K., Lawson, G.L., Benfield, M.C., Copley, N., 2007. Determining dominant scatterers of sound in mixed zooplankton populations. J. Acoust. Soc. Am. 122, 3304–3326.
Levin, L.A., 2003. Oxygen minimum zone benthos: adaptation and community response to hypoxia. Oceanogr. Mar. Biol. Annu. Rev. 41, 1–45.
Li, L., Stramski, D., Reynolds, R.A., 2014. Characterization of the solar light field within the ocean mesopelagic zone based on radiative transfer simulations. Deep Sea Res. Part I Oceanogr. Res. Pap. 87, 53–69.
Luo, J., Ortner, P.B., Forcucci, D., Cummings, S.R., 2000. Diel vertical migration of zooplankton and mesopelagic fish in the Arabian Sea. Deep Sea Res. II 47, 1451–1473.
Maas, A.E., Frazar, S.L., Outram, D.M., Seibel, B.A., Wishner, K.F., 2014. Fine-scale vertical distribution of macroplankton and micronekton in the Eastern Tropical North Pacific in association with an oxygen minimum zone. J. Plankton Res. 0, 1–19.
Maas, A.E., Wishner, K.F., Seibel, B.A., 2012. The metabolic response of pteropods to acidification reflects natural CO_2-exposure in oxygen minimum zones. Biogeosciences 9, 747–757.
Matear, R.J., Hirst, A., 2003. Long-term changes in dissolved oxygen concentrations in the ocean caused by protracted global warming. Glob. Biogeochem. Cycles, 17.
McClatchie, S., Goericke, R., Cosgrove, R., Auad, G., Vetter, R., 2010. Oxygen in the Southern California Bight: Multidecadal trends and implications for demersal fisheries. Geophys. Res. Lett. 37, 1–5.
Melzner, F., Gutowska, M.A., Langenbuch, M., Dupont, S., Lucassen, M., Thorndyke, M.C., Bleich, M., Pörtner, H.-O., 2009. Physiological basis for high CO2 tolerance in marine ectothermic animals: pre-adaptation through lifestyle and ontogeny. Biogeosciences 6, 2313–2331.
Nasby-Lucas, N., Dewar, H., Lam, C.H., Goldman, K.J., Domeier, M.L., 2009. White shark offshore habitat: a behavioral and environmental characterization of the eastern Pacific shared offshore foraging area. PLoS One 4, e8163.
Oozeki, Y., Hu, F., Kubota, H., Sugisaki, H., Kimura, R., 2004. Newly designed quantitative frame trawl for sampling larval and juvenile pelagic fish. Fish. Sci. 70, 223–232.
Pakhomov, E., Yamamura, O., 2010. Report of the advisory panel on micronekton sampling inter-calibration experiment. PICES Scientific Report No. 38. Sidney, BC Canada.
Paulmier, A., Ruiz-Pino, D., 2009. Oxygen minimum zones (OMZs) in the modern ocean. Prog. Oceanogr. 80, 113–128.
Powell, J.R., Ohman, M.D., 2015. Covariability of zooplankton gradients with glider-detected density fronts in the Southern California Current System. Deep Res. Part II Top. Stud. Oceanogr. 112, 79–90.
Prince, E.D., Goodyear, C.P., 2006. Hypoxia-based habitat compression of tropical pelagic fishes. Fish. Oceanogr. 15, 451–464.
Rabalais, N.N., Turner, R.E., Wiseman, W.J., 2002. Gulf of Mexico Hypoxia, a.k.a. "the Dead Zone". Annu. Rev. Ecol. Syst. 33, 235–263.
Ramirez-Llodra, E., Tyler, P.A., Baker, M.C., Bergstad, O.A., Clark, M.R., Escobar, E., Levin, L.A., Menot, L., Rowden, A.A., Smith, C.R., Dover, C.L. Van, 2011. Man and the last great wilderness: human impact on the deep sea. PLoS One 6, e22588.
Ricker, W.E., 1973. Linear regressions in fishery research. J. Fish. Res. Board Canada 30, 409–434.
Robinson, C., Steinberg, D.K., Anderson, T.R., Arístegui, J., Carlson, C.A., Frost, J.R., Ghiglione, J.-F., Hernández-León, S., Jackson, G.A., Koppelmann, R., 2010. Mesopelagic zone ecology and biogeochemistry – a synthesis. Deep Sea Res. Part II Top. Stud. Oceanogr. 57, 1504–1518.
Robison, B.H., 2009. Conservation of deep pelagic biodiversity. Conserv. Biol. 23, 847–858.
Sarmiento, J., Hughes, T., Stouffer, R., Manabe, S., 1998. Simulated response of the ocean carbon cycle to anthropogenic climate warming. Nature 393, 1–2.
Seibel, B.A., 2011. Critical oxygen levels and metabolic suppression in oceanic oxygen minimum zones. J. Exp. Biol. 214, 326–336.
Seibel, B.A., Häfker, N.S., Trübenbach, K., Zhang, J., Tessier, S.N., Pörtner, H.-O., Rosa, R., Storey, K.B., 2014. Metabolic suppression during protracted exposure to hypoxia in the jumbo squid, *Dosidicus gigas*, living in an oxygen minimum zone. J. Exp. Biol. 217, 2555–2568.
Seibel, B.A., Maas, A.E., Dierssen, H.M., 2012. Energetic plasticity underlies a variable response to ocean acidification in the pteropod, *Limacina helicina* antarctica.

PLoS One 7, e30464.
Seibel, B.A., Drazen, J.C., 2007. The rate of metabolism in marine animals: environmental constraints, ecological demands and energetic opportunities. Philos. Trans. R. Soc. Lond. Ser. B 362, 2061–2078.
Seibel, B.A., Walsh, P.J., 2001. Carbon cycle. Potential impacts of CO2 injection on deep-sea biota. Science 294, 319–320.
Send, U., Nam, S., 2012. Relaxation from upwelling: The effect on dissolved oxygen on the continental shelf. J. Geophys. Res. 117, C04024.
Shaffer, G., Olsen, S.M., Pedersen, J.O.P., 2009. Long-term ocean oxygen depletion in response to carbon dioxide emissions from fossil fuels. Nat. Geosci. 2, 105–109.
Stauffer, B., Gellene, A., Schnetzer, A., Seubert, E., Oberg, C., Sukhatme, G., Caron, D., 2012. An oceanographic, meteorological, and biological "perfect storm" yields a massive fish kill. Mar. Ecol. Prog. Ser. 468, 231–243.
Stramma, L., Johnson, G.C., Sprintall, J., Mohrholz, V., 2008. Expanding oxygen-minimum zones in the tropical oceans. Science 320, 655–658.
Stramma, L., Johnson, G.C., Firing, E., Schmidtko, S., 2010. Eastern Pacific oxygen minimum zones: supply paths and multidecadal changes. J. Geophys. Res. 115, C09011.
Stramma, L., Prince, E.D., Schmidtko, S., Luo, J., Hoolihan, J.P., Visbeck, M., Wallace, D.W.R., Brandt, P., Körtzinger, A., 2011. Expansion of oxygen minimum zones may reduce available habitat for tropical pelagic fishes. Nat. Clim. Change, 1–5.
Sydeman, W.J., García-Reyes, M., Schoeman, D.S., Rykaczewski, R.R., Thompson, S.A., Black, B.A., Bograd, S.J., 2014. Climate change. Climate change and wind intensification in coastal upwelling ecosystems. Science 345, 77–80.
Sverdrup, H.U., 1938. On the explanation of the oxygen minima and maxima in the oceans. ICES J. Mar. Sci. 13, 163–172.
Tont, S.A., 1975. Deep scattering layers: patterns. CalCOFI Rep. 18, 112–117.
Urmy, S.S., Horne, J.K., Barbee, D.H., 2012. Measuring the vertical distributional variability of pelagic fauna in Monterey Bay. ICES J. Mar. Sci. 69, 184–196.
Warren, J., 2001. In situ measurements of acoustic target strengths of gas-bearing siphonophores. ICES J. Mar. Sci. 58, 740–749.
Watanabe, Y.W., Wakita, M., Maeda, N., 2003. Synchronous bidecadal periodic changes of oxygen, phosphate and temperature between the Japan Sea deep water and the North Pacific intermediate water. Geophys. Res. Lett. 30.
Whitney, F.A., Freeland, H.J., Robert, M., 2007. Persistently declining oxygen levels in the interior waters of the eastern subarctic Pacific. Prog. Oceanogr. 75, 179–199.
Williams, A., Koslow, J.A., 1997. Species composition, biomass and vertical distribution of micronekton over the mid-slope region off southern Tasmania, Australia. Mar. Biol. 130, 259–276.
Wishner, K.F., Outram, D.M., Seibel, B.A., Daly, K.L., Williams, R.L., 2013. Zooplankton in the eastern tropical north Pacific: boundary effects of oxygen minimum zone expansion. Deep Sea Res. Part I Oceanogr. Res. Pap. 79, 122–140.
Wishner, K.F., Gelfman, C., Gowing, M.M., Outram, D.M., Rapien, M., Williams, R.L., 2008. Vertical zonation and distributions of calanoid copepods through the lower oxycline of the Arabian Sea oxygen minimum zone. Prog. Oceanogr. 78, 163–191.
Wyrtki, K., 1962. The oxygen minima in relation to ocean circulation. Deep Sea Res. Oceanogr. Abstr. 9, 11–23.

ACKNOWLEDGEMENTS

Chapter 2, in full, is a reprint of the material as it appears in Deep-Sea Research I, 2015, Netburn, A.N., and J.A. Koslow, Elsevier Press, 2015. The dissertation author was the primary investigator and author of this paper.

CHAPTER 3

SURVIVAL IN A DEOXYGENATING OCEAN: EVIDENCE OF REDUCED METABOLIC ACTIVITY IN MESOPELAGIC FISHES IN AN OXYGEN MINIMUM ZONE

3.1 Abstract

Global climate models predict declines in oceanic dissolved oxygen concentrations, which are expected to be particularly severe in some oxygen minimum zone regions. Observed trends of generally declining oxygen concentrations in the California Current Ecosystem over the last several decades support these predictions. Living already in hypoxic waters, mesopelagic fishes in some oxygen minimum zones may be particularly vulnerable to the ocean deoxygenation predicted to accompany climate change in oxygen minimum zones. In order to test the effects of variable midwater oxygen concentrations on their metabolism, we measured the activities of aerobic (Citrate Synthase (CS), Malate Dehydrogenase (MDH)) and anaerobic (Lactate Dehydrogenase (LDH) and Alcohol Dehydrogenase (ADH)) metabolic enzymes in a suite of 20 species of mesopelagic fishes from the families Bathylagidae, Gonostomatidae, Melamphaidae, Myctophidae, Phosichthyidae, and Sternoptychidae collected throughout the southern California Current Ecosystem. Our data provide evidence that there may be overall suppression of metabolic enzyme activity in areas with relatively low oxygen concentrations. However, we did not observe an increased reliance on anaerobic respiration under more hypoxic conditions. Diel vertical migrators had elevated activities of CS, MDH, and LDH compared with the non-migratory mesopelagic residents, and there were some significant differences in enzyme activities among families. Our results suggest that in a future deoxygenating ocean, mesopelagic fishes in the California Current may need to shift vertical and/or horizontal habitat ranges in order to survive, with possible consequences to species diversity, predator-prey interactions, and carbon transport to the deep sea.

3.2 Introduction

Dissolved oxygen concentrations in the ocean have experienced global declines in recent decades (Helm et al. 2011) due to decreased solubility of warming surface waters, increased stratification, and changes to ocean circulation (Sverdrup 1938, Wyrtki 1962, Karstensen et al. 2008). These losses are particularly severe at upper mesopelagic depths of oxygen minimum zones (OMZs), which occur worldwide in eastern boundary currents and tropical (Gilly et al. 2013), and are regions where animals are already living at the edge of their hypoxia tolerance (Seibel 2011b). In the California Current Ecosystem (CCE), the hypoxic boundary has shoaled by as much as 80 m since the 1980s (Bograd et al. 2008, McClatchie et al. 2010), linked to intensification of the California Undercurrent (Bograd et al. 2014). Global climate models predict further expansion of OMZs in both horizontal and vertical extent (Deutsch et al. 2006, 2011b, Shaffer et al. 2009, Keeling et al. 2010), although there is evidence that this trend could reverse in response to weakening tropical trade winds (Deutsch et al. 2014b). Models predict a poleward shift in distributions of many ectotherms due to metabolic limitations of warming and deoxygenation. Acoustically-detected deep scattering layers, comprised of both fish and zooplankton (Warren 2001, Benfield et al. 2003, Lavery et al. 2007), appear depth-limited by hypoxic conditions (Bianchi et al. 2013, Netburn & Koslow 2015), and declines in oceanic oxygen content have been associated with the concurrent loss of mesopelagic fish ichthyoplankton by as much as over 60% (Koslow et al. 2011), attributed in part to habitat compression (Koslow et al. 2011, Netburn & Koslow 2015). Some mesopelagic fish species live constantly in deep, low oxygen waters; however, others make nightly migrations into shallow (200-0 m), well-oxygenated waters, where

they feed on the more abundant prey resources. Thus, non-migrating fishes live constantly in low oxygen waters, while migrating fishes experience intermittent hypoxia. The apparent deoxygenation in the CCE raises questions about the effects of variable midwater oxygen concentrations on the metabolic physiology of mesopelagic fishes living within the southern CCE.

Citrate Synthase (CS) and Malate Dehydrogenase (MDH) are two enzymes of the Krebs cycle that are commonly used as indicators of aerobic respiratory capacity (Torres et al. 2012). In vertebrates, the last step of anaerobic respiration involves the conversion of pyruvate to lactate, catalyzed by Lactate Dehydrogenase (LDH). Lactate production is energetically expensive and accumulation of lactate is toxic (Hochachka & Somero 2002), so respiration via the LDH pathway cannot be sustained for long periods of anoxic exposure. There exists only one alternative metabolic pathway in vertebrates, thus far only demonstrated in the Cyprinidae (Crucian carp and goldfish), in which lactate is ultimately converted to ethanol, which can diffuse from the cells and be excreted, avoiding the accumulation of toxic molecules within muscle tissue (Shoubridge & Hochachka 1980, Vornanen et al. 2009). Activities of CS, MDH, and LDH have been found to decline with the minimum depth of occurrence for mesopelagic fishes regardless of other environmental characteristics, typically attributed to the reduced energy demands required by taking refuge from visually-oriented predators in relatively dark mesopelagic waters (Childress 1995, Seibel & Drazen 2007). Torres et al. (2012) found evidence for the ADH pathway in some species of Myctophidae, including three species considered in this study (i.e., *Nannobrachium ritteri*, *Stenobrachius leucopsarus*, *Triphotorus mexicanus*), with ADH activities detected of similar magnitude as that measured in carp

and goldfish. However, these fishes' ability to metabolically produce ethanol has not been confirmed.

To investigate the metabolic response of mesopelagic fishes to natural variability in ambient oxygen concentrations over space, we measured the activities of CS, MDH, LDH, and ADH in a suite of mesopelagic fishes collected in variable oxygen conditions throughout the southern CCE. We specifically sought to answer the following questions:

(1) Does aerobic metabolic activity change in relation to spatial variations in midwater oxygen concentrations?

We expect that aerobic metabolic enzyme activities will decline in response to declining midwater oxygen concentrations.

(2) Does the relative contribution of anaerobic metabolic enzyme activity to total metabolic enzyme activity vary in response to variations in midwater oxygen concentration?

We expect that LDH enzymatic activity will be higher in fish from the lowest dissolved oxygen concentrations, due to the limited oxygen.

(3) How do a) diel vertical migration behavior, b) phylogeny, and c) tissue composition affect aerobic and anaerobic metabolic enzyme activities?

a) Since non-vertical-migrating fish species are permanent residents of oxygen-limited waters, we expect they will have a higher LDH:CS ratio and lower overall metabolic enzyme activities. On the other hand, migrators will have elevated overall metabolic enzyme activities due to both the high metabolic cost of migration and their periodic exposure to well-oxygenated epipelagic water. b) We expect there will be differences in activities among families, in a manner related to their phylogenetic history.

c) We expect fish with lower water content and higher protein concentrations to have elevated activities of all metabolic enzymes because of higher maintenance costs associated with swimming and feeding.

(4) Is there evidence for an ethanol-production anaerobic pathway mesopelagic fishes in the CCE?

The presence of the ADH pathway would suggest mesopelagic fishes in the CCE can produce ethanol as an end product of anaerobic metabolism, which is more easily excreted and less toxic compared to lactate.

3.3 Methods

We collected the fish specimens on two research cruises: the California Cooperative Oceanic Fisheries Investigations Fall 2012 cruise (CalCOFI 1210; 19 Oct - 5 Nov 2012) and the California Current Ecosystem Long-Term Ecological Research Summer 2014 process cruise (CCE-P1408; 6 Aug – 4 Sept, 2014) with oblique profiles of a Matsuda-Oozeki Hu Trawl net (Oozeki 2004) (**Figure 3.1**). On CalCOFI 1210, we conducted trawls at a subset of stations of the standard CalCOFI grid. Five of fourteen tows were made during daytime, to approximately 500 m depth. The remainder of the tows were to ~150 m at night, capturing only the vertically migrant component of the assemblage. On CCE-P1408, we conducted both daytime (≤500 m) and nighttime (≤150m) trawls at each of three sampling stations. We identified and sorted the fish at sea in chilled seawater, immediately froze them whole in liquid nitrogen, and later transferred them to a -80° C freezer. Within 2 years of collection, we subsequently measured and weighed the samples, dissected them on dry ice to avoid protein

degradation, and homogenized a piece of tissue at 0-4° C in buffer solution (50 mM imidazole buffer, 2 mM EDTA, pH 6.6 at 20° C) at a ratio of 1 g tissue to 9 ml buffer solution. For the Sternoptychidae *Argyropelecus affinis*, *Argyropelecus hemigymnus*, *Argyropelecus lychnus*, *Argyropelecus sladeni*, the Gonosotomatidae *Cyclothone acclinidens*, Stomiidae *Stomias atriventer*, Myctophidae *Diaphus theta*, *Nannobrachium ritteri*, *Protomyctophum crockeri*, *Stenobrachius leucopsarus Symbolophorus californiensis*, and *Triphoturus mexicanus*, the Bathylagidae *Bathylagoides wesethi*, *Leuroglossus stilbius*, and *Lipolagus ochotensis*, and Melamphaidae *Malamphaes parvus*, we homogenized dorsal white muscle. For specimens too small to obtain an adequate piece of isolated white muscle tissue - *Cyclothone signata*, *Vinciguerria lucetia*, and small specimens of *Idiacanthus antrostomus*, the specimens were instead skinned, beheaded, and gutted, and we used the whole or a piece of the remaining tissue, which was mostly white muscle, for analysis (as per Somero & Childress 1980). We homogenized the samples by hand in a glass homogenizer, and sonicated them for 10 seconds before centrifuging at 12,000 rcf for 10 minutes. We held the supernatant on ice until assaying within 1-2 hours. All assays were conducted in triplicate in 96-well plates, with 160 µl total volume of solution. Ten µl of supernatant was added to 100 µl assay solutions, and the reaction initiated with the addition of 50 µl of the substrate. The reactions for each enzyme assay are as follows (solution and substrate concentrations listed are the final concentrations in the well):

CS: (acetyl-CoA + oxaloacetate + H2O ↔ citrate + HS-CoA + H^+)

Assay solution: 2.0 mM $MgCl_2$, 0.1 mM DTNB, 0.1 mM Acetyl CoA, and 80 mM Tris buffer, and the substrate is 0.5 mM oxaloacetate.

MDH: (oxaloacetate + NADH ↔ malate + NAD^+)

Assay solution: 20 mM $MgCl_2$, 0.15 mM NADH, 80 mM Tris buffer, and the substrate is 0.4 mM oxaloacetate.

LDH: (pyruvate + NADH ↔ lactate + NAD^+)

Assay solution: 0.15 mM NADH, 100 mM KCL ↔ 50 mM Imidazole buffer, and the substrate is 1.0 mM pyruvate.

ADH: (acetaldehyde + NADH ↔ ethanol + NAD^+)

Assay solution: 1.0 mM glutathione, 0.2 mM NADH, 100 mM potassium phosphate buffer, and the substrate is 8.9 mM acetaldehyde.

All assays were conducted at 27° C in a spectrophotometer. We calculated the enzyme activity rates for MDH, LDH, and ADH using the slope of the decrease in absorbance of NADH at 340 nm. The CS rate was calculated using the slope of the increase of absorbance of 412 nm due to the reaction of reduced acetyl-CoA with DTNB. CS, MDH, and LDH enzyme activities were corrected to 10° C using a Q_{10} of 2.0, and are expressed as Units (micromoles substrate converted to product per min) per gram wet mass of white muscle tissue.

We conducted CS, MDH, and LDH activity assays for each specimen. Results that exceeded ± 2 standard deviations were excluded. For ADH, we assayed a minimum of two specimens of each species at the most hypoxic station for which that species was collected for the following species: Myctophidae *N. ritteri*, *S. leucopsarus*, *T. mexicanus*,

P. crockeri, *S. californiensis*, *C. townsendi*, *D. theta*, Bathylagidae *L. ochotensis*, *B. wesethi*, Stomiidae *I. antrostomus*, *S. atriventer*, Sternoptychidae *A. affinis*, *A. hemigymnus*, Gonostomatidae *C. acclinidens*, *C. signata*, and Phosichthyidae *V. lucetia.* We did not have material available to conduct the ADH assay for *A. lychnus*, *A. sladeni*, *L. stilbius*, and *M. parvus*.

As a positive control for ADH, we also conducted assays for 10 individual common goldfish (*Carassius auratus*) that had been exposed to hypoxia for approximately 24 hours (IACUC-approved protocol S10320). We also conducted the ADH assay for two specimens each of the three species for which there were previously reported ADH activities (Torres et al. 2012) using an alternative cuvette assay method. We calculated the LDH:CS ratio as an indicator of the relative contribution of anaerobic respiration to total respiration (Yang et al. 1992, Friedman et al. 2012). CS was chosen over MDH for this metric because MDH serves multiple roles in the cell, and interpretation of its activity is not straightforward (Thuesen & Childress 1994, Torres et al. 2012).

Diel vertical migration behavior was assigned for fish from this region as per Davison et al. (2014). The data were determined by the Kolmogorov-Smirnov test to be non-normal, even when transformed. Therefore, we made comparisons between median enzyme activities of families using the non-parametric Kruskal-Wallis test, followed by pairwise comparisons using the Dunn method. Two different indices of tissue composition were used in the analysis: (1) published estimates of % water weight, and (2) white muscle tissue protein concentration, which we measured for most of the specimens in the study. We performed linear regressions to test whether these indices predict

enzyme activity. Mean water weight values were obtained from Childress & Nygaard (1973) and Bailey & Robison (1986). Concentration of protein for each supernatant was measured using a standard Bradford Assay (Bio-Rad Protein Assay Kit).

Dissolved oxygen was measured as a function of depth with a CTD-rosette equipped with dual SBE43 oxygen sensors, and corrected with Winkler titration measurements on discrete depth bottle samples at each station. Because we do not know the precise depth at which each specimen was collected, we used the concentration of dissolved oxygen at 300 m (in ml l^{-1}) as a proxy for the relative dissolved oxygen concentrations experienced by the fish at each station.

3.4 Results

We measured activities of the enzymes CS, MDH, and LDH of a total of 481 individual specimens comprising 20 species of mesopelagic fishes, as well as the ADH activity of an additional 38 specimens (from 16 species). Activities for the aerobic enzymes CS and MDH, and the anaerobic enzyme LDH are summarized by species in **Figure 3.3**, as well as the LDH:CS ratio. Measurements are further detailed in **Appendix 3.1**. There were some significant differences in enzyme activities ($p<0.05$) between samples collected during the day and during the night for some of the migrating species (**Table 3.1**). We measured elevated MDH activity for daytime samples for *D. theta*, and elevated LDH by day for *S. californiensis*. Nighttime activities were elevated for CS for *T. mexicanus* and *V. lucetia,* MDH for *L. ochotensis* and *T. mexicanus*, and LDH for *S. leucopsarus*.

Midwater Dissolved Oxygen

Dissolved oxygen concentrations at 300 m varied from 0.46-2.02 ml l^{-1} across our sampling locations (**Figure 3.2**). Activities for the two aerobic enzymes covaried with concentration of dissolved oxygen (linear regression) for only a subset of the families investigated: CS: Phosichthyidae ($p < 0.01$), MDH: Phosichthyidae ($p < 0.01$), and Stomiidae ($p < 0.05$). The LDH:CS ratio for Phosichthyidae ($p < 0.05$) and Bathylagidae ($p < 0.01$) also covaried with oxygen concentrations (Fig. 4). Even where statistically significant, a relatively small proportion of the variance (0-31%) in enzyme activity was explained by ambient dissolved oxygen. However, both aerobic and anaerobic enzyme activity and the ratio of LDH:CS were consistently reduced at the lowest concentrations of dissolved oxygen (**Figure 3.4**).

Diel vertical migration behavior, phylogeny, and tissue composition

Diel vertical migrators exhibited significantly higher activities of CS ($p < 0.01$), MDH ($p<0.01$), and LDH ($p<0.05$) than non-vertically migrating fishes, but there was no statistical difference in the LDH:CS ratio between the two groups ($p = 0.13$, Mann-Whitney U Test, **Figure 3.5**). For all three enzymes, there were some significant pairwise differences in activities at the family level (**Figure 3.6**), with the following groups clustering together using the Dunn procedure for multiple non-parametric pairwise comparisons:

CS: (a) Phosichthyidae, Myctophidae, Sternoptychidae, and Bathylagidae, and (b) Gonostomatidae and Stomiidae. Activity of Melamphaidae was indistinguishable from the other families, due to the extremely low sample size in this family.

MDH: (a) Phosichthyidae, (b) Myctophidae and Sternoptychidae, and (c) Bathylagidae, Gonostomatidae, and Stomiidae. Melamphaidae activity was indistinguishable from the others.

LDH: (a) Phosichthyidae, Myctophidae, Sternoptychidae, (b) Bathylagidae, and (c) Gonostomatidae and Stomiidae. LDH activity in Bathylagidae was much higher compared to the other families, which also resulted in a higher LDH:CS ratio.

Previously published values of percent water content were not correlated with the magnitude of enzyme activity for any of the species (**Figure 3.7**), although the relationship with the LDH:CS ratio was significant at $p<0.05$ ($r^2=0.30$). CS and MDH activities were, however, reduced in fishes with water content >0.8. The activities of both aerobic enzymes, CS ($r^2=0.27$, $p<0.05$) and MDH ($r^2=0.33$, $p<0.01$), covaried with the measured protein concentration (**Figure 3.8**).

ADH Activity

No ADH activity was detected by either the microplate or cuvette methods for any of the specimens sampled of Myctophidae, Bathylagidae, Stomiidae, Sternoptychidae, Gonostomatidae, and Phosichthyidae. However, samples from common goldfish (*C. auratus*) had a mean ADH activity of 4.04 (±0.44) U g^{-1} at 27° C (measured using the microplate method) which served as a positive control.

3.5 Discussion

In this study, we observed a general reduction in maximum metabolic enzyme activities of CS, MDH, and LDH for all species combined with declines in environmental

oxygen concentrations. We found no increase in LDH activity at low dissolved oxygen levels (~0.5 ml l^{-1} compared to 2.0 ml l^{-1}), and no evidence of an alternate anaerobic ethanol production pathway. In addition, we found that diel vertically migrating fishes have higher aerobic and anaerobic metabolic activities than their non-migrating counterparts, and revealed differences in activities based on phylogenetic relationships and fish tissue composition. As would be expected due to the relatively low energy expenditure of mesopelagic fishes (Seibel & Drazen 2007), the enzyme activities of the fishes measured in this study are lower than activities typical of epipelagic fishes. The maximum activity of CS for any species of mesopelagic fish in our study (~2.5 U g^{-1} for *D. theta*) is approximately 5 times lower than that of epipelagic tunas (~7.5 U g^{-1}), and LDH activity (~80 U g^{-1} for *B. wesethi*) is approximately 30 times lower than in tuna white muscle (>2500 U g^{-1}, Dickson 1995). The California anchovy *Engraulis mordax*, which is more similar in size to many of the mesopelagic fishes in our study, and also has a comparable plankton diet, has MDH and LDH activities about twice the temperature-corrected maximum in our study (Childress & Somero 1979). The mean enzyme activities in our study are similar to those reported in previous studies on this assemblage (**Table 3.2**). The greatest exception is the MDH and LDH activities of *Vinciguerria lucetia*, which are about one-third of those measured by Childress & Somero (1979), who did not measure CS. It is possible that the generally smaller size of our specimens (17-34 mm) compared with those in their study (26-52 mm) accounts for the difference in magnitude of enzyme activities due to size-scaling effects. However, although LDH typically increases with size, MDH activity decreases with size (Somero & Childress 1980). A more likely explanation for the discrepancy lies in the somatic tissues used for

the assay. With all of our specimens measuring under 35 mm standard length, we homogenized whole gutted and fin-removed specimens for our enzyme activity measurements. However, Childress & Somero (1979) used gutted and fin-removed specimens for the smaller specimens, and dorsal white muscle tissue alone for the larger specimens. Further, there is inherent variability in all of our measurements because the fishes may spend up to 2-3 hours in the net between the time of capture in the water column and being frozen for storage, during which time the enzyme concentrations may change due to stress effects and/or degradation.

We observed the same general trend of declining metabolic activities with depth (**Appendix 3.3**) as has previously been reported for visually-orienting fishes (Childress & Somero 1979), crustaceans (Cowles et al. 1991), and cephalopods (Seibel et al. 1997). This declining trend in metabolic activity is attributed primarily to the decline of light irradiance with depth rather than oxygen, temperature, or food availability (Seibel & Drazen 2007), as the "Visual Interactions Hypothesis" predicts decreased energy demands of organisms that take refuge from their predators in the darkness of the deep open ocean, thereby reducing the high energy requirement of locomotory predator avoidance (Childress 1995). The metabolic activities for *Protomyctophum crockeri*, however, are higher than expected based on their minimum depth of occurrence. A potential explanation for this exception to the pattern of declining metabolic rates with increased minimum depth of occurrence is that *P. crockeri* may be evolutionary constrained, as most of their closest relatives, the other members of the family Myctophidae, migrate into surface waters at night, and therefore have high metabolic rates.

There were diel differences in the enzyme activities for some migratory species. Nighttime activities were higher for three of the four species for which there was a significant diel difference in activities of either of the aerobic enzymes CS & MDH. This may be due to the higher locomotory activity of migrators at night, during which time they are actively feeding. Additionally, LDH activity was elevated for *S. californiensis* during the day, when they reside within the OMZ. LDH activities were elevated at night for *S. leucopsarus*, however individuals of this species are not consistent migrators, so would not be expected to fit the pattern.

In interpreting our results, we revisit the questions set forth in the Introduction.

(1) Does aerobic metabolic activity change in relation to spatial variations in midwater oxygen concentrations?

In order to understand the potential metabolic consequences of ongoing and potential future ocean deoxygenation in the CCE, we have investigated the responses of mesopelagic fishes to natural variability in dissolved oxygen concentrations within their environment. The activities of CS and MDH covaried with midwater oxygen content for only two of the seven families tested, and these relationships explain only a relatively small proportion of the variance. We did not detect a statistically significant trend of decreasing metabolic rates with decreasing midwater oxygen concentration (from ~2.0-0.5- ml l^{-1} at 300 m) within the sampling region. However, our data suggest that at low environmental oxygen concentrations, the mesopelagic community as a whole may be metabolically constrained to lower maximum activities of both aerobic and anaerobic enzymes, while a full range of activity rates may be exhibited at higher oxygen concentrations. Previous studies (as well as the data we present here) have found that

metabolic enzyme activities, compared among species, decline with increasing minimum depth of occurrence regardless of other environmental factors (Childress & Somero 1979). Yet our data suggest that across a single region, environmental oxygen concentrations may also influence the metabolism within a taxon, with depressed metabolic rates in specimens collected within the low range of oxygen concentrations. Although we know of no other studies that have investigated the metabolic response of organisms to variable oxygen within a region (as opposed to with depth), a few have made comparisons between regions. Cowles et al. (1991) found lower metabolic rates in crustaceans living shallower than 400 m in the OMZ-containing California region compared to those in Hawaii, although not for those living deeper than 400 m. As we conducted midwater trawls to only 500 m in this study, we did not collect deep mesopelagic and bathypelagic fish species to test whether their metabolic activities respond to changes in midwater oxygen concentrations. Additionally, our results do not rule out the Visual Interactions Hypothesis (Childress 1995), as oxygen concentration can covary with irradiance.

(2) Does the relative contribution of anaerobic metabolic enzyme activity to total metabolic enzyme activity vary in response to variations in midwater oxygen concentration?

Ratios of anaerobic to aerobic enzymes have been used in previous studies to investigate the relative contribution of anaerobic respiration to total respiration in OMZ regions (Yang et al. 1992, Friedman et al. 2012). Although we did not observe a significant correlation between the LDH:CS ratio and dissolved midwater oxygen

concentrations, we did observe a tendency for the lowest ratios to occur at low (~0.5-1.0 ml l^{-1}) dissolved oxygen concentrations. We speculate that there is an increase in total metabolic potential of mesopelagic fishes in well-oxygenated regions that is accompanied by an increase in LDH activity in muscle tissues due to increased physical activity. Even in normoxic conditions, fish rely on anaerobic metabolism in their muscle tissue when under high energy demands, so more active fish are likely to have higher LDH activities, regardless of environmental dissolved oxygen concentration. Our results are in agreement with other studies that did not find evidence of an increased reliance on anaerobic respiration for deep-sea fishes living in hypoxia (Childress & Somero 1979, Vetter & Lynn 1997, Thuesen et al. 1998, Friedman et al. 2012), although an increased ratio of anaerobic to aerobic metabolic enzymes has been observed in a scorpaenid fish that lives in deep hypoxic water compared with a shallower-dwelling confamilial (Yang et al. 1992). Similarly, Torres et al. (2012) found higher LDH and lower CS values in myctophids collected in the OMZ-containing Arabian Sea compared to those collected in the Gulf of Mexico (but higher MDH activities in the Gulf of Mexico fishes). However, Torres et al. (2012) also found higher LDH activities in well-oxygenated Antarctic waters compared to California myctophids. Many studies have found that fishes have mechanisms to increase uptake of oxygen from their environment, such as increasing the gill surface area, reducing diffusion distances, and enhancing the oxygen affinity of hemoglobin (Childress & Seibel 1998, Friedman et al. 2012). These factors may account at least to some extent for the ability of the mesopelagic fishes to survive low oxygen concentrations without increasing anaerobic respiration.

(3) How do a) diel vertical migration behavior, b) phylogeny, and c) tissue composition affect aerobic and anaerobic metabolic enzyme activities?

a) Vertical Migration Behavior: In agreement with our expectation, vertically migrating fishes had higher activity levels for all enzymes than the non-migrators. However, the expected pattern of elevated LDH:CS ratios and overall suppressed activity levels for non-migrating animals compared to migrators was only evident within the family Stomiidae. We do not observe the same distinction within Myctophidae; the one non-migrator, *P. crockeri* has an average LDH:CS ratio compared with its migrating con-familials. *P. crockeri*, however, is considered an "active" myctophid (Barham 1971, Childress & Nygaard 1973), and has quite high activities of both of the aerobic enzymes. Although both members of the Gonostomatidae are non-migratory, the LDH:CS ratio is elevated for *C. acclinidens*, which is deeper-dwelling (500-1000 m) than its congener *C. signata* (300-500 m, Miya & Nishida 1996), perhaps attributable to its more hypoxic environment. The Sternoptychidae do not exhibit particularly low levels of any of the enzymes, however they typically live within the shallower portion of the non-migrating layer, so are likely not exposed to the same severity of hypoxia as are the Gonostomatidae and *S. atriventer*. The high LDH:CS ratios of the Bathylagidae could be due to a generally higher physical activity level, leading to more anaerobic activity in the muscle tissue overall.

b) Phylogeny: There were significant differences in enzyme activities between some of the families, however these differences were not consistent across all enzymes. The Phosichthyidae (represented by just one species, *V. lucetia*) stand out as having the highest activities of the two aerobic enzymes. Childress & Somero (1979) similarly found

elevated MDH (CS was not studied) activities in *V. lucetia* compared with other species in that study. *V. lucetia* dominate in regions with pronounced and shallow oxygen minimum zones (Cornejo & Koppelmann 2006), however they are most abundant in the CCE in years with relatively high oxygen concentration (Koslow et al. 2011). Our specimens for *V. lucetia* were relatively small, so our results could reflect a size-related bias. The Stomiidae consistently have the lowest activities for all enzymes. Activities are also relatively low for the two Gonostomatidae, which is likely explained by their less active lifestyle than other groups in the study (Barham 1971).

c) Tissue Composition: Tissue protein content was a good explanatory variable for the two aerobic enzymes (CS and MDH, **Fig. 3.8**); probably because organisms with high protein concentrations tend to be more active and contain more metabolic enzymes per unit tissue mass (Moyes et al. 1992). We did not find a linear relationship of enzyme activities with water weight, although aerobic activities were reduced at higher water weight as expected (**Fig. 3.7**).

(4) Is there evidence for an ethanol-production anaerobic pathway mesopelagic fishes in the CCE?

We did not detect ADH activity in any of the 16 species we assayed and do not find support for the hypothesis that these fishes have an ethanol-production pathway. These results contrast with those of Torres et al. (2012), who found activity in all of the myctophids they assayed (from 4.03 U g^{-1} white muscle tissue for *Electrona antarctica* in the Antarctic to 345.2 U g^{-1} for *Lampanyctus sp*. in the Arabian Sea). The reason for this discrepancy is not clear. Our method differed only in the assay volume (160 µl instead of

1 ml) and temperature (27° C instead of 15° C). Our methods appear robust, as the Q_{10}-corrected results for the other enzymes were all within range of previous studies on this assemblage (Childress & Somero 1979, Torres et al. 2012) and we detected ADH activity in *C. auratus*, a species for which presence of the ADH ethanol-production pathway is verified. The ADH activity rates that we measured for *C. aurautus* were detectable, at 4.0 ± 0.4 U g^{-1} (n=10), however were lower than the published value of 29.2 ± 7.0 U g^{-1} (n=4, Shoubridge & Hochachka 1980). The ethanol-production anaerobic pathway is thus far known only from animals that are exposed to environmental anoxia, and is rare even within the one family of fish that exhibits it (Hochachka & Somero 2002). While the mesopelagic fishes in the California Current are indeed adapted to live in low oxygen conditions, they are not known to inhabit anoxic waters. We recommend further studies to determine the discrepancy between our and published estimates of ADH activity. The preferred way to verify the presence of an ethanol-production pathway is to collect live fish and directly measure the production of ethanol in a closed system. Although mesopelagic fishes are difficult to maintain alive in the lab, such experiments are feasible. There are a number of limitations of our sampling procedure that introduce variability into the data- several hours can pass from collection to preservation of specimens, the specimens were preserved for up to 2 years before conducting assays, and assay preparation conditions (such as room temperature) may have been inconsistent. Finally, these enzymes are a measure of maximum metabolic scope and not necessarily the actual metabolic activity in the in situ organism.

3.6 Conclusions

To our knowledge this is the first study to examine the variable metabolic activities for a suite of mesopelagic fish species across relatively small-scale horizontal gradients in oxygen concentrations, although previous studies have used species distributions across vertical gradients in oceanographic features as a means to investigate metabolic response to environmental cues (e.g., Childress & Somero 1979, Friedman et al. 2012). Through the extensive sampling conducted on the CalCOFI and LTER programs, specimens of the same species were collected at multiple locations, thereby allowing us to resolve how these animals respond to horizontal gradients in midwater oxygen availability within a single region.

Given the predictions of future deoxygenation in the CCE region and beyond, we speculate that there could be a decrease in individual metabolic potential of fishes as the mesopelagic zone becomes more hypoxic. We further speculate that if populations of mesopelagic fishes decline in abundance in years of decreased oxygen (as suggested by Koslow et al. 2011), there could be a decline in the maximum theoretical metabolic activity of the midwater community. Respiration by mesopelagic organisms is a process that contributes to oxygen minimum zone formation (Bianchi et al. 2013), and a decline in total respiration could potentially create a self-regulatory loop to curb the expansion of OMZs. However, our back of the envelope calculations suggest that respiration from the fish component is likely negligible in contributing to oxygen depletion in the midwater (**Appendix 3.4**). Another possible implication for this work is that if habitat compression occurs with OMZ expansion (Netburn & Koslow 2015), mesopelagic fishes could be forced into shallower waters where warmer temperatures would increase the demand for both oxygen and food (Bickler & Buck 2007), and potentially force the fishes into still

shallower water, where they will be more vulnerable to predators. Entire species could eventually be forced out of the region, decreasing diversity, and with it the resilience of the system. Other processes beyond respiratory metabolism may affect the survival of mesopelagic fishes under hypoxic conditions. The visual performance of fishes is diminished in hypoxic conditions (Scherer 1971, Johansson et al. 1997, Robinson et al. 2013). Loss of visual acuity could lead to decreased survival of mesopelagic fishes under hypoxic conditions by diminishing the ability of these fishes to detect prey and avoid predators. Finally, the co-occurring stressors of ocean acidification and ocean warming could combine to create a more inhospitable environment than deoxygenation alone (Bopp et al. 2013, Levin & Le Bris 2015), and further work is required to understand the combine effects of these multiple stressors.

Only long-term measurements of both individual and assemblage-level responses to environmental changes, such as are possible in the CalCOFI and CCE-LTER programs, will reveal the response of mesopelagic animals to climate change-associated effects like ocean deoxygenation. Further, we recommend that comparative studies be carried out in regions with shallower and more hypoxic OMZs such as the Eastern Tropical Pacific, Peru-Chile Current, and the northern Indian Ocean to study metabolic responses to conditions that may develop in the CCE. In the interim, the space-for-time approach presented here, suggests that mesopelagic animals in oxygen-limited regions experience suppression of their maximum metabolic capacity, and are therefore vulnerable to a changing ocean climate.

3.7 Acknowledgements

We extend a special thanks to Qianyun ("Wendy") Luo, who volunteered many hours preparing samples for the metabolic enzyme assays. We further thank Pete Davison, Jaime Chang, and Jian Liu for assistance in collecting, sorting, and identifying specimens at sea, as well as Yuzo Yanagitsuru and Lauren Linsmayer for advising on the assay protocols. Tony Koslow provided the MOHT, which was purchased with funds from the Gordon and Betty Moore Foundation. Shiptime on both cruises was provided by the NSF-funded California Current Ecosystem LTER program. We thank the captains and crews of the R/V New Horizon and R/V Melville for all of their assistance, as well as the CalCOFI and CCE-LTER science parties for accommodating and aiding this sampling. Finally, we thank Tony Koslow, Lisa Levin, and Frank Powell for their feedback on a preliminary draft of the manuscript.

Chapter 3 is currently submitted for publication in Marine Ecology Progress Series. Netburn, A.N., Tresguerres, M., and M.D. Ohman. Inter-Research Science Center, 2016. The dissertation author was the primary investigator and author of the paper.

3.8 Figures

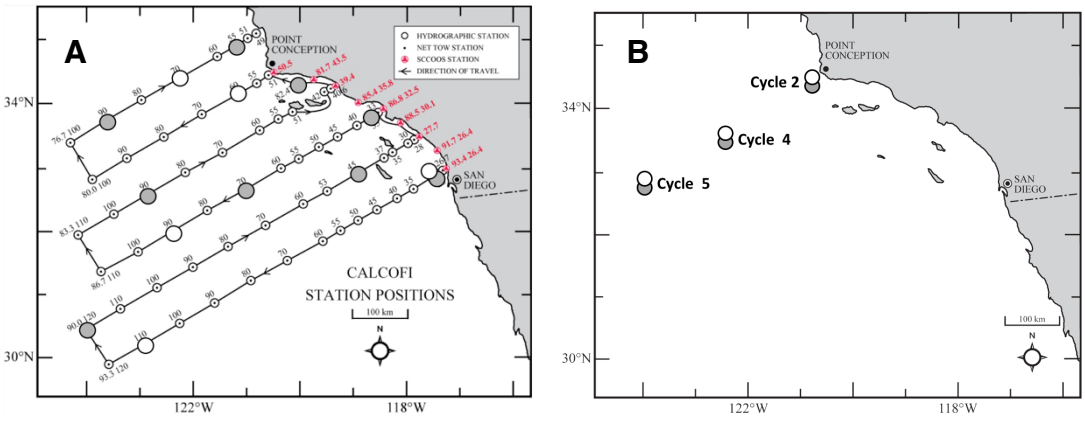

Figure 3.1. The two collection surveys: (a) California Cooperative Oceanic Fisheries Investigation, sampled in October 2012. Each circle represents the location of a single trawl. (b) The California Current Ecosystem Long-Term Ecological Research program's August 2014 Process Cruise. The sampling Cycles are sites where ecosystem-wide sampling was conducted over several days using a quasi-Lagrangian design. The circles indicate locations where multiple trawls were conducted in close proximity to each other. Open and filled circles indicate samples collected at day and night, respectively.

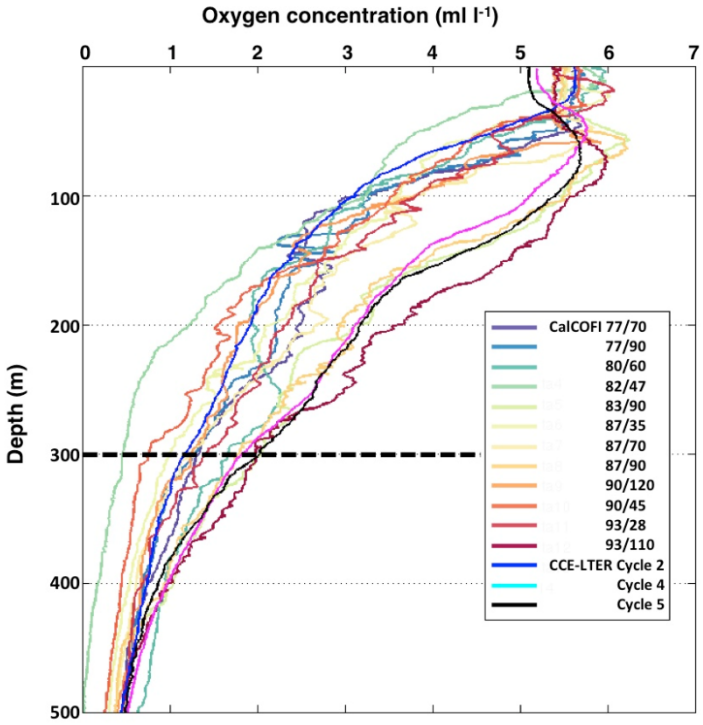

Figure 3.2. Oxygen concentration (ml l^{-1}) against depth for all stations where specimens were collected. The profiles for the CalCOFI station are from single CTD casts at each station, while those of each of the CCE-LTER stations are the mean of measurements from multiple CTD casts conducted over several days while following a water parcel. The thick broken bar highlights the 300 m depth. Oxygen concentration at this depth was used as the indicator of the extent of midwater hypoxia, although collections were to either 500 m (daytime) or 150 m (nighttime).

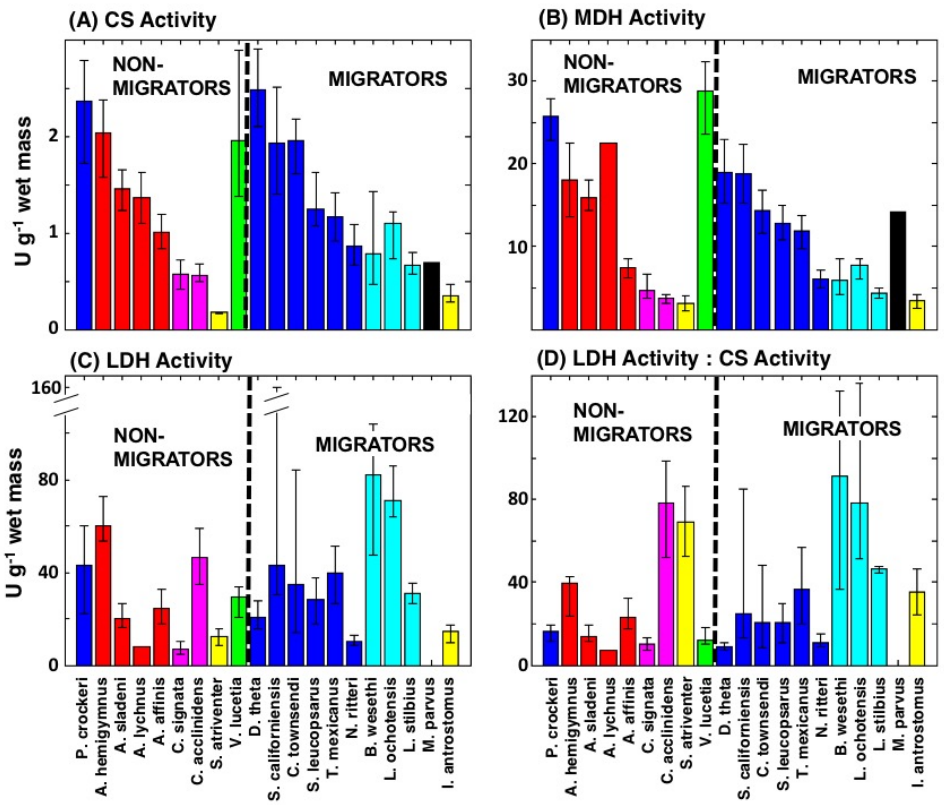

Figure 3.3. Median enzyme activities by species for (a) Citrate Synthase, (b) Malate Dehydrogenase, and (c) Lactate Dehydrogenase. Panel (d) is the LDH:CS ratio. Units (U) are μmoles of substrate converted per minute, and the data are pooled across sampling stations. Bars are color-coded by family. All species to the left of the broken line are non-migrators, while those to the right are species that undergo diel vertical migrations. The error bars indicate the 25-75th percentile range.

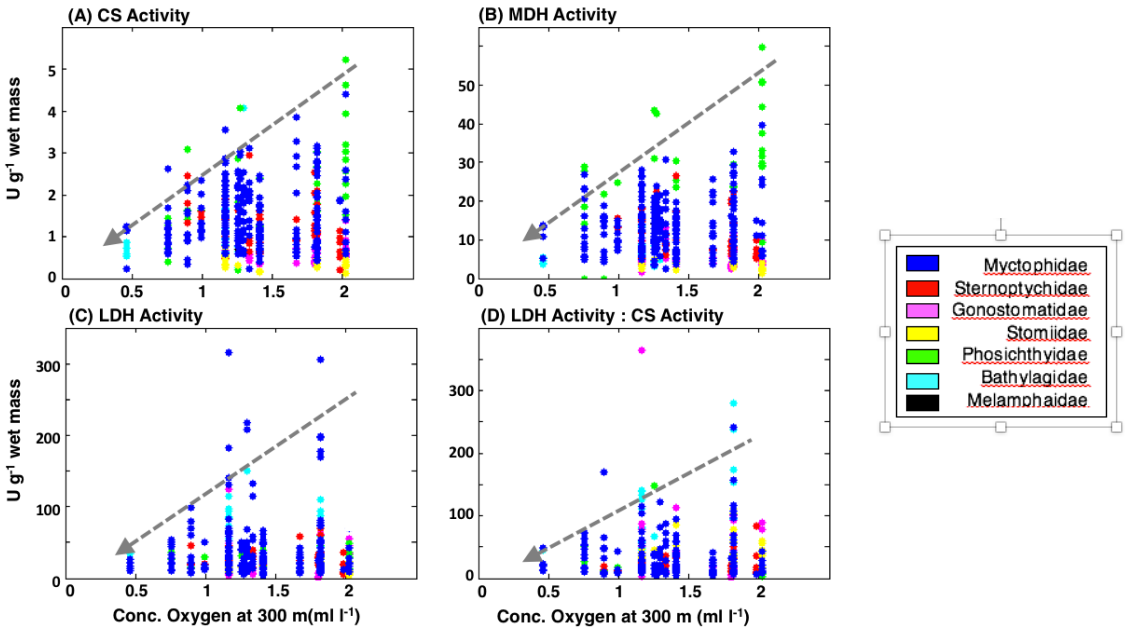

Figure 3.4. Enzyme activities in relation to the concentration of dissolved oxygen at 300 m (measured at the station where the corresponding specimen was collected) for: (a) Citrate Synthase (b) Malate Dehydrogenase, and (c) Lactate Dehydrogenase. Panel (d) is the LDH:CS ratio. Units (U) are µmoles of substrate converted per minute. Each point represents a single specimen, labeled by family, with linear regressions fit by family. Points are color-coded by family. Linear regression lines are not shown. The following fits were significant: CS: Phosichthyidae (r^2=0.24, $p < 0.01$), MDH: Phosichthyidae (r^2=0.26, $p < 0.01$), Stomiidae (r^2=0.16, $p < 0.05$). LDH:CS ratio: Phosichthyidae (r^2=0.14, $p < 0.05$) and Bathylagidae (r^2=0.31, $p < 0.01$). The broken grey arrows illustrate the approximate upper boundary of enzyme activities as a function of dissolved oxygen concentrations. See **Appendix 3.2** for plots by species.

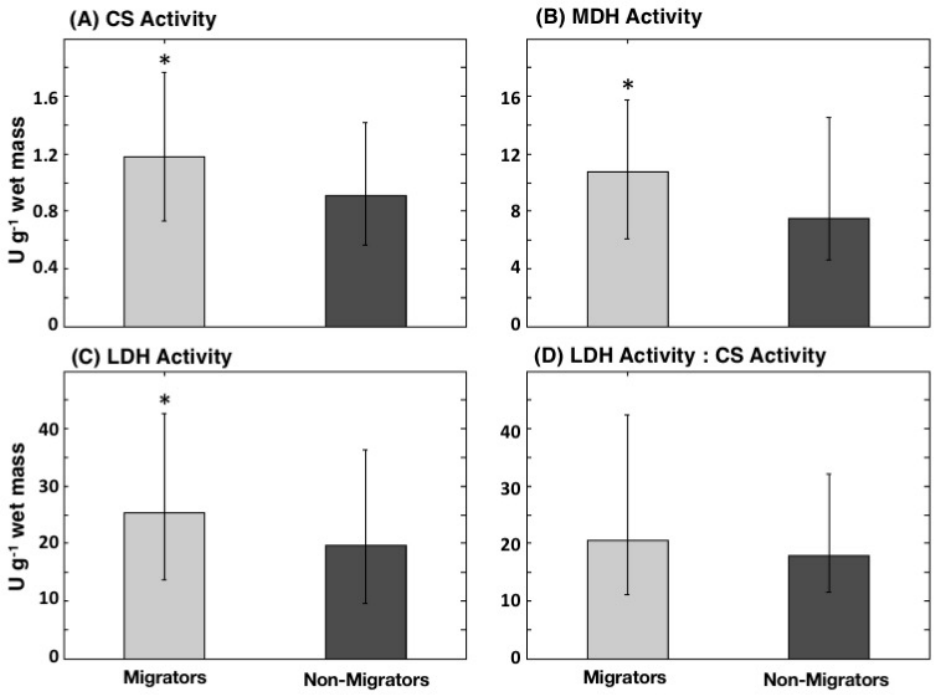

Figure 3.5. Median enzyme activities by diel vertical migration behavior of (a) Citrate Synthase, (b) Malate Dehydrogenase, and (c) Lactate Dehydrogenase. Panel (d) is the LDH:CS ratio. Units (U) are μmoles of substrate converted per minute. The errorbars indicate the 25-75th percentile range, and asterisks denote significant differences.

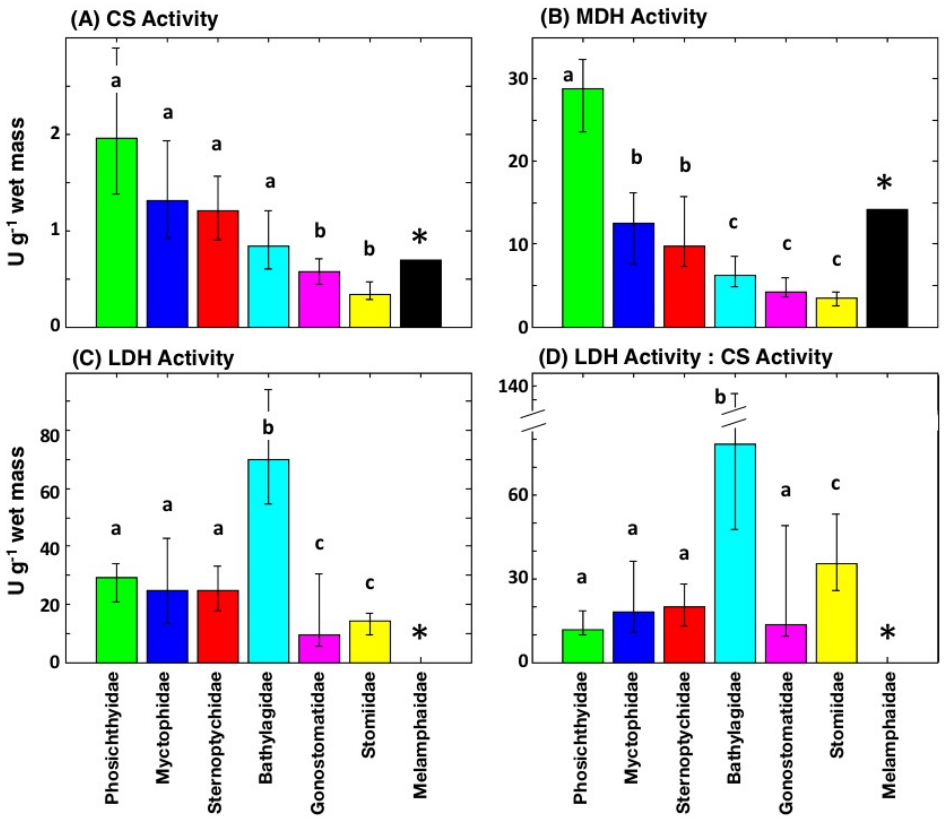

Figure 3.6. Median enzyme activities by family for (a) Citrate Synthase, (b) Malate Dehydrogenase, and (c) Lactate Dehydrogenase. Panel (d) is the LDH:CS ratio. Units (U) are µmoles of substrate converted per minute. Bars indicate the 25-75th percentile range. Letters indicate groups that are indistinguishable based on the Dunn method for multiple non-parametric pairwise comparisons. The enzyme activities for Melamphaidae were indistinguishable from all other families, denoted by asterisks.

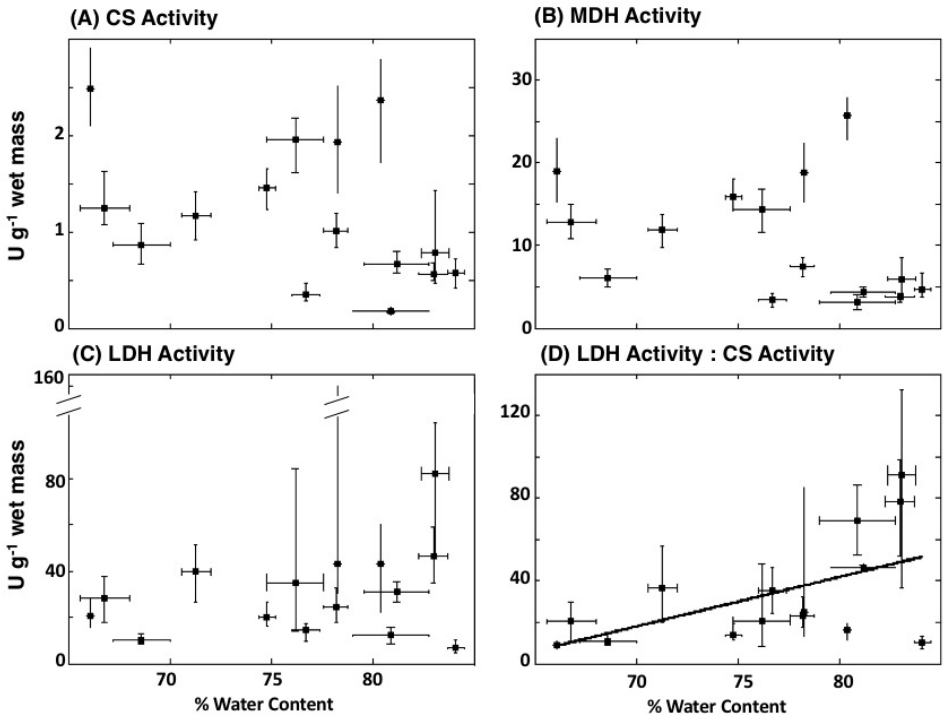

Figure 3.7. Median enzyme activities by family in relation to published values of mean % water content for: (a) Citrate Synthase ($p=0.13$), (b) Malate Dehydrogenase ($p=0.21$), and (c) Lactate Dehydrogenase ($p=0.26$). Panel (d) is the LDH:CS fratio ($r^2=0.30$, $p<0.05$). Units (U) are µmoles of substrate converted per minute. Water content values are from Childress & Nygaard (1973) and Bailey & Robison (1986). The y-axis error bars indicate the 25-75th percentile range, and the x-axis error bars the standard error of the mean.

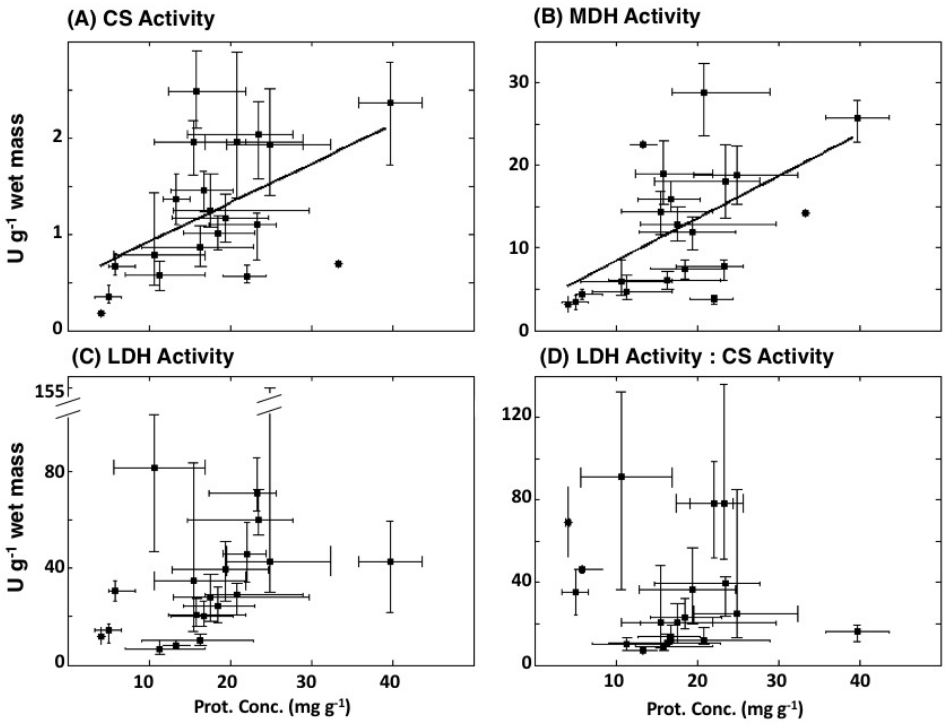

Figure 3.8. Median enzyme activities by family in relation to median protein concentrations by species for: (a) Citrate Synthase (linear regression, r^2 =0.27, $p<0.05$), (b) Malate Dehydrogenase (r^2 =0.33, $p<0.01$), and (c) Lactate Dehydrogenase ($p=0.10$). Panel (d) is the LDH:CS ratio ($p=0.46$). Units (U) are μmoles of substrate converted per minute. Bars indicate 25-75thpercentile range.

3.9 Tables

Table 3.1. Significance values of Mann-Whitney U tests comparing enzyme activities of samples collected by day versus night for vertically migrating species in this study. *L. stilbius* and *M. parvus* specimens were only collected during the day, so they are not included in the table. Values shaded in grey are significant at the $p<0.5$ level, and an asterisk denotes that the enzyme activity of daytime-collected samples was significantly higher than the activity of nighttime samples.

	p-value (day-night comparison)		
Species	**CS**	**MDH**	**LDH**
Bathylagoides wesethi	0.13	0.41	0.39
Ceratoscopelus townsendi	0.29	0.42	0.51
Diaphus theta	0.79	0.05*	0.16
Idiacanthus antrostomus	0.55	0.45	0.81
Lipologus ochotensis	0.09	0.03	0.22
Nannobrachium ritteri	0.53	0.73	0.15
Symbolophorus californiensis	0.50	0.70	0.02*
Stenobrachius leucopsarus	0.12	0.14	0.01
Triphotorus mexicanus	0.00	0.05	0.92
Vinciguerria lucetia	0.03	0.48	0.71

Table 3.2. Median enzyme activities (25th percentile, 75th percentile) by mesopelagic fish species measured in our Southern California study compared to previously reported values in the region (mean ± standard error). We only report the activities for which there are published estimates available. Units (U) are μmoles of substrate converted per minute. No error is available where only 1 sample or pooled samples were assayed.

		Enzyme Activity (U g^{-1} WW)	
Species	**Enzyme**	**This Study**	**Previously Reported**
Argyropelecus affinis	LDH	24.5 (17.8, 32.4)	19.6 (± 1.2)[a]
Bathylagoides wesethi	MDH	5.9 (4.2, 8.4)	9.3[a]
	LDH	82.0 (47.3, 103.7)	83.6[a]
Leuroglossus stilbius	MDH	4.3 (3.8, 5.0)	8.1[a]
	LDH	30.9 (26.6, 35.2)	45.0[a]
Nannobrachium ritteri	CS	0.9 (0.7, 1.1)	1.5 (± 0.2)[b]
	MDH	6.0 (5.0, 7.2)	8.9 (± 0.4)[a], 17.3 (± 6.7)[b]
	LDH	10.0 (8.4, 12.9)	31.0 (± 9.8)[a], 20.3 (± 12.4)[b]
Stomias atriventer	MDH	3.1 (2.2, 4.1)	3.2[a]
	LDH	12.1 (8.5, 15.7)	7.9[a]
Symbolophorus californiensis	MDH	18.8 (15.3, 22.4)	24.6 [a]
	LDH	43.1 (30.4, 154.9)	188.1[a]
Stenobrachius leucopsarus	CS	1.2 (1.1, 1.6)	2.4 (± 0.82)[b]
	MDH	12.9 (10.8, 14.9)	34.9 (± 9.23)[b]
	LDH	28.1 (18.0, 37.4)	38.6 (± 17.65)[b]
Triphotorus mexicanus	CS	1.2 (0.9, 1.4)	4.8 (± 1.91)[b]
	MDH	11.9 (9.8, 13.7)	22.1[a], 39.1 (± 17.70)[b]
	LDH	39.6 (26.8, 51.1)	46.1 (± 6.0)[a], 47.7 (± 13.55)[b]
Vingiguerria lucetia	MDH	28.8 (23.6, 32.4)	89.5 (± 8.4)[a]
	LDH	29.3 (20.6, 33.9)	90.3 (± 16.1)[a]

[a] Childress & Somero (1979)

[b] Torres et al. (2012)

+

3.10 Appendices

Appendix 3.1. Activities of CS, MDH, and LDH. Cycles 2, 4, and 5 are CCE-P1408 sampling sites (see map in Figure 1). The remaining stations are CalFOFI 1210, and labelled by line/station. The mean mass and length are indicated, followed by the range of measurements for each species at each station. The mean activities for each of the enzymes are given in Units (μmoles of substrate converted per minute) per gram of wet weight, followed by the standard error, and the n-value. Gray shading indicates nighttime sampling. Specimens indicated by unshaded rows were collected by day.

					Enzyme Activity (Units g-1 ww)		
Family	**Species**	**Station**	**Mass (g)**	**Length (mm)**	**CS (± SE, n)**	**MDH (± SE, n)**	**LDH (± SE, n)**
Bathylagidae	*Bathylagoides wesethi*	Cycle 2 (D)	3.275 (1.311-6.644)	52 (42-61)	1.05 ± 0.31 (3)	6.95 ± 1.03 (3)	82.05 ± 9.35 (2)
		Cycle 2 (N)	0.775 (0.300-1.432)	43 (33-53)	1.28 ± 0.19 (5)	8.91 ± 1.41 (5)	75.50 ± 18.61 (4)
		Cycle 4 (D)	4.449 (3.186-5.104)	78 (71-82)	0.41 ± 0.06 (5)	4.46 ± 0.55 (5)	87.58 ± 12.09 (3)
		Cycle 4 (N)	0.321 (0.321-0.321)	39	1.42 (1)	8.5 (1)	44.46 (1)
		77/90	3.872 (3.892-3.892)	76	4.06 (1)	4.77 (1)	150.59 (1)
		90/120	2.727 (0.335-5.119)	66 (35-84)	0.55 ± 0.11 (3)	5.22 ± 1.27 (3)	50.15 (1)
	Lipolagus ochotensis	Cycle 2 (D)	3.083 (0.506-6.663)	62 (40-88)	0.94 ± 0.10 (5)	6.82 ± 0.57 (5)	84.13 ± 8.65 (5)
		Cycle 2 (N)	0.782 (0.274-1.820)	41 (30-58)	1.23 ± 0.05 (5)	8.55 ± 0.22 (5)	69.02 ± 7.24 (5)
		Cycle 4 (D)	3.911 (2.815-5.007)	70 (61-79)	0.48 ± 0.02 (2)	5.31 ± 0.31 (2)	78.07 ± 8.86 (2)
	Leuroglossus stilbius	82/47	2.671 (0.461-5.008)	63 (46-84)	0.68 ± 0.06 (4)	4.41 ± 0.32 (4)	30.93 ± 2.48 (2)
Gonostomatidae	*Cyclothone acclinidens*	Cycle 2 (D)	0.434 (0.110-0.916)	45 (28-55)	0.52 ± 0.07 (5)	3.42 ± 0.45 (5)	51.79 ± 19.07 (5)
		Cycle 4 (D)	0.462 (0.144-0.714)	45 (31-52)	0.74 ± 0.10 (5)	6.31 ± 1.58 (5)	57.58 ± 6.71 (5)
		Cycle 5 (D)	0.397 (0.210-0.522)	44 (34-49)	0.58 ± 0.03 (5)	3.53 ± 0.40 (5)	45.10 ± 4.71 (3)
		93/28(D)	0.084 (0.049-0.119)	26 (21,30)	0.17 ± 0.002 (2)		12.59 ± 6.60 (2)
	Cyclothone signata	Cycle 2 (D)	0.127 (0.087-0.165)	31 (28-33)	0.68 ± 0.11 (5)	5.49 ± 1.16 (5)	6.87 ± 1.52 (5)
		Cycle 4 (D)	0.114 (0.070-0.147)	28 (23-32)	0.96 ± 0.18 (5)	5.66 ± 0.77 (5)	11.72 ± 1.76 (5)
		Cycle 5 (D)	0.112 (0.071-0.157)	30 (24-37)	0.87 ± 0.14 (5)	5.71 ± 1.11 (5)	7.37 ± 1.65 (5)
		77/70	0.203 (0.050-0.640)	26 (22-32)	0.51 ± 0.03 (5)	10.45 ± 1.46 (5)	7.45 ± 1.15 (3)
		80/60	0.096 (0.052-0.154)	27 (22-32)	0.64 ± 0.09 (4)	4.96 ± 0.43 (3)	10.09 ± 1.27 (4)
		87/90	0.097 (0.058-0.124)	28 (22-30)	0.45 ± 0.04 (7)	3.56 ± 0.41 (7)	2.56 ± 0.80 (7)
		93/28 (D)	0.092 (0.058-0.125)	25 (21-30)	0.36 ± 0.02 (3)	4.83 ± 0.28 (3)	8.59 ± 3.10 (3)
Melamphaidae	*Memphaes parvus*	90/120	0.819	35	0.70 (1)	14.23 (1)	
Myctophidae	*Ceratoscopelus townsendi*	77/70	0.904 (0.329-2.195)	40 (31-55)	2.18 ± 0.19 (5)	12.35 ± 2.10 (5)	80.24 ± 19.09 (4)
		77/90	1.425 (0.661-3.394)	46 (38-62)	2.04 ± 0.13 (6)	17.11 ± 1.26 (5)	99.96 ± 36.07 (6)
		83/90	1.522 (0.500-2.344)	46 (35-55)	1.94 ± 0.11 (5)	14.03 ± 0.52 (5)	55.04 ± 12.49 (5)
		87/70	0.442 (0.244-0.743)	33 (28-40)	1.00 ± 0.32 (3)	13.84 ± 3.28 (3)	12.27 ± 3.36 (3)
		87/90	0.653	32	0.77 (1)	16.24 (1)	24.43 (1)
		90/120	1.367 (0.676-2.056)	45 (38-53)	2.00 ± 0.09 (6)	14.09 ± 0.95 (6)	

Appendix 3.1. Enzyme activities, Continued.

Family	Species	Station	Mass (g)	Length (mm)	Enzyme Activity (Units g-1 ww) CS (± SE, n)	MDH (± SE, n)	LDH (± SE, n)
		93/110	0.263 (0.239-0.286)	29 (28-30)	1.87 ± 0.01 (2)	13.10 ± 1.92 (2)	11.65 ± 0.17 (2)
	Diaphus theta	77/70	0.208 (0.156-0.254)	24 (22-25)	1.53 ± 0.51 (3)	17.69 ± 6.36 (3)	23.7 ± 2.30 (4)
		77/90	0.154 (0.136-0.185)	23 (21-26(		16.27 ± 0.86 (2)	19.87 ± 6.20 (3)
		80/60	0.739 (0.223-2.730)	25 (24-27)	2.95 ± 0.30 (5)	20.17 ± 2.34 (5)	26.05 ± 5.56 (5)
		87/35	2.220	46	2.34 (1)	14.91 (1)	17.74 (1)
		87/70	1.794 (1.112-2.475)	46 (40-52)	2.99 ± 0.04 (2)	22.08 ± 1.73 (2)	26.12 ± 1.75 (2)
		90/120	0.196 (0.168-0.224)	22 (20-24)	2.54 ± 0.03 (2)	16.90 ± 1.19 (2)	17.38 (1)
		90/45	0.235 (0.205-0.263)	24 (22-25)	1.61 ± 0.82 (2)	24.34 ± 1.20 (3)	22.83 ± 2.54 (3)
		93/28(D)	1.110 (0.084-3.924)	31 (17-57)	2.20 ± 0.19 (3)	15.17 ± 0.77 (4)	17.02 ± 3.43 (4)
	Nannobrachium ritteri	Cycle 2 (D)	2.865 (1.190-5.255)	64 (49-82)	0.98 ± 0.11 (5)	6.5 ± 0.52 (5)	14.26 ± 2.44 (5)
		Cycle 2 (N)	1.729 (0.217-2.660)	54 (40-65)	1.05 ± 0.09 (5)	6.24 ± 0.41 (5)	11.38 ± 1.07 (5)
		Cycle 4 (D)	4.560 (0.822-9.082)	72 (45-101)	0.97 ± 0.20 (5)	7.02 ± 0.39 (5)	11.85 ± 1.25 (5)
		Cycle 4 (N)	2.694 (0.530-6.983)	58 (38-85)	0.71 ± 0.09 (5)	5.28 ± 0.36 (5)	9.48 ± 1.64 (5)
		Cycle 5 (D)	5.446 (0.807-10.398)	77 (48-100)	0.81 ± 0.20 (4)	6.5 ± 0.33 (4)	17.14 ± 3.88 (4)
		77/90	2.008 (1.348-2.427)	61 (52-68)	0.88 ± 0.25 (3)	9.9 ± 2.27 (3)	10.81 ± 1.27 (3)
		80/60	3.158 (2.280-4.776)	68 (60-79)	0.71 ± 0.06 (6)	5.59 ± 0.61 (6)	11.91 ± 1.84 (6)
		82/47	1.323	54	0.22 (1)	5.13 (1)	10.92 (1)
		83/90	0.875 (0.564-1.513)	47 (40-56)	0.97 ± 0.03 (4)	5.43 ± 0.39 (4)	8.58 ± 0.28 (4)
		87/70	2.750 (0.675-7.196)	59 (43-80)	1.06 ± 0.09 (5)	8.00 ± 0.20 (5)	10.11 ± 1.29 (5)
		90/120	1.425 (0.737-3.355)	48 (35-62)	1.08 ± 0.15 (5)	5.18 ± 0.62 (5)	9.47 (1)
		90/45	2.325 (0.375-5.623)	51 (34-78)	0.99 ± 0.10 (5)	5.99 ± 0.47 (5)	11.91 ± 0.61 (3)
		93/28(D)	3.585 (2.149-7.605)	66 (57-85)	0.70 ± 0.13 (4)	4.96 ± 0.62 (4)	12.46 ± 5.76 (4)
		93/28(N)	0.779 (0.216-1.730)	42 (30-56)	0.81 ± 0.05 (8)	6.01 ± 0.41 (8)	7.86 ± 1.07 (8)
	Protomyctophum crockeri	Cycle 2 (D)	0.488 (0.217-1.098)	27 (21-40)	1.98 ± 0.37 (5)	25.42 ± 1.01 (5)	45.08 ± 9.14 (5)
		Cycle 4 (D)	1.065 (1.065-1.065)	39 (34-39)	2.32 ± 0.46 (5)	26.95 ± 2.03 (5)	50.38 ± 9.05 (5)
		Cycle 5 (D)	0.126 (0.084-0.186)	18 (15-23)	2.41 ± 0.56 (5)	22.99 ± 5.02 (5)	32.66 ± 10.83 (5)
	Symbolophorus californiensis	Cycle 2 (D)	2.415 (0.329-7.351)	50 (33-82)	2.42 ± 0.20 (8)	20.38 ± 1.37 (8)	116.24 ± 29.16 (7)
		Cycle 4 (D)	3.197 (0.156-9.967)	58 (27-93)	1.65 ± 0.13 (7)	17.31 ± 1.82 (7)	155.22 ± 30.57 (6)
		Cycle 4 (N)	3.079 (0.264-9.533)	51 (31-90)	2.60 ± 0.19 (6)	22.98 ± 1.64 (6)	62.30 ± 23.53 (6)
		77/90	0.444	35	2.00 (1)	17.54 (1)	43.76 (1)
		83/90	0.578 (0.198-1.193)	36 (29-47)	0.42 ± 0.03 (3)	16.82 ± 0.99 (3)	36.81 ± 11.82 (3)
		87/70	0.296	32	1.89 (1)	16.19 (1)	20.20 (1)
		90/120	0.687 (0.222-1.151)	40 (30-50)	1.15 ± 0.35 (3)	13.13 ± 3.41 (3)	14.10 ± 3.18 (2)
		93/28(D)	0.813 (0.371-1.255)	41 (33,48)	1.82 ± 0.10 (2)	17.56 ± 2.04 (2)	49.05 ± 13.47 (2)
	Stenobrachius leucopsarus	Cycle 2 (D)	1.795 (0.851-5.055)	53 (44-78)	1.71 ± 0.07 (7)	13.92 ± 0.72 (7)	32.50 ± 2.42 (7)
		Cycle 2 (N)	1.375 (0.136-2.965)	47 (23-62)	1.53 ± 0.15 (7)	14.03 ± 1.59 (7)	31.38 ± 4.47 (7)

Appendix 3.1. Enzyme activities, Continued.

Family	Species	Station	Mass (g)	Length (mm)	Enzyme Activity (Units g-1 ww) CS (± SE, n)	MDH (± SE, n)	LDH (± SE, n)
		Cycle 4 (D)	0.380 (0.088-0.785)	31 (20-41)	1.73 ± 0.16 (3)	12.96 ± 0.33 (7)	16.23 ± 1.33 (3)
		Cycle 5 (D)	0.068	20	0.87 (1)	6.92 (1)	9.12 (1)
		77/70	3.468 (0.450-5.596)	62 (36-73)	1.43 ± 0.16 (4)	12.4 ± 1.37 (4)	54.45 (1)
		77/90	1.084 (0.293-2.529)	43 (33-60)	1.51 ± 0.19 (3)	12.99 ± 0.46 (3)	26.38 ± 8.49 (3)
		80/60	3.893 (3.292-4.523)	68 (64-73)	0.97 ± 0.10 (4)	12.56 ± 0.90 (4)	30.82 ± 1.14 (4)
		82/47	0.859 (0.455-1.628)	45 (32-58)	1.19 ± 0.02 (5)	11.28 ± 1.15 (5)	20.74 ± 1.85 (5)
		87/35	0.357 (0.261-0.478)	31 (28-34)	1.50 ± 0.15 (4)	10.6 ± 0.87 (4)	12.78 ± 2.47 (5)
		87/70	0.406 (0.177-0.675)	33 (27-39)	2.11 ± 0.27 (3)	18.84 ± 1.31 (3)	26.85 ± 9.27 (3)
		90/120	4.034 (3.213-4.855)	68 (63,73)	0.96 ± 0.05 (2)	9.92 ± 0.61 (2)	20.41 ± 14.43 (2)
		90/45	1.801 (0.236-4.184)	49 (28-71)	1.23 ± 0.10 (5)	13.31 ± 2.01 (5)	35.44 ± 4.64 (4)
		93/28(D)	2.501 (1.124-4.412)	59 (48-70)	1.06 ± 0.07 (3)	6.21 ± 0.73 (3)	16.75 ± 7.24 (3)
		93/28(N)	1.930 (0.643- 3.627)	55 (39-69)	1.03 ± 0.07 (7)	14.14 ± 0.83 (7)	39.21 ± 6.50 (7)
	Triphotorus mexicanus	Cycle 2 (D)	1.065 (0.484-1.755)	48 (37-58)	1.20 ± 0.28 (5)	11.32 ± 2.03 (5)	65.06 ± 18.43 (5)
		Cycle 2 (N)	0.801 (0.374-1.473)	44 (36-55)	1.61 ± 0.16 (5)	13.41 ± 0.77 (5)	49.72 ± 9.61 (5)
		Cycle 4 (D)	1.657 (1.316-2.129)	58 (54-62)	1.13 ± 0.12 (5)	11.49 ± 0.83 (5)	50.59 ± 12.17 (5)
		Cycle 4 (N)	0.913 (0.457-2.129)	46 (39-56)	1.28 ± 0.13 (5)	12.74 ± 1.07 (5)	35.97 ± 9.70 (5)
		77/90	0.998 (0.940,1.055)	50 (50, 50)	1.00 ± 0.09 (2)	13.65 ± 1.36 (2)	47.01 ± 4.26 (2)
		87/35	0.393 (0.168-0.478)	34 (27-48)	1.18 ± 0.05 (4)	9.22 ± 0.39 (4)	23.87 ± 9.00 (4)
		90/120	1.524 (0.712-1.996)	55 (46-61)	1.23 ± 0.05 (4)	12.94 ± 1.65 (4)	45.10 ± 2.10 (4)
		90/45	2.190 (1.624-2.750)	63 (58-68)	0.76 ± 0.06 (4)	7.18 ± 1.32 (4)	46.26 ± 4.65 (4)
		93/28(D)	0.614 (0.388-0.754)	42 (37-45)	1.61 ± 0.10 (5)	12.90 ± 0.69 (5)	27.09 ± 1.57 (5)
		93/28(N)	1.868 (1.164-2.477)	59 (54-64)	1.00 ± 0.12 (7)	12.53 ± 0.89 (7)	40.60 ± 5.90 (7)
Phosichthyidae	*Vinciguerria lucetia*	Cycle 4 (D)	0.058	17	2.26 (1)	26.49 (1)	18.00 (1)
		Cycle 4 (N)	0.064 (0.040-0.085)	20 (18-22)	2.27 ± 0.34 (4)	25.98 ± 1.43 (4)	31.39 ± 5.08 (4)
		Cycle 5 (D)	0.080 (0.058-0.100)	20 (18-22)	1.86 ± 0.35 (5)	28.30 ± 4.88 (5)	22.30 ± 5.29 (4)
		Cycle 5 (N)	0.489 (0.089-1.138)	34 (22-56)	3.58 ± 0.40 (7)	41.91 ± 4.76 (7)	29.10 ± 4.7 (6)
		83/90	0.048 (0.026-0.064)	19 (17-22)	2.03 ± 0.52 (3)	13.54 ± 6.82 (3)	18.14 ± 1.44 (3)
		87/35	0.066	20	1.62 (1)	24.73 (1)	29.32 (1)
		87/70	0.100	24	4.06 (1)	44.04 (1)	35.02 (1)
		90/120	0.528 (0.030-1.517)	29 (17-52)	1.62 ± 0.67 (3)	37.25 ± 4.40 (2)	30.59 (1)
		90/45	0.072 (0.043-0.099)	20 (17-23)	1.02 ± 0.20 (3)	17.78 ± 5.25 (5)	35.07 ± 3.44 (5)
		93/28(D)	.055 (0.050-0.059)	19	1.54 ± 0.44 (3)	26.45 ± 2.00 (3)	26.48 ± 6.73 (3)
Sternoptychidae	*Argyropelecus affinis*	Cycle 2 (D)	0.514 (0.267-0.761)	34 (25-47)	1.10 ± 0.14 (4)	7.68 ± 0.86 (4)	25.48 ± 7.12 (4)
		Cycle 4 (D)	2.277 (0.2870-4.329)	43 (24-59)	1.18 ± 0.12 (5)	8.21 ± 0.85 (5)	28.37 ± 7.10 (5)
		77/70	2.986 (0.446-5.503)	49 (29-62)	0.84 ± 0.05 (4)	7.67 ± 0.45 (4)	27.47 ± 3.35 (4)
		80/60	1.174 (0.309-2.010)	33 (16-46)	1.15 ± 0.11 (5)	7.25 ± 0.15 (4)	32.62 ± 6.69 (5)
		87/90	1.501 (1.210-2.319)	41 (39-45)	1.33 ± 0.18 (5)	7.98 ± 0.60 (5)	27.63 ± 2.02 (5)
		93/110	3.150 (0.198-7.493)	46 (23-67)	0.73 ± 0.14 (6)	6.75 ± 0.70 (6)	15.77 ± 4.57 (6)

Appendix 3.1. Enzyme activities, Continued.

					Enzyme Activity (Units g-1 ww)		
Family	**Species**	**Station**	**Mass (g)**	**Length (mm)**	**CS (± SE, n)**	**MDH (± SE, n)**	**LDH (± SE, n)**
		93/28(D)	4.639 (2.989- 6.288)	56 (49-62)	0.62 ± 0.03 (2)	8.09 ± 1.87 (2)	18.61 ± 0.56 (2)
	Argyropelecus hemigymnus	Cycle 4 (D)	0.563 (0.354-0.700)	28 (25-31)	2.02 ± 0.34 (5)	17.71 ± 2.23 (5)	63.64 ± 5.19 (5)
	Argyropelecus lychnus	87/70	0.945	30	1.10 (1)	22.48 (1)	56.55 ± 48.27 (2)
		90/120	0.990	31	1.63 (1)		
	Argyropelecus sladeni	Cycle 2 (D)	0.408 (0.198-0.768)	24 (19-29)	1.27 ± 0.19 (6)	13.87 ± 1.98 (6)	13.64 ± 1.29 (6)
		77/70	2.339 (2.084-2.593)	45 (43-46)	1.89 ± 0.75 (2)	11.56 (1)	31.58 ± 1.59 (2)
		83/90	0.951 (0.581-1.277)	31 (27-33)	1.85 ± 0.23 (3)		28.25 ± 6.43 (3)
		87/35	0.928 (0.521-1.334)	31 (27-35)	1.54 ± 0.06 (2)	14.48 ± 0.94 (2)	18.90 ± 0.91 (2)
		87/90	1.460 (1.074-1.845)	36 (34-38)	2.05 ± 0.48 (2)	19.86 ±0.39 (2)	21.86 ± 2.96 (3)
		93/28(D)	1.181 (0.761-1.854)	33 (28-39)	1.34 ± 0.11 (6)	18.25 ± 1.69 (6)	27.23 ± 1.85 (2)
Stomiidae	*Idiacanthus antrostomus*	Cycle 2 (D)	3.719 (0.137-17.549)	134 (65-337)	0.51 ± 0.08 (5)	4.78 ± 0.91 (5)	13.62 ± 1.81 (5)
		Cycle 2 (N)	1.157 (0.131-3.332)	126 (61-209)	0.39 ± 0.05 (5)	3.19 ± 0.15 (5)	11.56 ± 1.40 (5)
		Cycle 4 (D)	0.179 (0.137-0.239)	78 (71-84)	0.41 ± 0.03 (5)	4.08 ± 0.23 (5)	19.82 ± 4.16 (5)
		Cycle 4 (N)	1.292 (0.015-3.239)	116 (55-193)	0.36 ± 0.05 (5)	3.93 ± 0.31 (5)	21.46 ± 3.23 (5)
		Cycle 5 (D)	0.378 (0.152-1.216)	95 (67-155)	0.28 ± 0.05 (5)	2.38 ± 0.49 (5)	11.15 ± 3.67 (5)
		Cycle 5 (N)	0.549 (0.150-1.676)	109 (80-165)	0.40 ± 0.07 (5)	2.36 ± 0.17 (5)	10.09 ± 0.68 (5)
		90/120	0.264	95	0.32 (1)	4.85 (1)	14.73 (1)
	Stomias atriventer	93/28(N)	1.556 (0.888-2.224)	140 (79, 200)	0.17 ± 0.01 (2)	3.13 ± 0.97 (2)	12.09 ± 3.60 (2)

Appendix 3.2. Plots by species of measured enzyme activities against the concentration of dissolved oxygen at 300 m (measured at the station where the corresponding specimen was collected) for: (a) Citrate Synthase (b) Malate Dehydrogenase, and (c) Lactate Dehydrogenase. Panel (d) is the LDH:CS ratio. Units (U) are µmoles of substrate converted per minute. Points are color-coded by family.

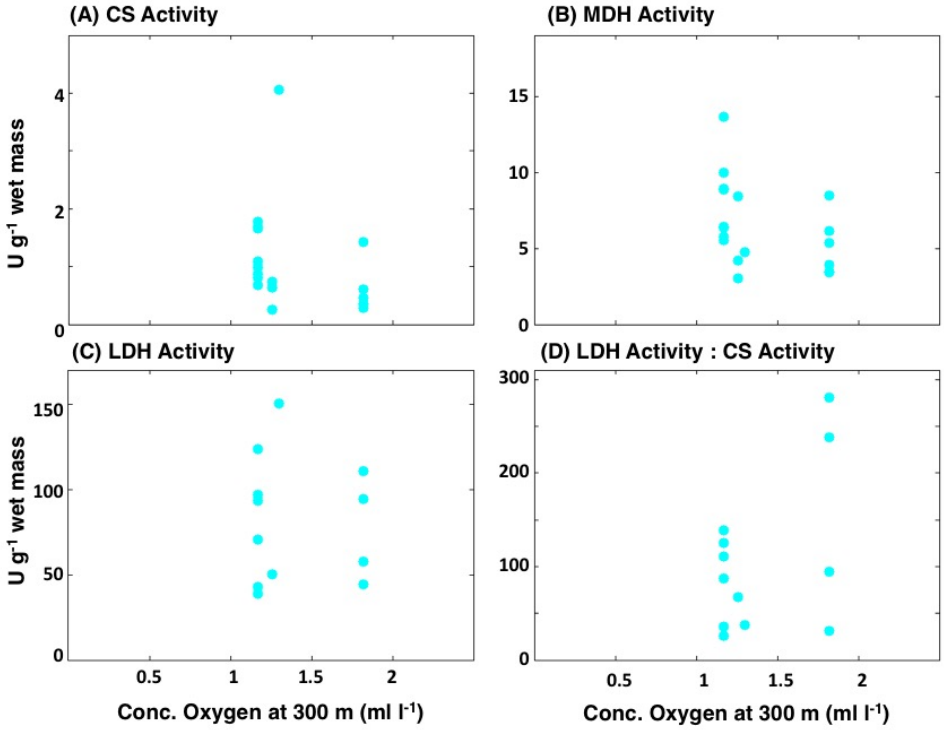

Appendix 3.2.1. *Bathylagoides wesethi*

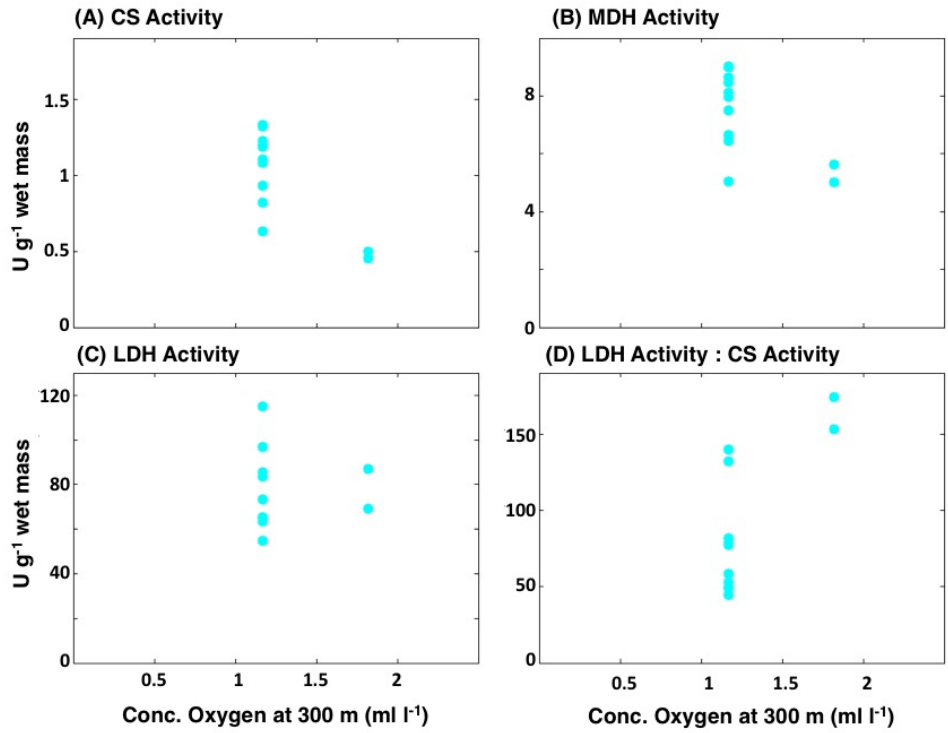

Appendix 3.2.2. *Lipolagus ochotensis*

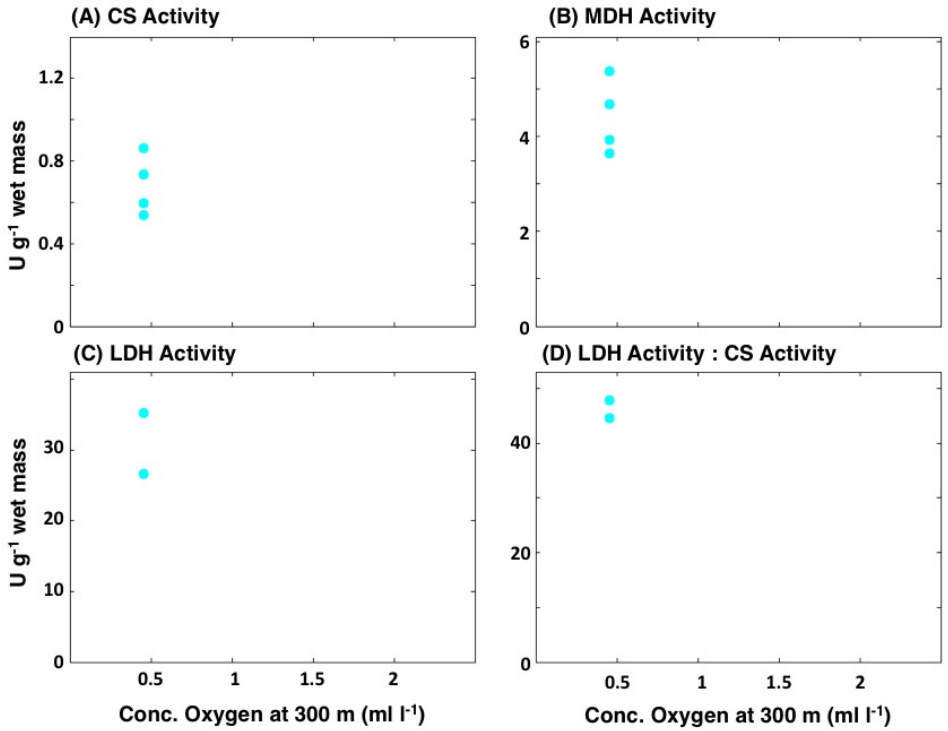

Appendix 3.2.3. *Leuroglossus stilbius*

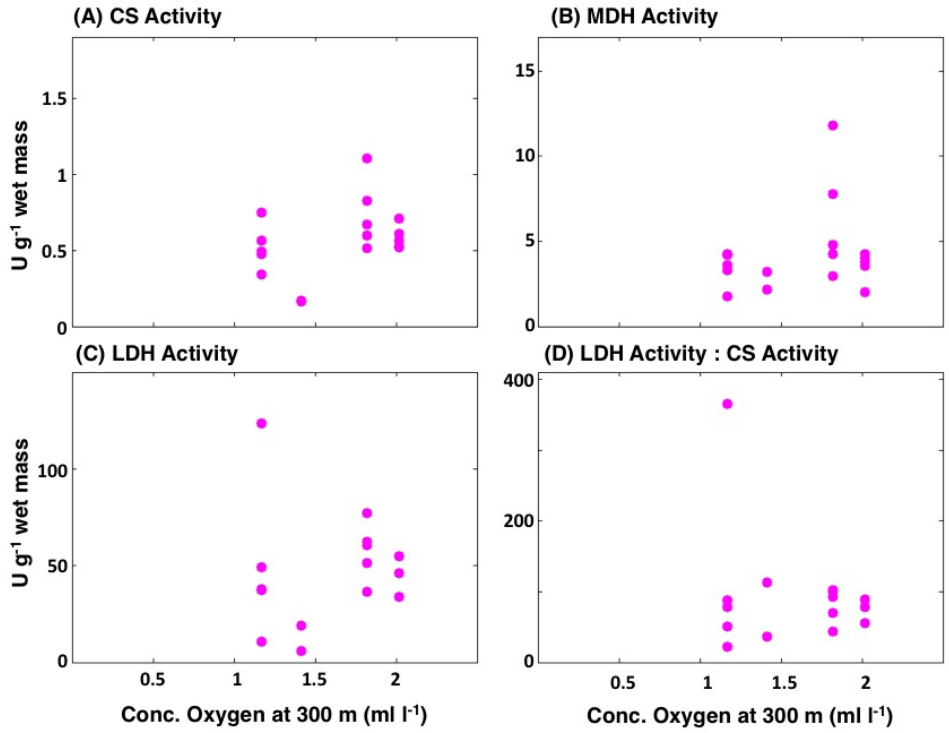

Appendix 3.2.4. *Cyclothone acclinidens*

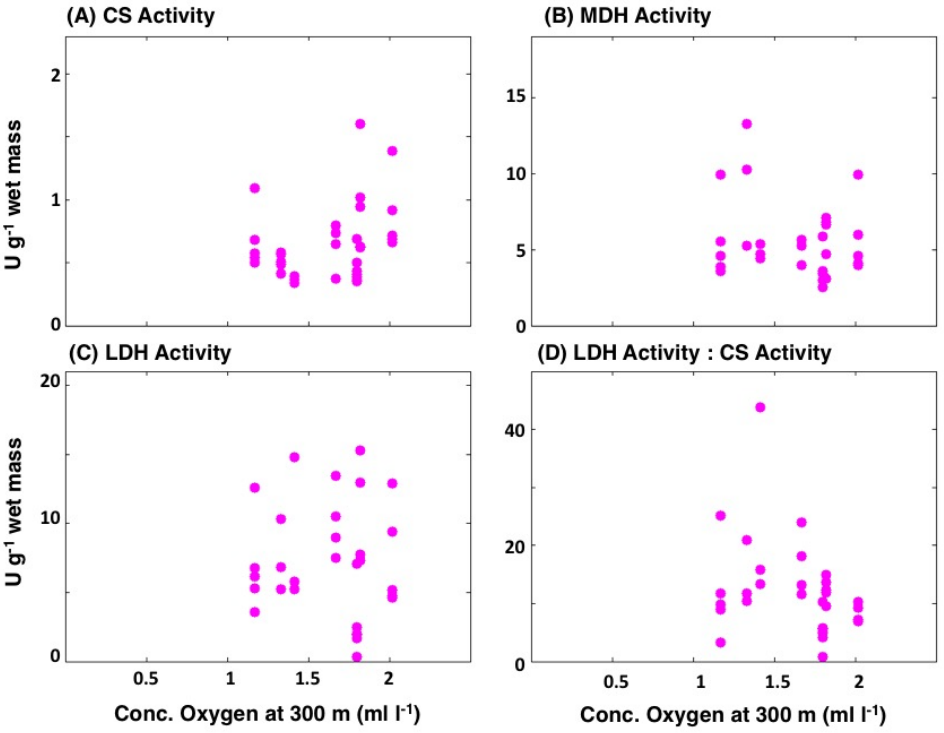

Appendix 3.2.5. *Cyclothone signata*

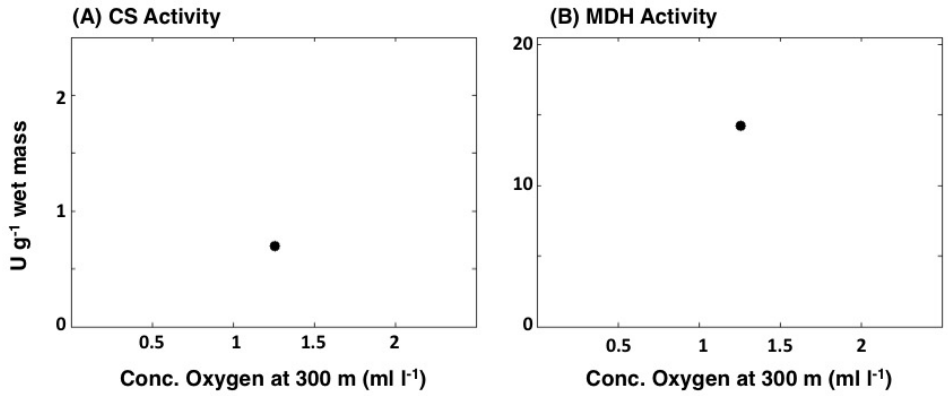

Appendix 3.2.6. *Melamphaes parvus* (No measurements were available of LDH activity)

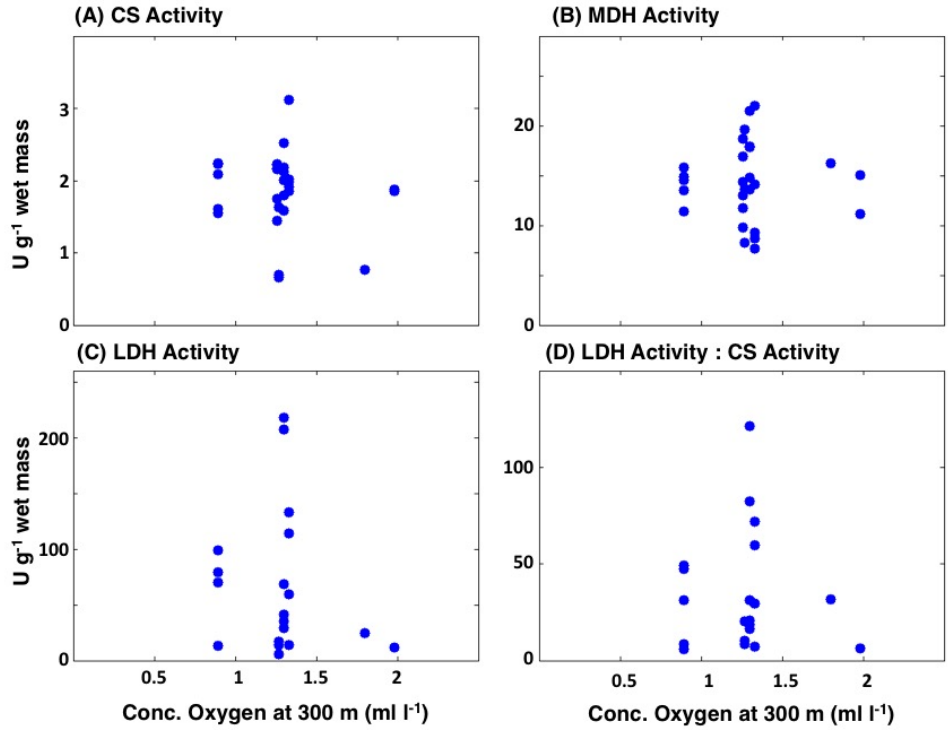

Appendix 3.2.7. *Ceratoscopelus townsendi*

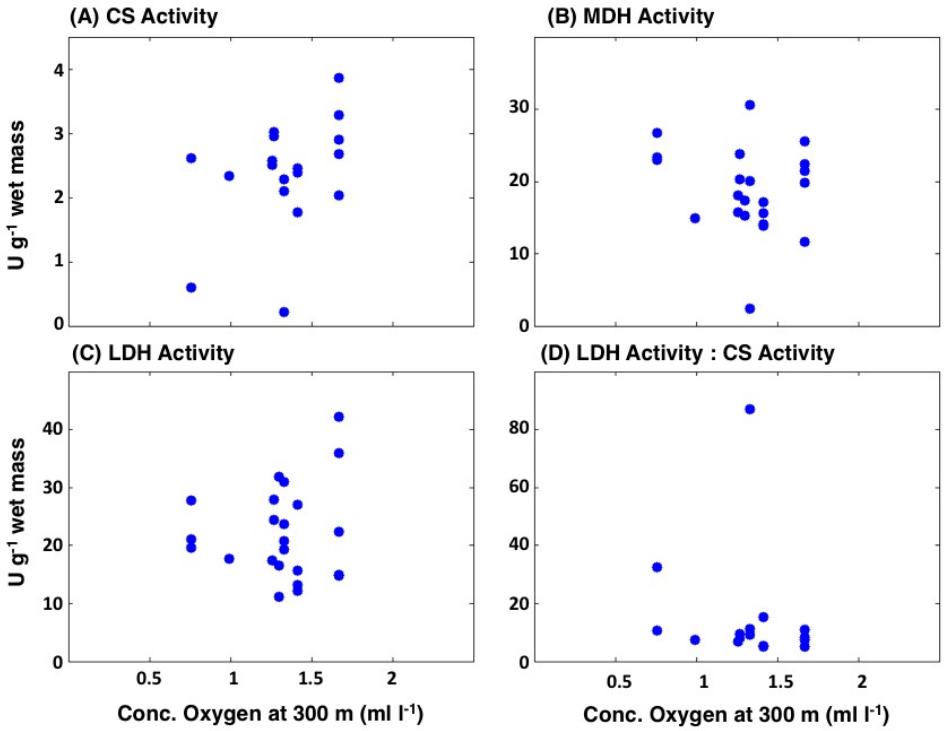

Appendix 3.2.8. *Diaphus theta*

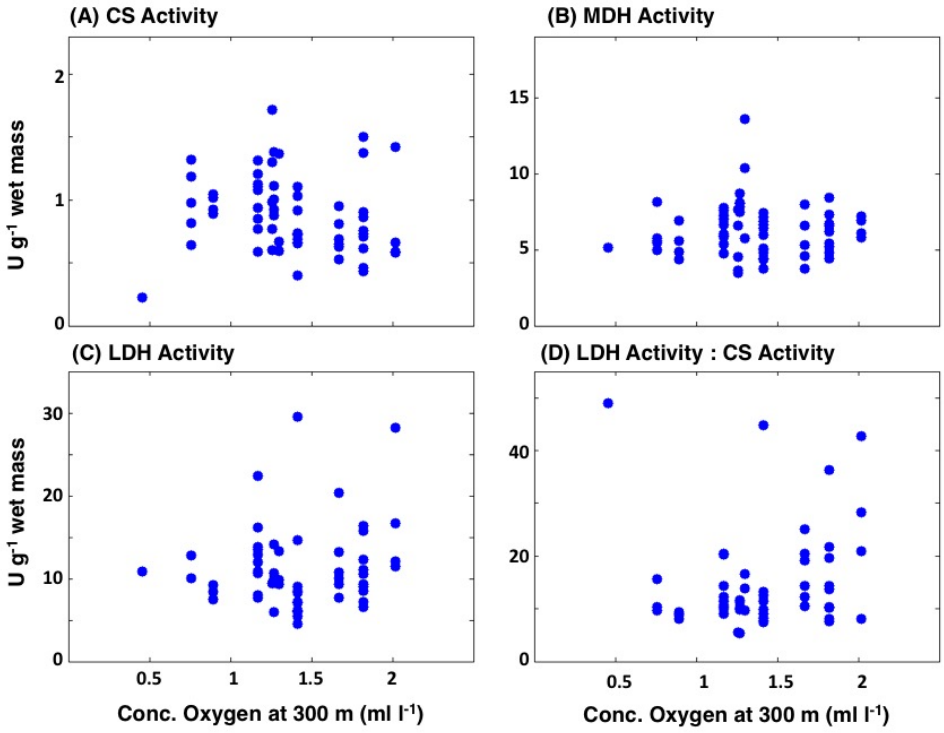

Appendix 3.2.9. *Nannobrachium ritteri*

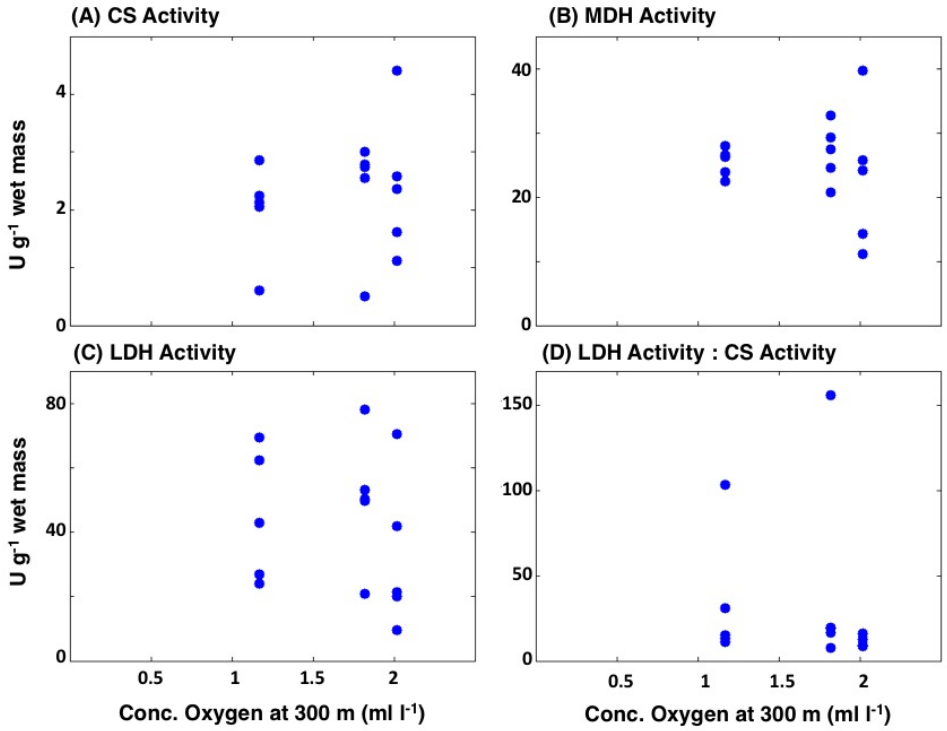

Appendix 3.2.10. *Protomyctophum crockeri*

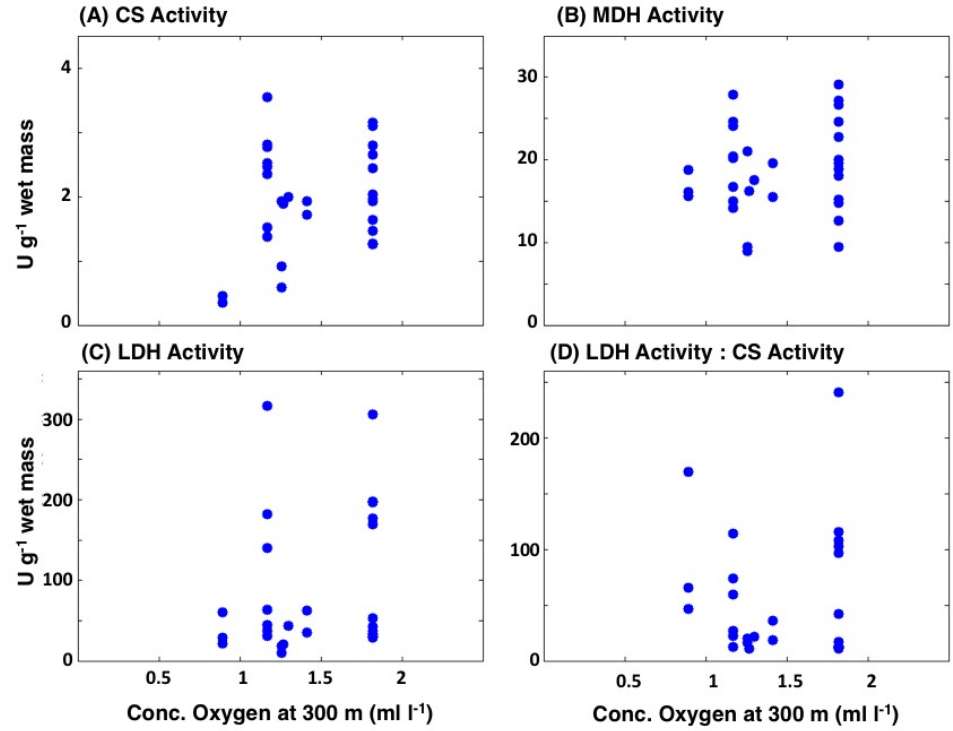

Appendix 3.2.11. *Symbolophorus californiensis*

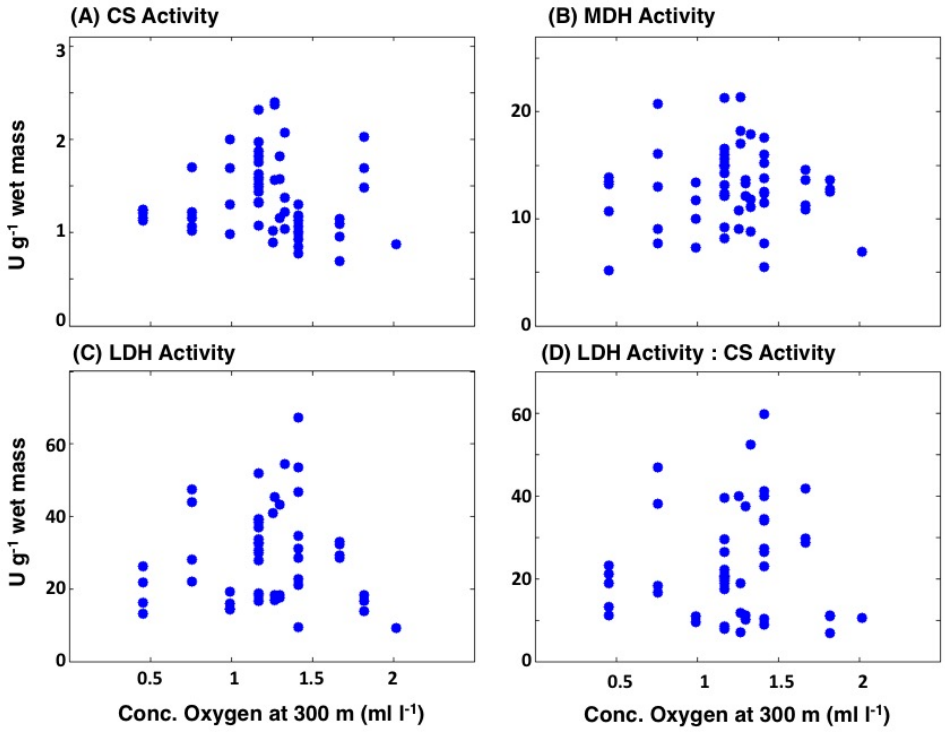

Appendix 3.2.12. *Stenobrachius leucopsarus*

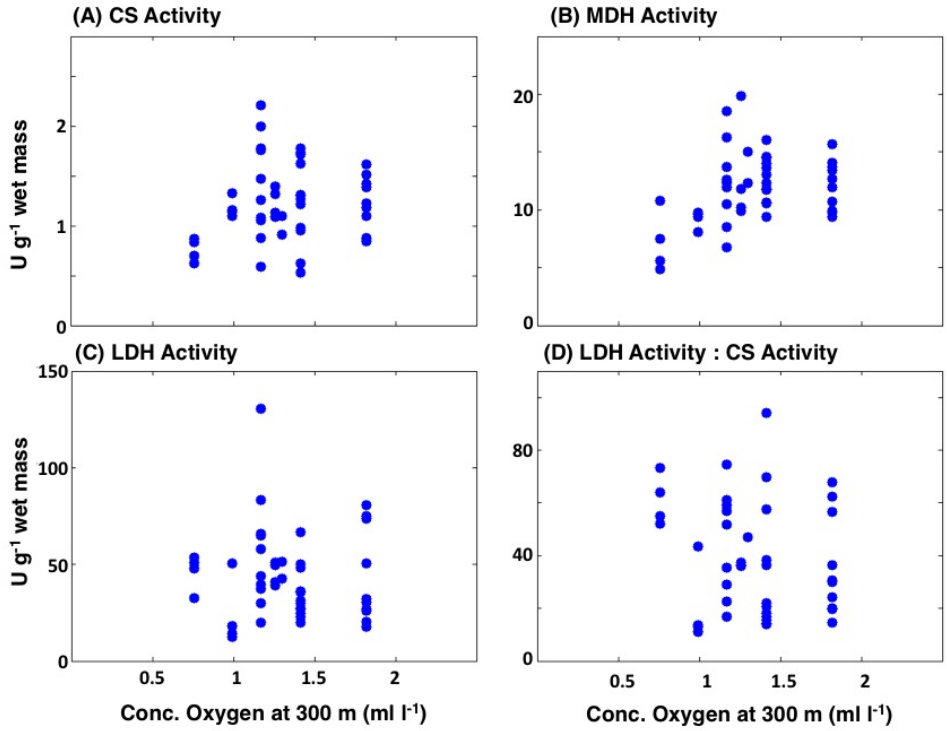

Appendix 3.2.13. *Triphotorus mexicanus*

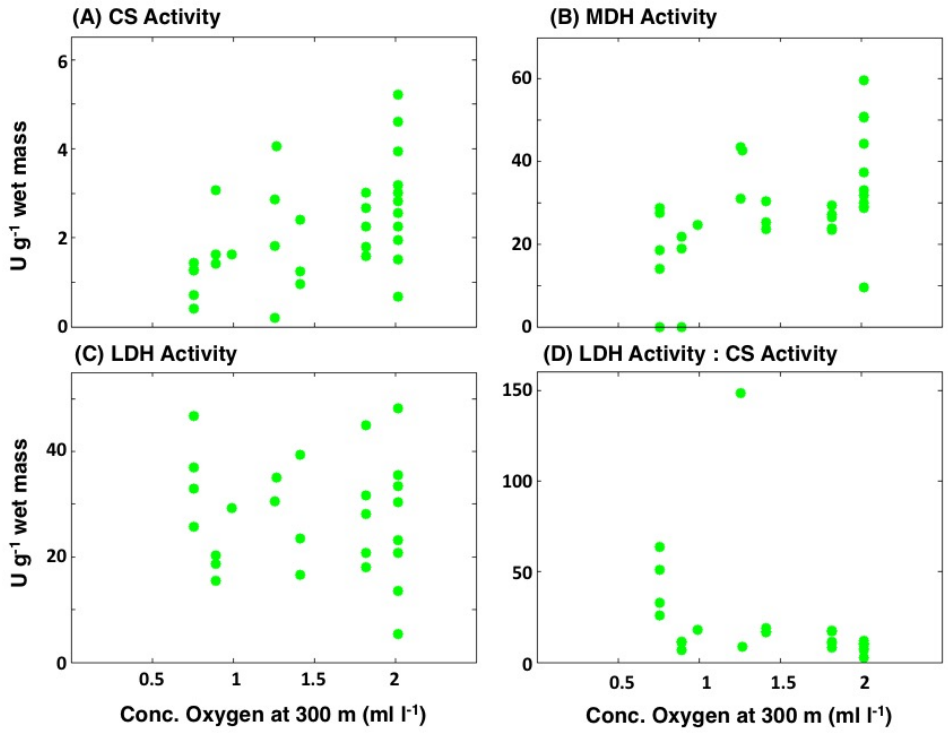

Appendix 3.2.14. *Vinciguerria lucetia*

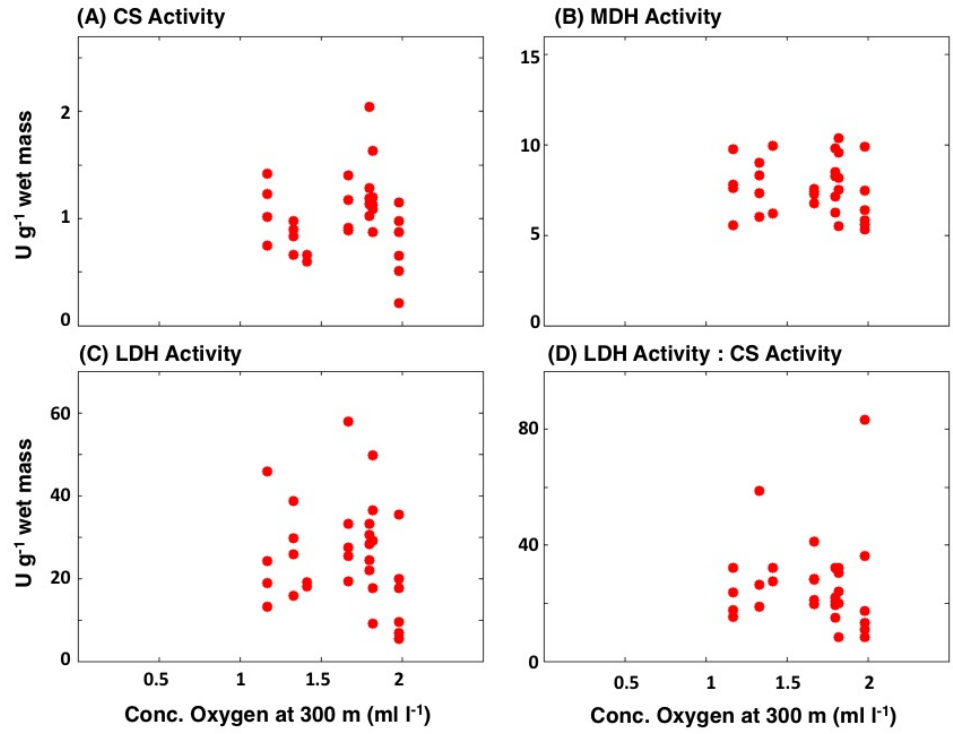

Appendix 3.2.15. *Argyropelecus affinis*

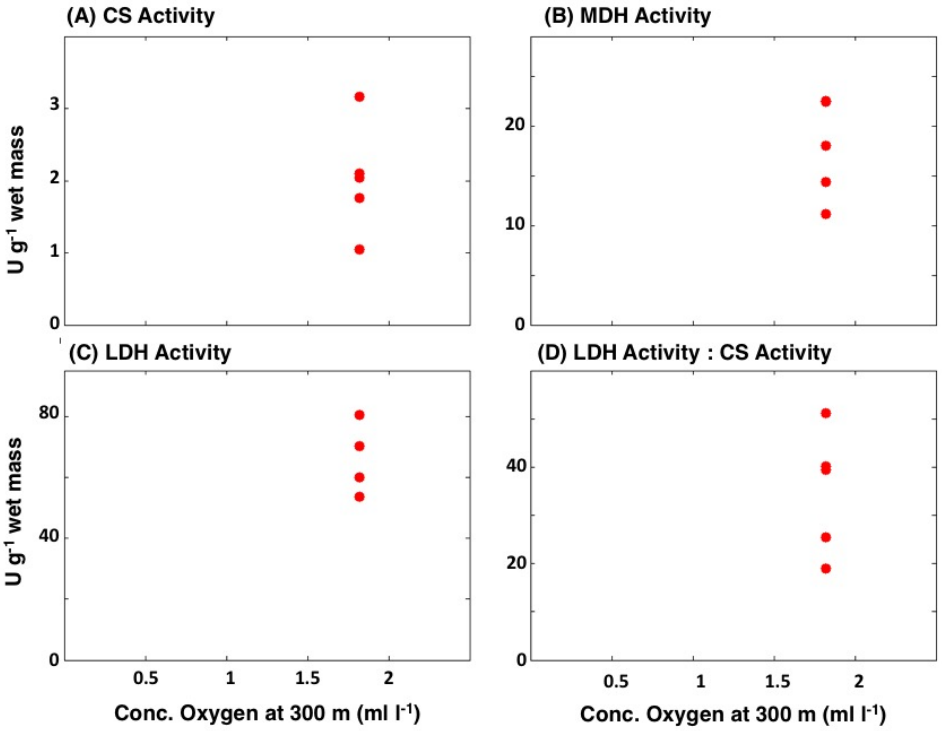

Appendix 3.2.16. *Argyropelecus hemigymnus*

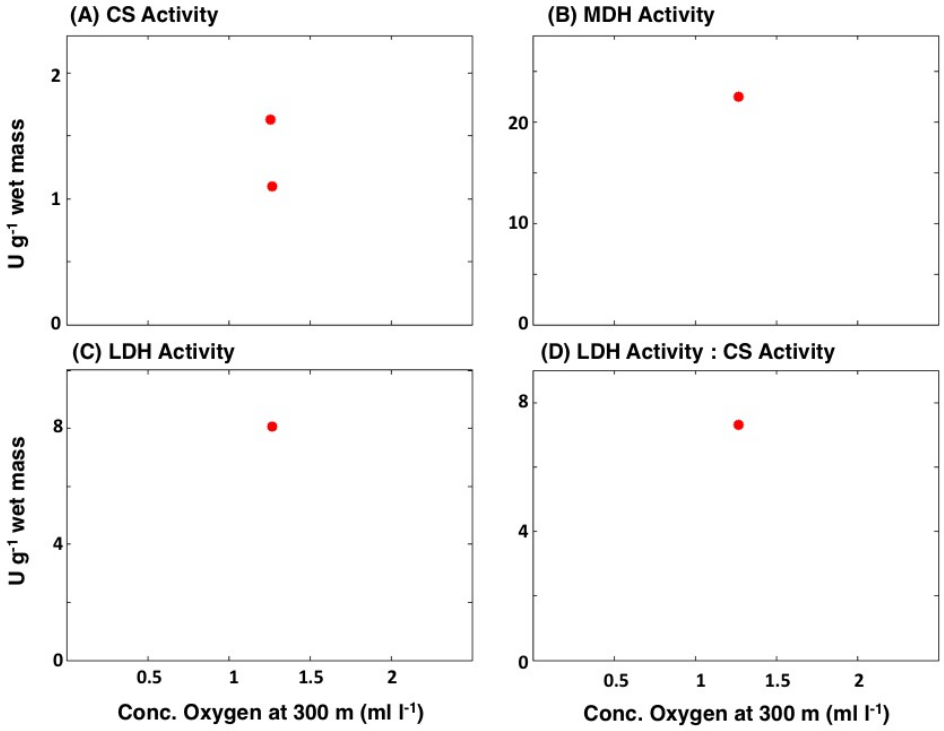

Appendix 3.2.17. *Argyropelecus lychnus*

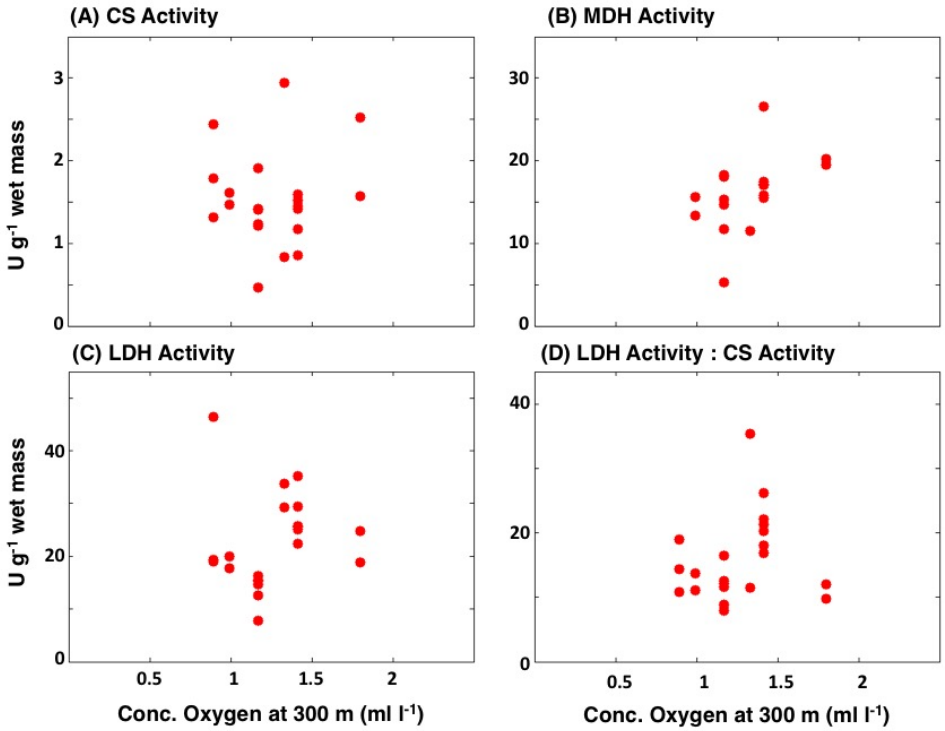

Appendix 3.2.18. *Argyropelecus sladeni*

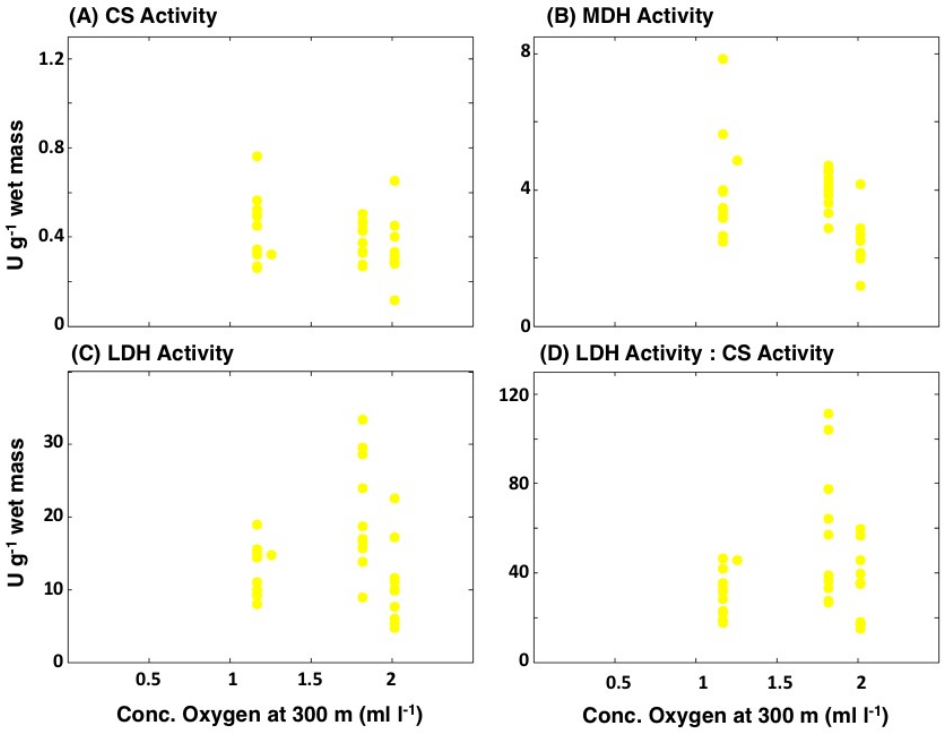

Appendix 3.2.19. *Idiacanthus antrostomus*

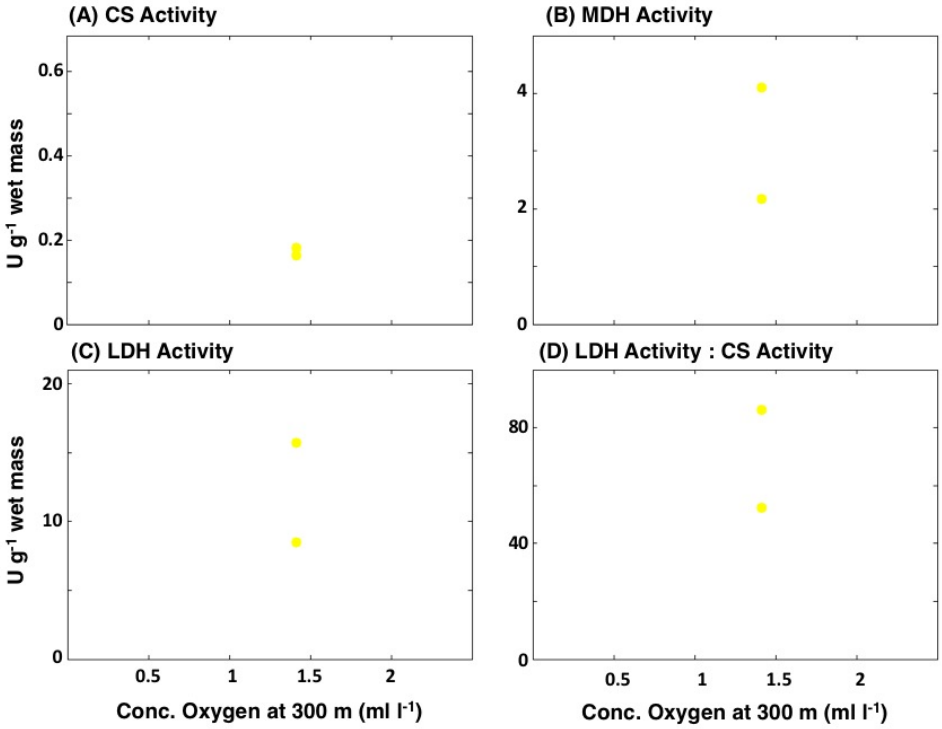

Appendix 3.2.20. *Stomias atriventer*

Appendix 3.3. A) CS, B) MDH, and C) LDH enzyme activities plotted against minimum depth of occurrence (A: *Protomyctophum crockeri*, B: *Argyropelecus hemigymnus*, C: *Argyropelecus sladeni*, D: *Argyropelecus lychnus*, E: *Argyropelecus affinis*, F: *Cyclothone signata*, G: *Cyclothone acclinidens*, H: *Stomias atriventer*, I: *Vinciguerria lucetia*, J: *Diaphus theta*, K: *Symbolophorus californiensis*, L: *Ceratoscopelus townsendi*, M: *Stenobrachius leucopsarus*, N: *Triphotorus mexicanus*, O: *Nannabrachium ritteri*, P: *Bathylagoides wesethi*, Q: *Lipologus ochotensis*, R: *Leuroglossus stilbius*, S: *Melamphaes parvus*, T: *Idiacanthus antrostomus*).

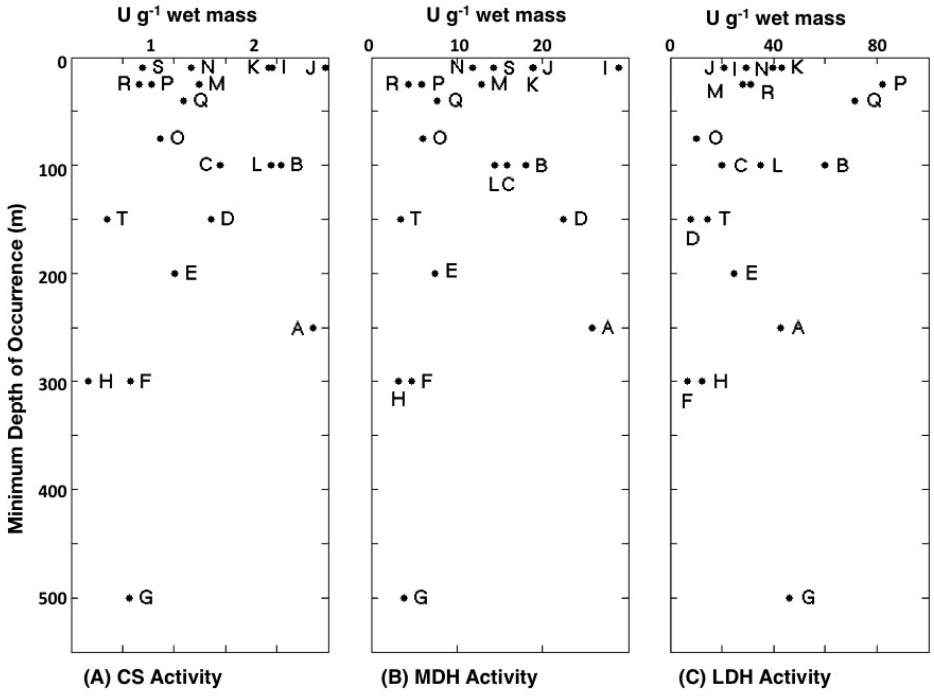

Appendix 3.4. Back of the envelope calculation of fish-mediated oxygen consumption in a 200 m thick midwater layer.

Given a range of oxygen consumption rates of 0.01-0.1 μmol O^2 mg^{-1} h^{-1} (Childress), a mean biomass of mesopelagic fishes of 25 g m^{-2} (Davison 2013), and assuming that biomass is confined to a layer 200 m thick, we estimate a fish-mediated oxygen consumption rate of 0.012-12 μmol O_2 h^{-1}, which is negligible compared to the oxygen contained in that layer (20,000,000 μmol O^2 m^{-2} over a 200 m layer, assuming an ambient oxygen concentration of 100 μmol O^2 kg^{-1}).

3.11 References

Bailey TG, Robison BH (1986) Food availability as a selective factor on the chemical compositions of midwater fishes in the eastern North Pacific. Mar Biol 91:131–141

Barham EG (1971) Deep-sea fishes: lethargy and vertical orientation. In: Farquhar GB (ed) Proceedings of the International Symposium on Biological Sound Scattering in the Ocean.p 100–118

Benfield MC, Lavery AC, Wiebe PH, Greene CH, Stanton TK, Copley NJ (2003) Distributions of physonect siphonulae in the Gulf of Maine and their potential as important sources of acoustic scattering. Can J Fish Aquat Sci 60:759–772

Bianchi D, Galbraith ED, Carozza DA, Mislan K, Stock CA (2013) Intensification of open-ocean oxygen depletion by vertically migrating animals. Nat Geosci 6:545–548

Bickler PE, Buck LT (2007) Hypoxia tolerance in reptiles, amphibians, and fishes: life with variable oxygen availability. Annu Rev Physiol 69:145–170

Bograd SJ, Buil MP, Lorenzo E Di, Castro CG, Schroeder ID, Goericke R, Anderson CR, Benitez-Nelson C, Whitney FA (2014) Changes in source waters to the Southern California Bight. Deep Sea Res Part II Top Stud Oceanogr:1–11

Bograd SJ, Castro CG, Lorenzo E Di, Palacios DM, Bailey H, Gilly W, Chavez FP (2008) Oxygen declines and the shoaling of the hypoxic boundary in the California Current. Geophys Res Lett 35:1–6

Bopp L, Resplandy L, Orr JC, Doney SC, Dunne JP, Gehlen M, Halloran P, Heinze C, Ilyina T, Séférian R, Tjiputra J, Vichi M (2013) Multiple stressors of ocean ecosystems in the 21st century: Projections with CMIP5 models. Biogeosciences 10:6225–6245

Childress JJ (1995) Are there physiological and biochemical adaptations of metabolism in deep-sea animals? Trends Ecol Evol 10:30–36

Childress JJ, Nygaard MH (1973) The chemical composition of midwater fishes as a function of depth of occurrence off southern California. Deep Sea Res 20:1093–1109

Childress J, Seibel B (1998) Life at stable low oxygen levels: adaptations of animals to oceanic oxygen minimum layers. J Exp Biol 201:1223–32

Childress JJ, Somero GN (1979) Depth-related enzymic activities in muscle, brain and heart of deep-living pelagic marine teleosts. Mar Biol 52:273–283

Cornejo R, Koppelmann R (2006) Distribution patterns of mesopelagic fishes with special reference to Vinciguerria lucetia Garman 1899 (Phosichthyidae: Pisces) in the Humboldt Current Region off Peru. Mar Biol 149:1519–1537

Cowles DL, Childress JJ, Wells ME (1991) Metabolic rates of midwater crustaceans as a function of depth of occurrence off the Hawaii Islands: food availability as a selective factor? Mar Biol 110:75–83

Davison P, Lara-Lopez A, Anthony Koslow J (2015) Mesopelagic fish biomass in the southern California current ecosystem. Deep Sea Res Part II Top Stud Oceanogr 112:129–142

Deutsch C, Berelson W, Thunell R, Weber T, Tems C, McManus J, Crusius J, Ito T, Baumgartner T, Ferreira V, Mey J, Geen A van (2014) Oceanography. Centennial changes in North Pacific anoxia linked to tropical trade winds. Science 345:665–8

Deutsch C, Brix H, Ito T, Frenzel H, Thompson L (2011) Climate-forced variability of ocean hypoxia. Science 333:336–9

Deutsch C, Emerson S, Thompson L (2006) Physical-biological interactions in North Pacific oxygen variability. J Geophys Res 111:1–16

Dickson KA (1995) Unique Adaptations of the Metabolic Biochemistry of Tunas and Billfishes for Life in the Pelagic Environment. Environ Biol Fishes 42:65–97

Friedman JR, Condon NE, Drazen JC (2012) Gill surface area and metabolic enzyme activities of demersal fishes associated with the oxygen minimum zone off California. Limnol Oceanogr 57:1701–1710

Gilly WF, Beman JM, Litvin SY, Robison BH (2013) Oceanographic and Biological Effects of Shoaling of the Oxygen Minimum Zone. Ann Rev Mar Sci:1–28

Helm KP, Bindoff NL, Church JA (2011) Observed decreases in oxygen content of the global ocean. Geophys Res Lett 38

Hochachka PW, Somero GN (2002) Biochemical adaptation: mechanism and process in physiological evolution. Oxford University Press, New York

Johansson D, Nilsson GE, Døving KB (1997) Anoxic depression of light-evoked

potentials in retina and optic tectum of crucian carp. Neurosci Lett 237:73–6

Karstensen J, Stramma L, Visbeck M (2008) Oxygen minimum zones in the eastern tropical Atlantic and Pacific oceans. Prog Oceanogr 77:331–350

Keeling RF, Körtzinger A, Gruber N (2010) Ocean deoxygenation in a warming world. Ann Rev Mar Sci 2:199–229

Koslow J, Goericke R, Lara-Lopez A, Watson W (2011) Impact of declining intermediate-water oxygen on deepwater fishes in the California Current. Mar Ecol Prog Ser 436:207–218

Lavery AC, Wiebe PH, Stanton TK, Lawson GL, Benfield MC, Copley N (2007) Determining dominant scatterers of sound in mixed zooplankton populations. J Acoust Soc Am 122:3304–3326

Levin LA, Bris N Le (2015) The deep ocean under climate change. Sci 350 :766–768

McClatchie S, Goericke R, Cosgrove R, Auad G, Vetter R (2010) Oxygen in the Southern California Bight: Multidecadal trends and implications for demersal fisheries. Geophys Res Lett 37:1–5

Miya M, Nishida M (1996) Molecular phylogenetic perspective on the evolution of the deep-sea fish genus Cyclothone. Ichthyol Res 43:375–398

Moyes D, Mathieu-Costello O a, Brill W, Hochachka W (1992) Mitochondrial metabolism of cardiac and skeletal muscles from a fast (Katsuwonus pelamis) and a slow (Cyprinus carpio) fish. Can J Zool 70:1246–1253

Netburn AN, Koslow JA (2015) Dissolved oxygen as a constraint on daytime deep scattering layer depth in the southern California current ecosystem. Deep Sea Res Part I Oceanogr Res Pap 104:149–158

Robinson E, Jerrett A, Black S, Davison W (2013) Hypoxia impairs visual acuity in snapper (Pagrus auratus). J Comp Physiol A Neuroethol Sens Neural Behav Physiol 199:611–7

Scherer E (1971) Effects of Oxygen Depletion and of Carbon Dioxide Buildup on the Photic Behavior of the Walleye (Stizostedion vitreum vitreum). J Fish Res Board Canada 28:1303–1307

Seibel BA (2011) Critical oxygen levels and metabolic suppression in oceanic oxygen

minimum zones. J Exp Biol 214:326–36

Seibel BA, Drazen JC (2007) The rate of metabolism in marine animals: environmental constraints, ecological demands and energetic opportunities. Philos Trans R Soc London Ser B 362:2061–78

Seibel BA, Thuesen E V., Childress JJ, Gorodezky LA (1997) Decline in pelagic cephalopod metabolism with habitat depth reflects differences in locomotory efficiency. Biol Bull 192:262–278

Shaffer G, Olsen SM, Pedersen JOP (2009) Long-term ocean oxygen depletion in response to carbon dioxide emissions from fossil fuels. Nat Geosci 2:105–109

Shoubridge EA, Hochachka PW (1980) Ethanol: a novel end product of vertebrate anaerobic metabolism. Science (80-) 209:308–309

Somero GN, Childress JJ (1980) A violation of the metabolism-size scaling paradigm: activities of glycotic enzymes in muscle increase in larger-size fish. Physiol Zool 53:322–337

Sverdrup HU (1938) On the explanation of the oxygen minima and maxima in the oceans. ICES J Mar Sci 13:163–172

Thuesen E, Childress JJ (1994) Oxygen-consumption rates and Metabolic Enzyme-Activities of Oceanic California-Medusae in Relation to Body-Size and Habitat Depth. Biol Bull 187:84–98

Thuesen E V., Miller CB, Childress JJ (1998) Ecophysiological interpretation of oxygen consumption rates and enzymatic activities of deep-sea copepods. Mar Ecol Prog Ser 168:95–107

Torres JJ, Grigsby MD, Clarke ME (2012) Aerobic and anaerobic metabolism in oxygen minimum layer fishes: the role of alcohol dehydrogenase. J Exp Biol 215:1905–14

Vetter R, Lynn E (1997) Bathymetric demography, enzyme activity patterns, and bioenergetics of deep-living scorpaenid fishes (genera Sebastes and Sebastolobus):paradigms revisited. Mar Ecol Prog Ser 155:173–188

Vornanen M, Steyk J, Nilsoon G (2009) The anoxia-tolerant crucian carp (Carassius carassius L.). In: Richards J, Farrell A, Brauner C (eds) Fish Physiology, Vol. 27: Hypoxia. Academic Press, Amsterdam, p 398–443

Warren J (2001) In situ measurements of acoustic target strengths of gas-bearing siphonophores. ICES J Mar Sci 58:740–749

Wyrtki K (1962) The oxygen minima in relation to ocean circulation. Deep Sea Res Oceanogr Abstr 9:11–23

Yang T, Lai N, Graham J, Somero G (1992) Respiratory, blood, and heart enzymatic adaptations of Sebastolobus alascanus (Scorpaenidae; Teleostei) to the oxygen minimum zone: A comparative study. Biol Bull 183:490–499

CHAPTER 4

MESOPELAGIC FISH ASSEMBLAGES ACROSS OCEANIC FRONTS: A COMPARISON OF THREE FRONTAL SYSTEMS IN THE SOUTHERN CALIFORNIA CURRENT ECOSYSTEM

4.1 Abstract

With strong horizontal gradients in physical properties, oceanic frontal regions can lead to disproportionately high biological productivity. Through the California Current Ecosystem (CCE) Long Term Ecological Research program we analyzed cross-frontal changes in mesopelagic fish assemblages at three separate frontal systems in the southern CCE. The A-Front was sampled in October 2008, the C-Front in June/July 2011, and the E-Front in July/August 2012. We tested for differential effects of front-associated regions on density, species composition, and a population growth index of vertically migratory and non-migratory mesopelagic fishes. The fronts did not have a strong effect on densities of any subset of the mesopelagic fish assemblage. The species composition of the vertical migratory fishes (and their larvae) was typically altered across fronts, with different assemblages on either side of each front. The migratory assemblages at fronts were indistinguishable from those at the more productive side of the frontal system. In contrast, the assemblage composition of the non-migratory fishes was indistinguishable between regions across all three of the fronts. A population growth index, expressed as the ratio of larvae to adults, was altered across two of the fronts for migratory species, elevated on the colder side of the A-Front, and the warmer side of the E-Front. The population growth index was indistinguishable for non-migratory species at all three frontal systems. The non-migratory component of the community is little influenced by the presence of a front, apparently because the regions of strongest horizontal spatial gradients were too shallow for them to experience directly. We speculate that there was no change in larval community composition and population growth index at the most dynamic frontal system compared to the other fronts surveyed

because the feature was short-lived relative to the time scale for population growth of the fish. If mesoscale features such as fronts persist, and continue to increase in the future, they have the potential to alter population growth potential and restructure mesopelagic fish assemblages.

4.2 Introduction

The California Current Ecosystem (CCE) is a dynamic system with complex mesoscale features, including fronts, eddies, meanders, and jets, which are particularly common in the core California Current region off of central and southern California (Checkley & Barth 2009, Powell & Ohman 2015). Fronts occur where two distinct water masses meet, and are characterized by strong horizontal gradients in physical properties such as temperature, salinity, and density. Fronts vary in size, strength, duration, and mechanism of formation (Sournia 1994). Fronts are typically associated with enhanced along-front currents (Sournia 1994, de Verneil & Franks 2015), and the physical dynamics at a front may lead to aggregations or accumulation of organisms (Franks 1992). Frontal regions are often accompanied by elevated primary production (Chekalyuk et al. 2012, Taylor et al. 2012), zooplankton density (Powell & Ohman 2015, Ohman et al. 2012), and density of higher trophic levels (Hoefer 2000, Polovina et al. 2001, Doniol-Valcroze et al. 2007).

A recent study found that the frequency of satellite-detectable fronts in the CCE is increasing (Kahru et al. 2012). As there can be disproportionately high biological production at frontal features, an increase in the frontal frequency could enhance integrated total productivity of the CCE region, with implications for fisheries, carbon

transport to the deep sea, and marine spatial management. The horizontal gradients at oceanic fronts typically diminish with depth, but may extend as deep as 1000 m (Bower et al. 1985). The frontal gradients in the present study are slight or undetectable by ~200 m (**Figs. 4.1 and 4.2**), below which lies the deep scattering layer (DSL), an acoustically-detected midwater aggregation of mesopelagic organisms that is ubiquitous throughout the ocean (Currie et al. 1969, Tont 1975, Irigoien et al. 2014). The mesopelagic fauna that comprises the DSL is an often overlooked component of oceanic ecosystems. However in the CCE, mesopelagic fish biomass is equal to or exceeds the biomass of the well-studied epipelagic clupeoid fishes (e.g., sardines, anchovies; Davison et al. 2015). Mesopelagic fishes are important forage for a number of predators such as such as tunas and billfishes (Bertrand et al. 2002, Potier et al. 2007), squids (Field et al. 2007), marine mammals (Pauly et al. 1998), and seabirds (Thompson et al. 1998). Mesopelagic fish are known to respond to environmental variability in physical and chemical factors, such as dissolved oxygen (Koslow et al. 2011, 2013, Netburn & Koslow 2015). Here, we consider the responses of the mesopelagic fish community to the mesoscale horizontal gradients expressed at fronts.

The CCE is a transitional region of the Pacific, with Subarctic waters transported southward into the region via the California Current, Subtropical waters transported northward from the Baja region, and Central Pacific Gyre waters at its western edge (Bograd & Lynn 2003, Checkley & Barth 2009). The dominant species collected at a site can be indicators of prevailing oceanographic and climate patterns (Moser & Smith 1993, Beamish et al. 1999, Hsieh et al. 2009, Koslow et al. 2011). Mesopelagic fish species in the CCE generally fall into one of two assemblages based on their biogeographic

affinities: Subarctic-Transition Zone and Subtropical-associated (including warm-water species whose distributions extend into the North Pacific Subtropical gyre) assemblages.

All adult mesopelagic fish have daytime minimum depths below 200 m, however a portion of the assemblage migrates vertically (Frost & McCrone 1979, Watanabe et al. 1999) into surface waters at night where they are potentially influenced by the frontal gradients. In addition, larvae of most mesopelagic fishes live in the epipelagic zone (Moser 1996, Bowlin 2015). It therefore is appropriate to separate the mesopelagic fish assemblage into two primary categories based on the diel vertical migration propensity of the adults. Non-migrators in this paper will refer to species whose adults remain in mesopelagic depths (>200 m) both day and night. Migrators will refer to species that traverse between the mesopelagic and epipelagic zones on a daily basis. Larval forms of all mesopelagic fish are considered to live primarily in the epipelagic zone (Moser 1996). The different ways in which these three groups –Non-migrators, Migrators, and Larvae- are distributed in the water column suggests they experience different environmental conditions and environmental gradients. In the case of epipelagic-intensified frontal features, the distinctive distributions of these groups provide an opportunity to test the differential influence of fronts on the density, assemblage composition, and population growth potential of different segments of the mesopelagic fish assemblage.

Three different deep-water frontal systems have been studied in the southern sector of the California Current System Long-Term Ecological Research (CCE-LTER) region between 2008 and 2012 (**Figure 4.1**). In all cases, quasi-Lagrangian sampling was conducted of environmental characteristics and biological components. The A-Front was oriented on an East-West axis, where colder saltier waters from the north met warmer

fresher southern waters (Landry et al. 2012), and was a relatively stationary and enduring feature. The confluence of northern and southern waters sampled in the A-Front study is a common and often persistent feature of the CCE (Haury et al. 1993, Chereskin & Niiler 1994, Lara-Lopez et al. 2012). However, more transient and dynamic fronts are common in the CCE, arising at the edge of mesoscale features such as eddies, jets, and filaments (Checkley & Barth 2009). The other two frontal studies addressed herein included sampling of the mesopelagic fish assemblage at the frontal regions themselves, as well as on either side of each front. In 2011, we surveyed the California Current Front (C-Front, Brzezinski et al. 2015, Krause et al. 2015) and in 2012 we surveyed the Eddy-Front (E-Front) (Bednaršek & Ohman 2015, de Verneil & Franks 2015). These features differed both from each other and from the A-Front in characteristics, intensity, and persistence, thus providing additional opportunities to analyze how different types of fronts affect mesopelagic fish density, species composition, and population growth potential.

In this paper we seek specifically to answer the following questions:

1) Is the density of mesopelagic fishes enhanced at fronts?
2) Is the species composition of mesopelagic fish assemblages altered across frontal regions?
3) Is population growth potential enhanced at the front or either side of the front?
4) Are the effects of fronts different for vertically migrating fishes than for non-migrating fishes?
5) Are effects of fronts similar across different frontal systems?

4.3 Methods

1. Sampling Locations

All cruises took place on the *R/V Melville*, and utilized the same quasi-Lagrangian sampling design (**Table 4.1**). Each cruise consisted of a series of experimental Cycles, in which a satellite-tracked drifter was followed for 3-4 days, with comprehensive physical and biological sampling conducted in close proximity to the drifter (Landry et al. 2009, 2012, Ohman et al. 2012). Fronts were identified prior to sampling using satellite imagery of temperature, ocean color, and Sea Surface Height (SSH), then more detailed site surveys with both a SeaSoar and Moving Vessel Profiler (Ohman et al. 2012, 2013) were used to identify specific locations for the drifter deployments. The A-Front study was located south of Point Conception and offshore of the Channel Islands, from ~32.25-32.75° N and ~120-121° W, and sampling occurred from 20-27 October, 2008 (**Figures 4.1a** & **b**, Lara-Lopez et al. 2012). This front was characterized by strong gradients in both temperature and chlorophyll concentration (Landry et al. 2012). Responses of the density, biomass, and community composition of the mesopelagic fish assemblage in relation to the front were reported in Lara-Lopez et al. (2012), and many of the results are included in this study for comparison. Assignment of species-specific migratory behavior (**Appendix 4.1**) has, however, been revised based on Davison et al. (2015) and Froese and Pauly (2015). There was no direct sampling of mesopelagic fishes at the A-Front itself, and we report on the two adjacent regions, the denser, warmer, and fresher Southern region and the less dense, colder, and saltier Northern region (**Figures 4.1a** & **b**, **2a**).

The California Current Front (C-Front) study took place at ~32.5-34° N and ~121-122° W, from 18 June - 17 July 2011 (**Figures 4.1a & c, 4.2b**). The C-Front was

located at the confluence of two eddies and was highly dynamic in space and time. The front shifted during the sampling period, which may have captured a period of frontogenesis (Brzezinski et al. 2015, Krause et al. 2015). The offshore ("Oceanic") stations were located within a warm-core eddy, nearshore ("Coastal") stations toward a cold-core eddy, and "Frontal" stations were located where the water masses met.

The Eddy Front (E-Front) study was located at ~33.5-34.5° N and ~122.75-123.75° W, and was sampled from 28 July - 26 August 2012 (**Figures 4.1a & d**). The E-Front was more stable over the sampling period than the C-Front, but was similarly characterized by a paired offshore warm-core eddy and nearshore cold-core eddy (Bednaršek and Ohman 2015). Based on differences in salinity and density, we designated stations as Oceanic, Coastal, or Frontal (**Figure 4.2c**).

We sampled mesopelagic fishes with oblique tows of a Matsuda-Oozeki Hu Trawl net (MOHT, Oozeki et al. 2004) with a 5 m^2 mouth opening and a net mesh size of 1.6 mm. For the A-Front and E-Front surveys, we typically collected daytime samples to ~500 m and nighttime samples to 150-200 m. We measured the volume of water filtered using a TSK flowmeter. For the C-Front study, we modified the MOHT frame with an opening-closing cod end system with a 1.7 mm mesh net. Net opening was typically triggered on ascent from 1000 m. There was contamination within the depth-stratified samples of the C-Front study, so we integrated them over the full depth sampled (0-1000 m) and estimated volume sampled based on the proportion of time the net was actually fishing.

We separated all fish at sea from the invertebrate component of the catch, and preserved them in 10% formaldehyde buffered with sodium tetraborate. We identified all

fish and larvae to the lowest possible taxonomic level, which was typically species, and assigned diel vertical migration behavior as per Davison et al. (2015; **Appendix 4.1**). Each fish was assigned as either a diel vertically-migrating adult or juvenile ("Migrator"), non-vertically migrating adult or juvenile ("Non-migrator"), or "Larva," and we assigned biogeographic provinces of abundant species based on published literature (Moser et al. 1987, Moser & Smith 1993, Brodeur & Yamamura 2005, Hsieh et al. 2005, 2009). We did not include incidentally-collected epipelagic and demersal taxa in any analyses.

2. Density

We tested for differences in densities between regions for each group of Migrators, Non-migrators, and Larvae using the Mann-Whitney U test for the A-Front and Kruskal-Wallis analysis of variance for the C- and E-Fronts.

3. Species composition

We log(x+1) transformed the count data and expressed them as % total density by species for each trawl before calculating Bray-Curtis distances. We used non-metric multidimensional scaling (nMDS) to visualize the differences in community composition among stations and Analysis of Similarity (ANOSIM) to test whether different regions had significantly different assemblages. We used Similarity Percentage (SIMPER) analysis to determine the relative contribution of specific taxa to the differences in assemblages. We conducted analyses separately on Migrators, Non-migrators, and Larvae first for all three frontal systems combined with groups assigned by frontal system (ie., A,C,E), and for each individual front with assignments based on frontal region.

4. Population growth index

To test whether the presence of the front affected population growth potential, we calculated the ratio of larvae to adults for each species at each sampling station. This index can be elevated due to either increased egg production or decreased larval mortality. We calculated the mean of these ratios separately for all Migrators and Non-migrators at each region of each front. We also calculated the larval to adult ratios for the 20 individual species for which our gear collected sufficient numbers of both adults and larvae, reported in **Appendix 4.2**. We used the non-parametric Mann-Whitney U test (A-Front) and Kruskal-Wallis test (C- and E-Fronts) to test for differences among these ratios between regions at each frontal system, followed by pairwise comparisons using the Dwass-Steel-Critchlow-Fligner method.

4.4 Results

Density

A list of all species collected over the course of the 3 studies is included in **Appendix 4.1**. There were no significant differences across fronts in the total densities of either Migrators or Non-migrators, apart from migrators across the C-Front ($P=0.05$, **Table 4.2**). There was a significant difference in Larval densities ($p< 0.03$) between the Northern and Southern regions of the A-Front, with higher density in the south, with no significant differences in Larval densities at either the C- or E-Fronts.

Community Composition

Comparisons between A, C, & E-Front assemblages:

Results of the nMDS ordinations are illustrated in **Figsures 4.3-4.6** and ANOSIM in **Table 4.3**. The three frontal studies had heterogeneous compositions of Migrators ($p < 0.001$) and Larvae ($p<0.001$), which was reflected in significant pairwise differences between each pair of studies (**Table 4.3**). Although there was weak heterogeneity among Non-migrators (ANOSIM, $p<0.05$), a posteriori pairwise comparisons revealed that there was no significant difference between the Non-migratory assemblages of the C- and E-Fronts ($p=0.86$). The C- and E-Front assemblages are therefore combined in **Figure 4.3**. We used SIMPER analysis to obtain relative differences in species' densities between groups, however SIMPER does not test for statistically significant differences between individual species' densities between groups. The Non-migratory assemblage of the A-Front study was differentiated through SIMPER analysis from the two more northern, eddy-associated fronts by relatively higher densities of *Cyclothone signata* and *Argyropelecus hemigymnus*, and lower *Cyclothone pseudopallida* and *Argyropelecus sladeni* (**Figure 4.3e**). These species all have relatively broad distributions in the North Pacific (Beamish et al. 1999), and the patterns of distribution we saw are not explained by distinctive biogeographic provinces (Beamish et al. 1999, Brodeur & Yamamura 2005).

The Migratory assemblage of the A-Front study had higher relative densities of the subtropical species *Triphotorus mexicanus* and *Vinciguerria nimbaria* and lacked the Subarctic-Transition Zone *Stenobrachius leucopsarus* and *Diaphus theta* that were abundant in the more northerly fronts (**Figure 4.3d**). The A-Front study larval community consisted of relatively high densities of Subarctic-Transition Zone

Bathylagoides wesethi, *Protomyctophum crockeri*, and *Chauliodus macouni*, and low *Lipologus ochotensis* compared with the C- and E-Fronts. The subtropical *V. nimbaria* larvae were only present at the A-Front, while Subtropical-Transition Zone *T. mexicanus* larval densities were substantially higher there as well. Several larval species were entirely absent at the A-Front, including the Subarctic-Transition Zone *Nannobrachium regale*, *Tactostoma macropus*, and *Leuroglossus stilbius*, as well as the subtropical/transitional *Ceratoscopelus townsendi*.

Non-migrators:

In comparisons of Non-migrator across individual fronts, we detected significant spatial heterogeneity in the assemblages by region at only the E-Front (**Figures 4.4a-c, Table 4.3**; $p<0.05$; A-Front: $p=0.14$, C-Front: $p=0.09$). However, none of the pairwise comparisons at the E-Front were found to be significantly different (Frontal/Oceanic: $p=0.07$, Frontal/Coastal: $p=0.10$, Oceanic/Coastal: $p=0.43$).

Migrators:

Comparing Migrators across individual frontal systems (**Figures 4.5a-c, Table 4.3**), there was significant heterogeneity of assemblages across all three fronts ($p<0.05$), though there were no pairwise differences between the Frontal and Coastal assemblages at either of the C- ($p=0.20$) or E-Fronts ($p=0.29$). The assemblage differences at the A-Front were caused by higher relative densities of the subtropical *V. nimbaria*, *Lampadena urophaos*, and *C. townsendi* on the Southern side, and higher densities of Subarctic-Transition Zone *Idiacanthus antrostomus*, *D.theta* and *Tarletonbeania crenularis* on the Northern side (**Figure 4.5d**). At the C-Front, we measured elevated densities of larval *D. theta*, and *Diogenichthys atlanticus* on the Oceanic side, and

elevated *L. ochotensis*, *T. mexicanus*, and *N. ritteri* at the coastal and frontal regions (**Figure 4.5e**). The E-Front varied from this pattern, with elevated *C. townsendi*, *D. theta*, and *Nannobrachium ritteri* on the Oceanic side, and high *L. stilbius*, *T. mexicanus*, and *T. crenularis* at the Coastal and Front-associated regions (**Figure 4.5f**).

Larvae:

Larval assemblages were significantly different ($p<0.001$) across the A-Front and E-Front (**Figures 4.6 a & c, Table 4.3**), with the Frontal and Coastal assemblages of the E-Front indistinguishable from each other ($p=0.55$). The larval assemblages were not statistically distinguishable by region across the C-Front ($p=0.10$, **Figure 4.6b**). Larval assemblages at the Southern side of the A-front were characterized by high densities of *V. nimbaria* and *D.theta* in the south (both completely absent in the north), and elevated densities of the broadly-distributed *Benthalbella dentata*, and Subarctic-Transition Zone *C. macouni* and *T. crenularis* in the North (**Figure 4.6d**). The oceanic side of the E-Front was characterized by high *I. antrostomus*, *S. californiensis*, *C. townsendi*, all warm-water associated species, while the coastal and frontal regions had high *C. macouni*, *T. macropus*, *T. crenularis*, and *L. stilbius* which are cold-water associated (**Figure 4.6f**). The Bray-Curtis similarities of the larval assemblages were on average much lower for the Larvae than for Migrators or Non-Migrators (**Table 4.4**), and there were a few species that were abundant at one region while entirely absent from others.

Larval Index

Due to the high number of zeroes (adults collected, but no larvae) in our data, we present the mean and individual ratios for each region of each front, although we report

p-values based on rank differences (Mann-Whitney U and Kruskal-Wallis). There was no significant difference in the mean ratio of larvae to adults for Non-migratory species at any of the frontal systems (**Figure 4.7**). For Migrators, we detected a significantly higher ratio of larvae to adults on the Northern side of the A-Front than the Southern side ($p<0.001$), and also detected differences at all regions of the E-Front with the highest larvae to adult ratio in the Oceanic region, followed by the Frontal region, and then the Coastal region ($p<0.01$ for all pairwise comparisons). There was no significant difference in the ratios of larvae to adults for the C-Front ($p=0.14$). We report the larval:adult ratio of 20 individual species in **Appendix 4.2**. There were no significant differences in the ratios between regions for any individual species ($p>0.05$).

4.5 Discussion

We found no change in density of vertically migrating and non-vertically migrating fishes between frontal regions at any of the three fronts (for the frontal regions sampled), and elevated density of Larvae at only the northern side of the A-Front relative to the southern side of that system. We observed front-associated changes in species composition for Migrators and Larvae, although not for Non-Migrators. The larval:adult ratio was enhanced in association with two of the three fronts for Migrators, with no change across frontal regions for Non-Migrators. Effects were generally diminished at the more transient C-Front.

Density

Due to the reassignment of migratory behavior for some species, our density results for the A-Front are slightly different from those of Lara-Lopez et al. (2012). In

agreement with their analysis, we detected significantly elevated Larval density on the southern side of the A-Front, however we did not detect a significant difference in the densities of Migrators between the two sides of the front as they did. Still, densities of Migrators showed a tendency to be higher on the colder side of each of the three fronts, although significantly so only in the case of the C-Front Migrators. Elevated densities of mesopelagic fishes at the cooler side of fronts have been observed before within the southern CCE (Haury et al. 1993, Moser & Smith 1993), as well as in the Atlantic Ocean (where most studies on the topic have occurred), with enhanced densities of mesopelagic fishes on the cooler side of an East-West oriented front (Backus et al. 1969), the edge of a warm-core ring (Olson & Backus 1985), at the Angola-Benguela Frontal Zone (John 2001) and at the Azores front (Angel 1989), associated with colder and more productive waters. There is acoustic evidence that there is elevated fish densities at both the A-Front (Lara-Lopez et al. 2012) and the C-Front (Koslow, unpublished data). However, there was no sampling directly at the A-Front. The trawl net may not have sufficiently sampled the frontal area, because we were limited by wind and current to towing across the front, integrating the community over as many as 10 nautical miles.

Assemblage Composition

With little sunlight reaching mesopelagic depths, the resident fauna are ultimately dependent on primary productivity from the above epipelagic zone to meet their energy demands. Zooplankton and fish transfer carbon into the deep sea through diel vertical migration and respiration (Steinberg et al. 2008a). The biomass of mesopelagic fish (Davison et al. 2013, Irigoien et al. 2014) and their prey (Steinberg et al. 2008b) correlates strongly with surface productivity at basin and global scales, and here we

tested for effects across small-scale features. We did not detect a significant effect of the frontal gradients on the composition of Non-migrators across regions of any of the fronts that we studied, although there were some differences between the different frontal systems that could not be explained by biogeographic affinities. Because they live at depths where the environment is relatively uniform, many Non-migrators have broad distributions (Beamish et al. 1999), and the fronts do not seem to act as a boundary or site of attraction for them. Consistent with these observations, the larval population growth index for the Non-migratory species was constant across all three frontal systems. Living at depths below the peak hydrographic gradients of the front, their populations appear to be largely unaffected by the processes above them at the scale that we studied. No studies we know of prior to Lara-Lopez et al. (2012) have investigated the differential response of Non-migratory mesopelagic fishes to fronts, and one of our most notable findings is that their density, assemblage composition, and larval indices were not influenced by the frontal features that we studied on the time and space scales examined.

Coastal and frontal assemblages of both Migrators and Larvae were not statistically distinguishable from each other at either of the C- or E-Fronts. The C- and E-Front assemblages of both groups appear to be disproportionately derived from the Coastal assemblage, with less contribution from Oceanic taxa. There is evidence that coastal water may be entrained into front-associated jets (Hood et al. 1990), and our results suggest that this water is accompanied by coastal taxa, though we cannot distinguish whether this process may occur through active (i.e., behavior) or passive (i.e., transport) processes.

We detected shifts in assemblages for Migrators at all fronts, and for Larvae at the A- and E-Fronts. As Migrators inhabit the epipelagic zone through their nocturnal excursions into surface waters and the Larvae reside in the epipelagic where environmental gradients associated with fronts are the strongest, their distributions are more directly affected by the presence of a front. Moser & Smith (1993) similarly found distinct larval fish assemblages across the Ensenada Front. The differences between the Northern and Southern assemblages at the A-Front were primarily based on biogeographic provinces (Lara-Lopez et al. 2012), while the assemblage at the E-Front were largely distinguishable by their oceanic or coastal associations. Most species collected at E-front stations were found in both Oceanic and Coastal/Frontal waters. Although mixing of assemblages occurred at all of the fronts, there is more similarity between regional assemblages at the C- and E-Fronts than for the A-Front (**Figures 4.4, 4.5, & 4.6**). The A-Front may be a more permanent feature that behaves more like a barrier between the distinctive Subtropical and Subarctic-Transition Zone provinces (Moser & Smith 1993, Chereskin & Niiler 1994, Brodeur & Yamamura 2005), while the more transitory eddy-associated C- and E-Fronts behave more as "blenders" (Bower et al. 1985, Sournia 1994), with more subtle distinctions in the associated assemblages across the frontal zone.

With substantially lower Bray-Curtis similarities between stations (**Table 4.4**), the larval assemblages were overall much more dissimilar to each other than either of the adult assemblages were, likely because in general larvae have both spatially and temporally patchier distributions than adults, so sampling is more variable for them. Still,

we detected higher densities of warm-water species in the offshore region, and higher densities of coastal-oriented species in the nearshore, as would be expected.

The population growth index for Migrators as well as the larval assemblage compositions were unaltered at the C-Front, which we attribute to the dynamic nature of that frontal system. The late-stage larvae that are effectively captured in the MOHT are at least 3-4 weeks old (Gartner & Brunswick 1991, Moser 1996), and were therefore spawned by adults living under different oceanographic conditions than at the time of our sampling. Younger larvae are smaller than our mesh size, and typically not retained. As several weeks are needed for larvae to accumulate at eddy-associated convergence zones (Olson & Backus 1985), an increase in larval:adult ratios was not realized in this region.

There were, however, altered larval:adult ratios of Migrators across the more stable A- and E-Fronts. The patterns in larval indices at these two fronts are different, with higher values on the cooler, northern (more productive) side of the A-Front and on the oceanic (less productive) side of the E-Front. Bakun (2006) describes a tradeoff between better nutritional access and high growth potential in more productive (cooler) regions of fronts, and refuge from predation on the less productive side. Where the tradeoff results in higher growth potential depends on a number of factors, including predator densities and prey densities. We speculate that at the more southerly and offshore A-Front, there was lower overall predation on migratory larvae that allowed for the more productive Northern side to be the preferred habitat for spawning, while at the E-Front, there was enhanced survival in the Oceanic region due to release from predation. Midwater oxygen concentrations are substantially lower on the colder sides of these fronts (**Figure 4.2a-d**), with a particularly wide discrepancy at the E-Front, and it is

possible that reproduction or larval survival at the Oceanic side of that front is a response to increased larval survival in better-oxygenated waters.

Although the differences were not significant, we did observe a tendency to higher larval to adult ratios of a number of species in both Southern and Offshore waters for both Subarctic-Transition Zone species and Subtropical species. *D. theta* are known to undergo spawning migrations into subtropical waters (Moku et al. 2003, Sassa & Kawaguchi 2004) despite their Subarctic-Transition Zone adult distribution, and our results suggest that a number of other species, such as *N. ritteri*, *B. wesethi*, and *I. antrostomus*, may employ a similar behavior (**Appendix 4.2**). Our results may be confounded by sampling within two different seasons (Fall and Summer), as some species exhibit seasonal spawning (Moser 1996).

Incorporating data on predator density, water clarity, and patch density could inform the underlying mechanisms leading to our differential results in population growth potential across the two different types of fronts. Our surveys did not sample water that was distant from the front (e.g., John 2001), so it is difficult to say whether observed patterns, such as altered larval:adult densities on one side of a front, are a result of the association with the front or a result of association with the water mass itself. Future studies on the topic should compare not only the edge of the water masses adjacent to the front, but also non-front associated waters.

4.6 Conclusions

Through sampling of three different frontal systems within the southern CCE, this study builds upon the current understanding of the effects of pelagic fronts on

mesopelagic fish assemblages. We found that within the CCE, there are different types of fronts – the more persistent East-West oriented feature that separates Northern and Southern water masses is associated with more distinct assemblages across its boundary than the more transient eddy-associated fronts. Living at depths beyond the influence of most of the front-associated gradients, the Non-migratory assemblage remained relatively uniform across frontal systems, while Migratory and Larval assemblages were altered by the presence of the front, likely because these groups respond more directly to the epipelagic gradients associated with the frontal systems. In the CCE, frontal frequency (Kahru et al. 2012) and upwelling (Sydeman et al. 2014) may be increasing, which could be a response to altered eddy activity (Strub & James 2000). Our results suggest that fishes may benefit from the edge of fronts (Northern in the case of the E-W associated fronts, and Oceanic in the case of the eddy-associated fronts) for reproduction and/or recruitment. This study shows that fronts can significantly alter the structure of mesopelagic communities, although frontal duration and location affect the magnitude of such changes. If the frequency of frontal occurrences in the southern CCE continues to increase, such features will likely differentially influence migratory and non-migratory mesopelagic fishes, through effects on their reproduction, survival, distributions, and their predators.

4.7 Acknowledgements

We extend especial thanks to Jamie Chang, who spent many hours identifying fish for this study. We thank Cindy Klepadlo and H.J. Walker for assistance with specimen identification and accession, Pete Davison and Ana Lara-Lopez for collecting and identifying fishes, Mark D. Ohman for assistance with study design, data analysis, and manuscript revisions. We thank Mati Kahru, Jeff Krause, and Ryan Rykaczewski for advice on interpreting satellite data and generating maps, Ralf Goericke for rapidly assembling the deep CTD data, and Robin Westlake-Storey for assistance with vertical profiles. We finally thank the CCE-LTER Chief Scientist Mike Landry and Lead PI Mark D. Ohman for accommodating our trawl schedule, the captains and crew of the *R/V Melville*, and the CCE-LTER science party for helping with trawling. The Gordon and Betty Moore Foundation provided funding for the MOHT, and shiptime was provided through the NSF-funded CCE-LTER program.

4.8 Figures:

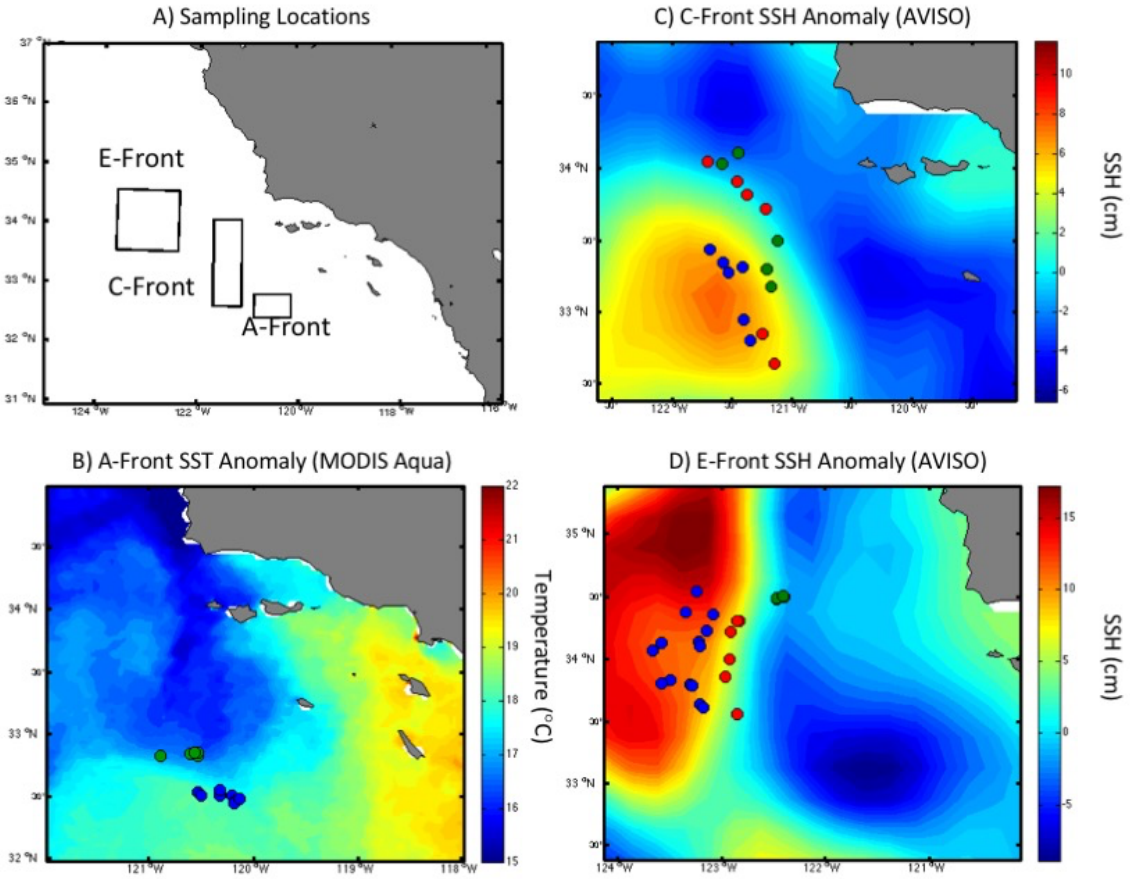

Figure 4.1. A) Locations of each of the 3 frontal systems in the Southern California Current System. MOHT trawl sampling locations at the: B) A-front (overlain on satellite-derived sea surface temperature (SST)), sampled from 20-27 October 2008, C) C-front (overlain on satellite-dervied sea surface height (SSH)), sampled from 18 June - 17 July 2011, and D) E-front (SSH), sampled from 30 July - 25 August 2012. Southern and Offshore stations are indicated by blue points, frontal stations by red, and Northern and Coastal stations by green.

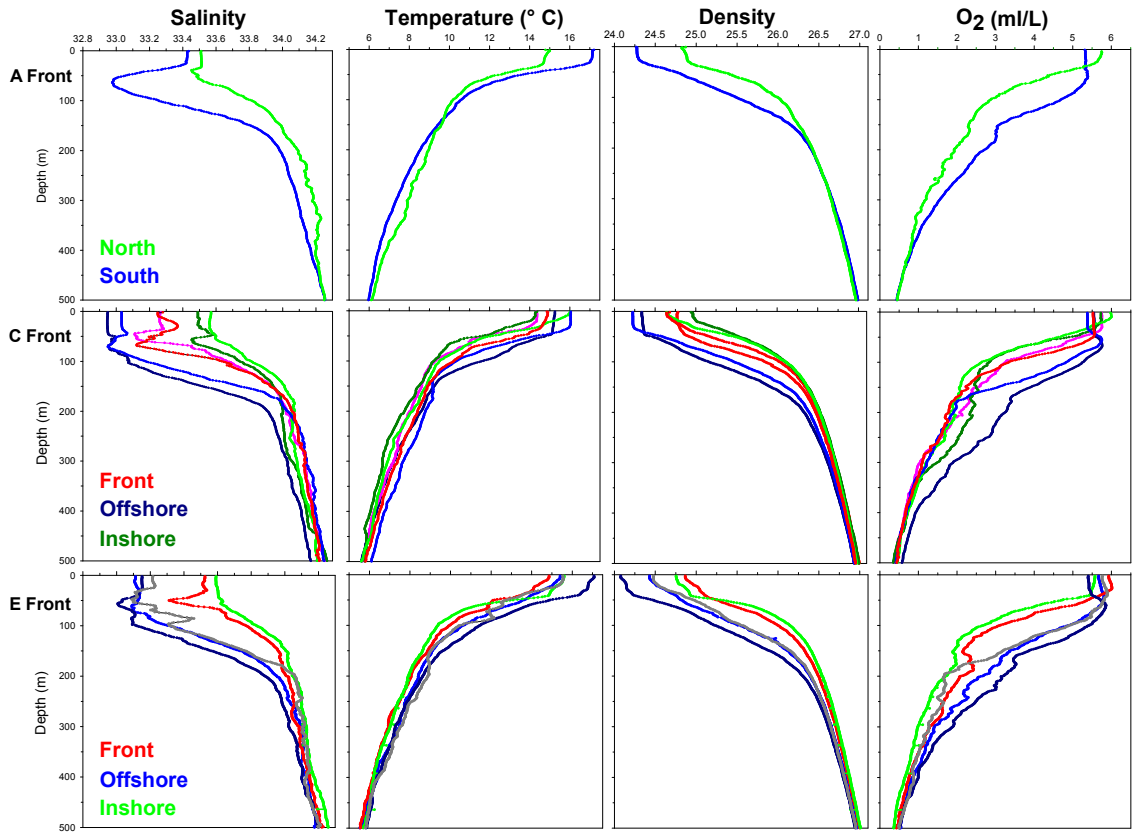

Figure 4.2. Salinity, temperature, density and oxygen profiles for each of the the A, C, and E-Fronts. Each individual trace is the mean for a single sampling Cycle, with the northern (A-front) and coastal (C-front and E-front) stations represented in shades of green, frontal stations in red and pink, and southern (A-front) or offshore stations (C-front and E-front) in shades of blue and grey.

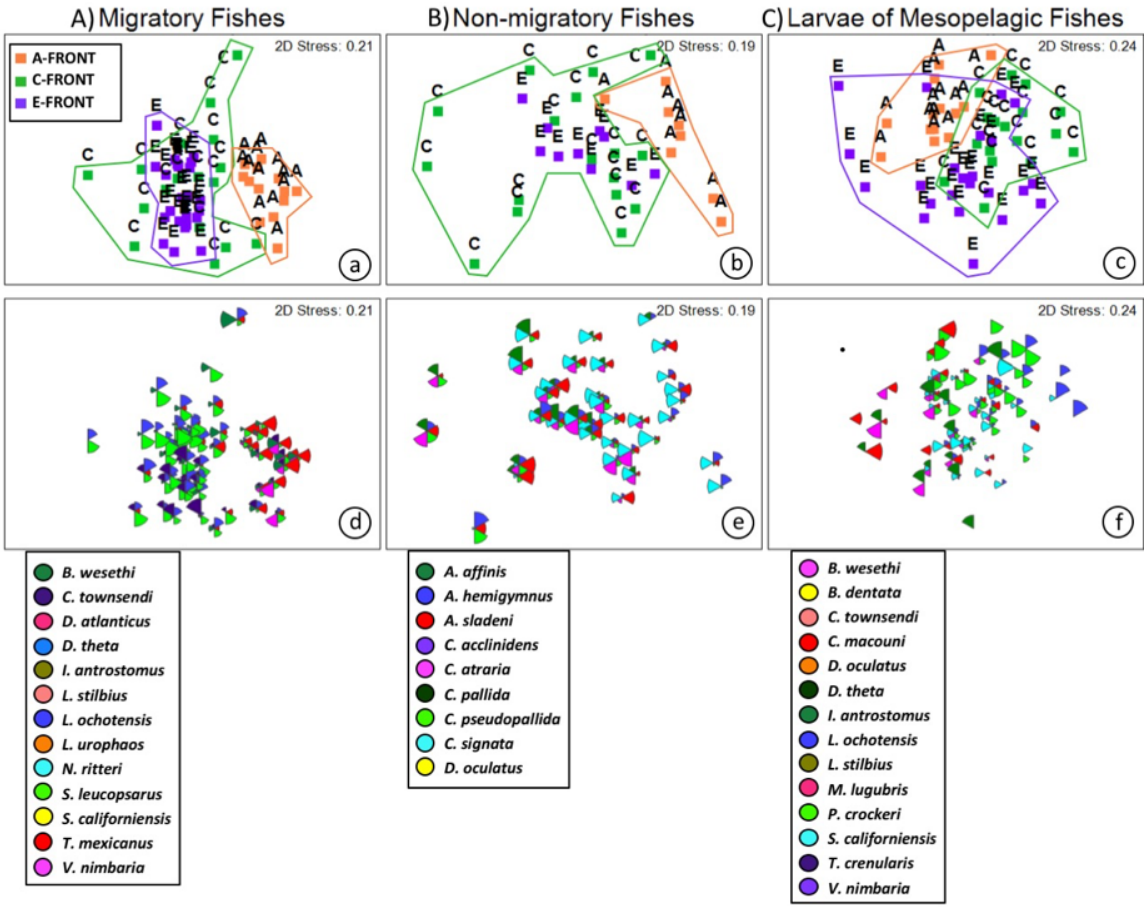

Figure 4.3. nMDS plots of A) vertically migrating fishes, B) non-vertically migrating fishes, and C) larvae of mesopelagic species for all three fronts. The upper panel (a-c) for each nMDS analysis is color-coded by frontal system. Groups that cluster significantly are outlined in solid lines. The lower panel of each nMDS analysis (d-f) shows a bubble plot indicating the relative densities of the species that were most informative for distinguishing between the systems according to the results of SIMPER analysis. We report the ANOSIM results and pairwise comparisons between regions in **Table 4.3**. The stress value, marked in the upper right-hand corner of each plot, is an indicator of how the distances on the nMDS plot represent the Bray-Curtis distances. Ordination with stress values of <0.20 for two dimensions are considered to represent the true distances reasonably well.

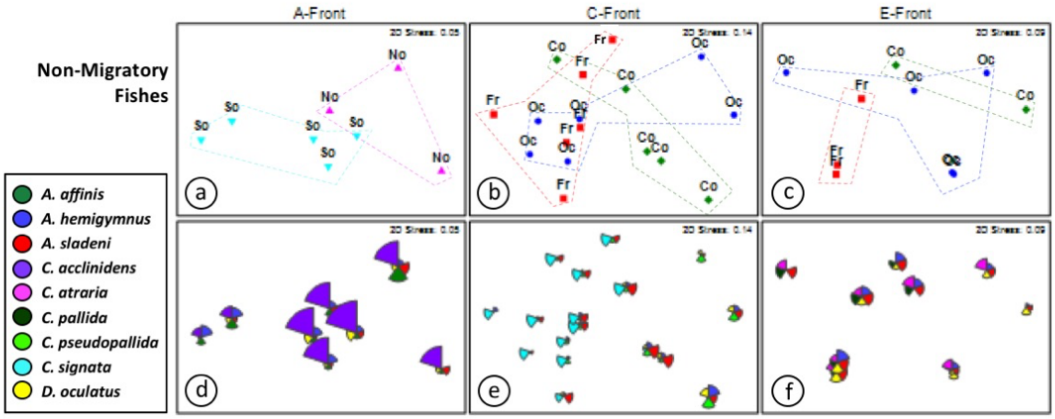

Figure 4.4. nMDS plots of non-vertically migrating fishes. For each frontal system, the upper panel (a-c) of each nMDS analysis is color-coded by region. The regions are Offshore, Frontal, and Coastal for the C- and E-Fronts, and North and South for the A-Front. Groups that cluster significantly are outlined in solid lines; faint dotted lines indicate regions that did not differ significantly. The lower panel (d-f) of each nMDS analysis shows a bubble plot indicating the relative densities of the species that were most informative for distinguishing between the regions according to the results of SIMPER analysis. We report the ANOSIM results and pairwise comparisons between regions in **Table 4.3**.

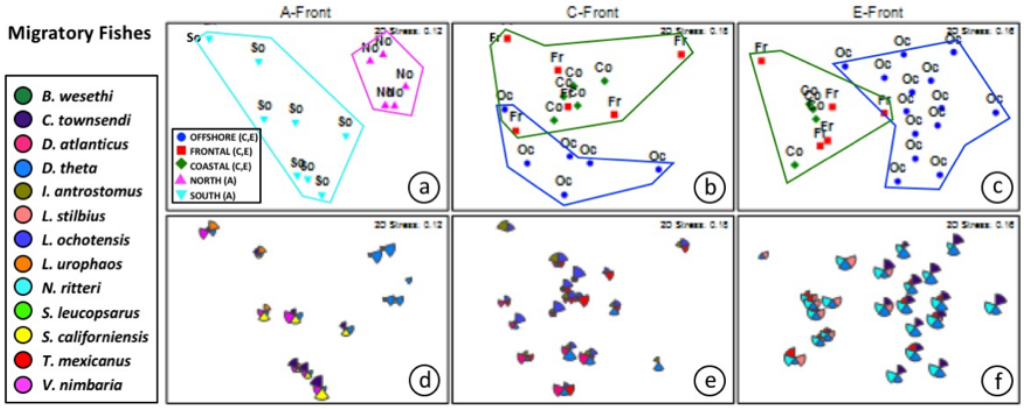

Figure 4.5. nMDS plots of vertically migrating fishes. For each frontal system, the upper panel (a-c) of each nMDS analysis is color-coded by region. The regions are Offshore, Frontal, and Coastal for the C- and E-Fronts, and North and South for the A-Front. Groups that cluster significantly are outlined in solid lines; faint dotted lines indicate regions that did not differ significantly. The lower panel (d-f) of each nMDS analysis shows a bubble plot indicating the relative densities of the species that were most informative for distinguishing between the regions according to the results of SIMPER analysis. We report the ANOSIM results and pairwise comparisons between regions in **Table 4.3**.

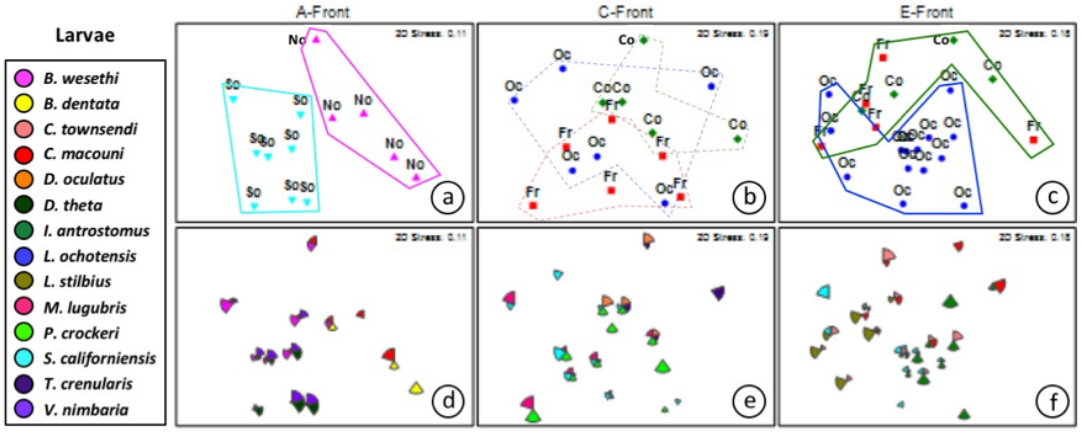

Figure 4.6. nMDS plots of larvae of mesopelagic species. For each frontal system, the upper panel (a-c) of each nMDS analysis is color-coded by region. The regions are Offshore, Frontal, and Coastal for the C- and E-Fronts, and North and South for the A-Front. Groups that cluster significantly are outlined in solid lines; faint dotted lines indicate regions that did not differ significantly. The lower panel (d-f) of each nMDS analysis shows a bubble plot indicating the relative densities of the species that were most informative for distinguishing between the regions according to the results of SIMPER analysis. We report the ANOSIM results and pairwise comparisons between regions in **Table 4.3**.

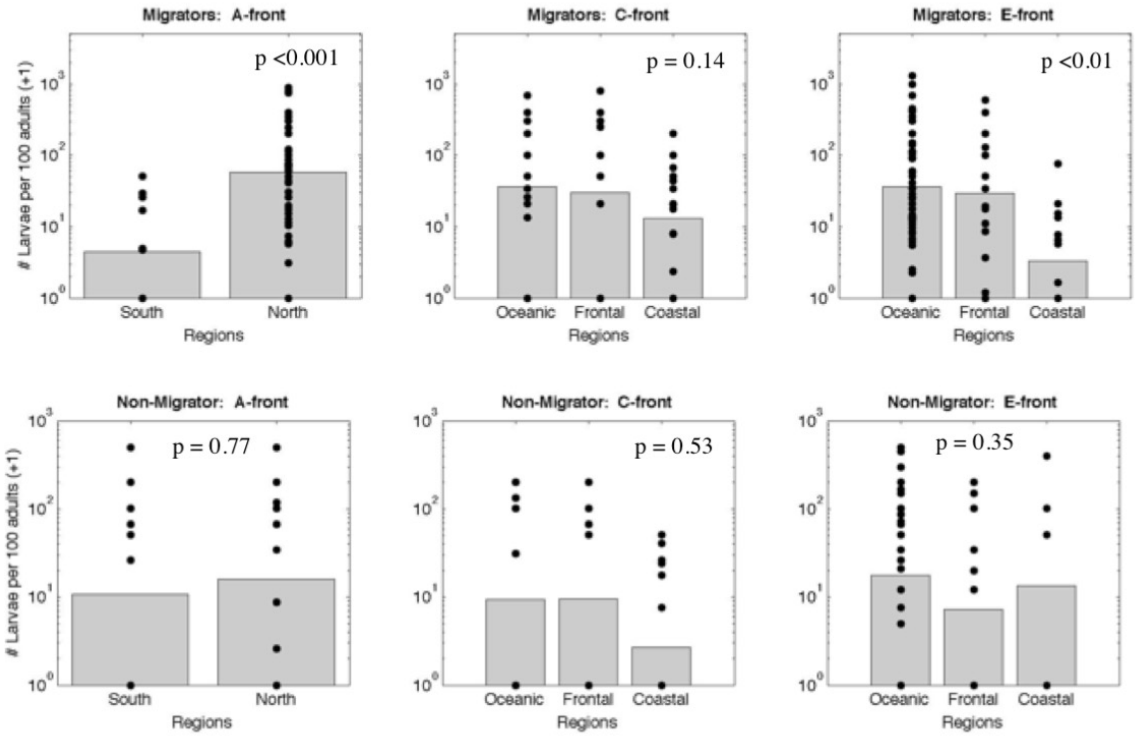

Figure 4.7. Ratio of larvae per 100 adults (log(X+1) transformed) for both vertically-migrating and non-migrating fishes. Bars indicate mean values of the ratios for all species, and points represent the ratio for each species at each station sampled in the region. See **Appendix 4.2** for results for individual species.

4.9 Tables

Table 4.1 Frontal systems sampled in this study.

System	Dates	Characteristics
A-Front	20-27 October, 2008	boundary between N/S waters, stable, long-lasting
C-Front	18 June - 17 July, 2011	eddy-associated, frontogenesis
E-Front	28 July - 26 August, 2012	eddy-associated, stable

Table 4.2. Median densities of vertical migrators, non-vertical migrators, and larvae of mesopelagic fishes at each region sampled for each of the three fronts. The reported p-values are based on non-parametric tests for difference in medians (Mann-Whitney U test for the A-front, and Kruskal-Wallis one-way analysis of variance for both the C- and E-Fronts).

	Indivs. m^{-2} (25-75th percentiles)			
	South		***North***	**p-value**
A-front (P0810)	n=8		n=5	
Migrators	1.96 (1.79-4.43)		3.65 (2.03-7.79)	0.31
Non-migrators	7.37 (0.60-8.53)		4.76 (0.84-5.70)	0.31
Larvae of mesopelagic fishes	0.73 (0.63-2.41)		0.19 (0.14-0.48)	0.03*
	Oceanic	***Front***	***Coastal***	**p-value**
C-Front (P1106)	n=6	n=6	n=5	
Migrators	0.92 (0.40-1.07)	0.76 (0.44-0.91)	2.28 (1.17-4.53)	0.05
Non-migrators	3.99 (3.75-5.38)	4.68 (3.14-8.62)	3.57 (3.02-4.33)	0.45
Larvae of mesopelagic fishes	0.29 (0.21-0.59)	0.36 (0.16-0.44)	0.19 (0.12-0.25)	0.39
E-Front (P1208)	n=5	n=14	n=4	
Migrators	2.07 (0.96-5.18)	1.84 (1.41-9.81)	5.79 (2.54-7.96)	0.30
Non-migrators	1.40 (0.89-2.27)	2.77 (0.81-3.62)	2.04 (0.54-5.01)	0.73
Larvae of mesopelagic fishes	0.26 (0.08-1.33)	0.22 (0.11-0.55)	0.13 (0.07-0.22)	0.49

Table 4.3. Results of Analysis of Similarity (ANOSIM) and a posteriori pairwise comparisons for species assemblages for all cruises combined and for each frontal system independently. For all studies combined, we conducted comparisons between frontal systems (A,C,E). For the individual frontal systems, we compared between frontal locations (pairwise comparisons columns). Subscripts for p-values are: A, C, or E demarcating each study, or F: Frontal, O: Oceanic, C: Coastal. (See **Figs. 3-6** for the nMDS ordination).

	p-value	Pairwise Comparisons		
ALL CRUISES				
Grouped by study		$p_{A,C}$	$p_{A,E}$	$p_{C,E}$
Migratory	***	***	***	***
Non-migratory	*	*	***	0.86
Larvae	***	***	***	***
Grouped by frontal location		$p_{F,O}$	$p_{F,C}$	$p_{O,C}$
A-FRONT				
Migratory	***			
Non-migratory	0.143	(only 2 regions)		
Larvae	***			
C-FRONT				
Migratory	*	*	0.20	*
Non-migratory	0.09	-	-	-
Larvae	0.10	-	-	-
E-FRONT				
Migratory	***	**	0.29	***
Non-migratory	*	0.07	0.10	0.43
Larvae	***	*	0.55	**

*p<0.05 **p<0.01 ***p<0.001

Table 4.4. Mean Bray-Curtis similarities within the groups of mesopelagic fishes. 95% confidence intervals are indicated in parentheses.

	Migratory fishes	Non-migratory fishes	Larvae of mesopelagics
All cruises	61.1 (± 0.6)	63.0 (± 0.7)	24.4 (± 0.9)
2008	71.8 (± 1.8)	70.1 (± 3.0)	39.0 (± 3.8)
2011	61.0 (± 1.8)	61.7 (± 1.5)	33.7 (± 2.5)
2012	71.7 (± 1.0)	70.6 (± 1.6)	25.7 (± 2.2)

4.10. Appendices

Appendix 4.1. All species captured in this study, listed by family. Migratory Behavior is indicated by the abbreviations M- Migrator and NM- Non-migrator.

	Behavior	Adults & Juvs	Larvae
Alepocephalidae			
Alepocephalus tenebrosus Gilbert, 1892	NM	X	X
Anoplogastridae			
Anoplogaster cornuta (Valenciennes, 1883)	NM	X	
Bathylagidae			
Bathylagoides wesethi (Bolin, 1938)	M	X	X
Bathylagus pacificus Gilbert 1890	NM	X	X
Leuroglossus stilbius Gilbert, 1890	M	X	X
Lipolagus ochotensis (Schmidt, 1938)	M	X	X
Pseudobathylagus milleri (Jordan & Gilbert, 1898)	NM	X	
Chiasmodontidae			
Chiasmodon niger Johnson, 1864	NM	X	X
Cyematidae			
Cyema atrum Günther, 1878	NM	X	X
Gonostomatidae			
Cyclothone acclinidens Garman, 1899	NM	X	
Cyclothone atraria Gilbert, 1905	NM	X	
Cyclothone pallida Brauer, 1902	NM	X	
Cyclothone pseudopallida Mukhacheva, 1964	NM	X	
Cyclothone signata Garman, 1899	NM	X	X
Howellidae			
Bathysphyraenops simplex Parr, 1933	M	X	
Howella sherborni (Norman, 1930)	NM	X	
Melamphaidae			
Melamphaes acanthomus Ebeling, 1962	NM	X	
Melamphaes lugubris Gilbert, 1890	NM	X	X
Melamphaes parvus Ebeling, 1962	NM	X	
Poromitra crassiceps (Günther, 1878)	NM	X	X
Scopeloberyx opisthopterus (Parr, 1933)	NM	X	
Scopelogadus bispinosus (Gilbert, 1915)	NM	X	
Scopelogadus mizolepis (Günther, 1878)	NM	X	X
Microstomatidae			
Nansenia candida Cohen, 1958	NM	X	
Microstoma microstoma (Risso, 1810)	NM	X	
Myctophidae			
Bolinichthys longipes (Brauer, 1906)	M	X	
Ceratoscopelus townsendi (Eigenmann & Eigenmann, 1889)	M	X	X
Diaphus kuroshio Kawaguchi & Nafpaktitis, 1978	M	X	
Diaphus theta Eigenmann & Eigenmann, 1890	M	X	X
Diogenichthys atlanticus (Tåning, 1928)	M	X	X
*Diogenichthys laternatus (*Garman, 1899)	M	X	

Appendix 4.1. Species in this study, Continued.

	Behavior	Adults & Juvs	Larvae
*Electrona risso (*Cocco, 1829)	M	X	
Hygophum reinhardtii (Lütken, 1892)	M		X
Lampadena urophaos Paxton, 1963	M	X	
Lampanyctus tenuiformes (Brauer, 1906)	M		X
Loweina rara (Lütken, 1892)	M		X
Myctophum nitidulum Garman, 1899	M	X	
Nannobrachium hawaiiensis Zahuranec, 2000	M	X	
Nannobrachium regale (Gilbert, 1892)	NM	X	X
Nannobrachium ritteri (Gilbert, 1915)	M	X	X
Notolychnus valdiviae (Brauer, 1904)	M	X	
Notoscopelus resplendens (Richardson, 1845)	M	X	X
Parvilux ingens Hubbs & Wisner, 1964	NM	X	
Protomyctophum crockeri (Bolin, 1939)	NM	X	X
Protomyctophum thompsoni (Chapman, 1944)	NM	X	
Stenobrachius leucopsarus (Eigenmann & Eigenmann, 1890)	M	X	X
Stenobrachius nannochir (Gilbert, 1890)	NM	X	
Symbolophorus californiensis (Eigenmann & Eigenmann, 1889)	M	X	X
Taaningichthys paurolychnus Davy, 1972	NM	X	
Tarletonbeania crenularis (Jordan & Gilbert, 1880)	M	X	X
Triphoturus mexicanus (Gilbert, 1890)	M	X	X
Nemichthyidae			
Avocettina infans (Günther, 1878)	NM	X	
Nemichthys scolopaceus Richardson, 1848	NM	X	
Neoscopelidae			
Scopelengys tristis Alcock, 1890	NM	X	
Notosudidae			
Scopelosaurus harryi (Mead, 1953)	NM	X	X
Opisthoproctidae			
Macropinna microstoma Chapman, 1939	NM	X	X
Paralepididae			
Arctozenus risso (Bonaparte, 1840)	NM	X	X
Lestidiops ringens (Jordan & Gilbert, 1880)	NM	X	X
Phosichthyidae			
Ichthyococcus irregularis Rechnitzer & Böhlke, 1958	NM	X	
Vinciguerria lucetia (Garman, 1899)	M	X	X
Vinciguerria nimbaria (Jordan & Williams, 1895)	M	X	X
Platytroctidae			
Holtbyrnia latifrons Sazonov, 1976	NM	X	X
Mirorictus taningi Parr, 1947	NM	X	
Sagamichthys abei Parr, 1953	NM	X	X
Saccopharyngidae			
Saccopharynx lavenbergi Nielsen & Bertelsen, 1985	NM	X	
Scopelarchidae			
Benthalbella dentata (Chapman, 1939)	M	X	X
Scopelarchus analis (Brauer, 1902)	M		X

Appendix 4.1. Species in this study, Continued

	Behavior	Adults & Juvs	Larvae
Serrivomeridae			
Serrivomer sector Garman, 1899	NM	X	
Sternoptychidae			
Argyropelecus affinis Garman, 1899	NM	X	X
Argyropelecus hemigymnus Cocco, 1829	NM	X	
Argyropelecus lychnus Garman, 1899	NM	X	X
Argyropelecus sladeni Regan, 1908	NM	X	X
Danaphos oculatus (Garman, 1899)	NM	X	X
Valenciennellus tripunctulatus (Esmark, 1871)	NM	X	
Sternoptyx diaphana Hermann, 1781	NM	X	
Sternoptyx obscura Garman, 1899	NM	X	
Sternoptyx pseudobscura Baird, 1971	NM	X	
Stomiidae			
Aristostomias scintillans (Gilbert, 1915)	NM	X	
Bathophilus flemingi Aron and McCrery, 1958	NM	X	
Borostomias panamensis Regan & Trewavas, 1929	NM	X	
Chauliodus macouni Bean, 1890	NM	X	X
Idiacanthus antrostomus Gilbert, 1890	M	X	X
Photonectes margarita (Goode & Bean, 1896)	NM	X	
Stomias atriventer Garman, 1899	NM	X	X
Tactostoma macropus Bolin, 1939	NM	X	X
Opostomias mitsuii Imai, 1941	NM	X	
Tetragonuridae			
Tetragonurus cuvieri Risso, 1810	NM	X	X
Trachipteridae			
Trachipterus altivelis Kner, 1859	M		X

Appendix 4.2. Ratio of larvae per 100 adults (log(X+1) transformed) for both vertically-migrating and non-migrating fishes. Bars indicate mean values of the ratios for all species, and points represent the ratio for each species at each station sampled in the region. We tested for differences between regions using Mann-Whitney U (A-front) and Kruskal-Wallis (C- and E-Front), followed by pairwise comparisons using the Dwass-Steel-Critchlow-Fligner Method, but found no significant differences. We have nonetheless classified these into 5 groups based on the qualitative differences across regions in larval:adult indices, an indirect measure of population growth potential.

Group I: Warm-water Spawners

This group has elevated larval:adult ratios in the warmer, lower productivity regions of the studied fronts- the Southern region of the A-front and the Oceanic region of the C and/or E-fronts. The group includes the vertically migrating fishes, *Diaphus theta*, *Nannobrachium ritteri, Symbolophorus californiensis, Bathylagoides wesethi* , and *Idiacanthus. antrostomus*, and the non-vertical migrator *Poromitra crassiceps*. Most of these species have a Subarctic-Transition Zone range, although *D. theta* are known to make spawning migrations into the southern end of their range. Our results suggest that the other members of this group may similarly spawn preferentially in warmer water. With the exception of *N. ritteri*, these species all exhibited high spawning potential at the frontal region of the C-front.

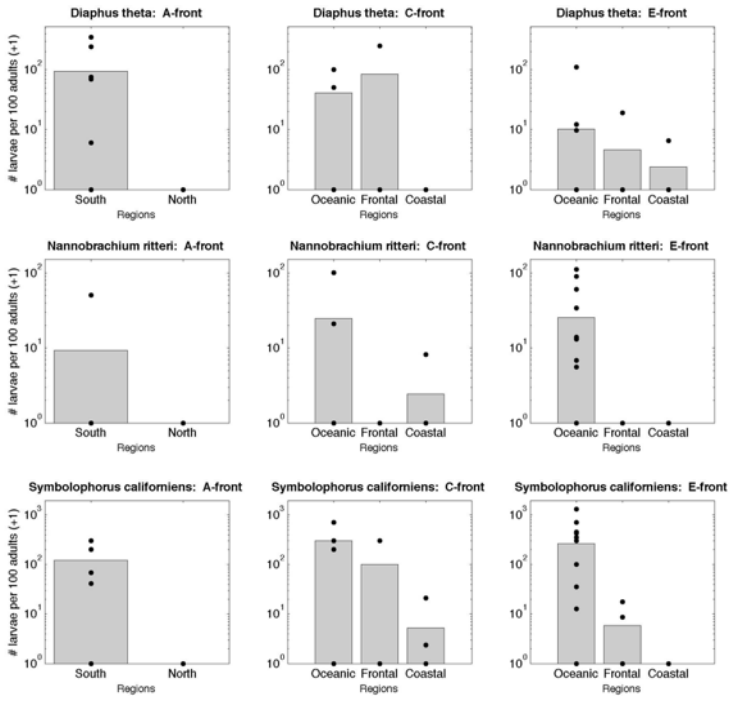

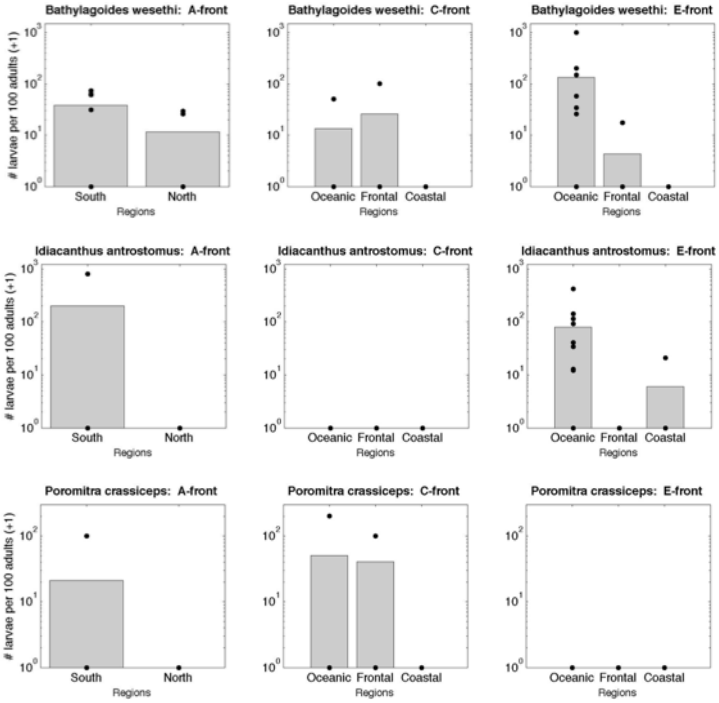
Bathylagoides wesethi: A-front
Bathylagoides wesethi: C-front
Bathylagoides wesethi: E-front
Idiacanthus antrostomus: A-front
Idiacanthus antrostomus: C-front
Idiacanthus antrostomus: E-front
Poromitra crassiceps: A-front
Poromitra crassiceps: C-front
Poromitra crassiceps: E-front
larvae per 100 adults (+1)
South
North
Oceanic
Frontal
Coastal
Regions

Group II: Southern Spawners

This group is defined by a peak ratio of larvae: adults in the southern side of the A-front, and includes the vertical migrators *Triphotorus mexicanus*, *Vinciguerria lucetia*, and *Vinciguerria nimbaria*, and the non-vertically migrating *Danaphos oculatus*. With the exception of *D. oculatus*, adult densities of all species were greatest at the A-front, and with the exception of *T. mexicanus*, the ratio of larvae: adults was highest at the south side of the A-front. *D. oculatus* are the only non-migrators in the group. All species in this group have a subtropical range.

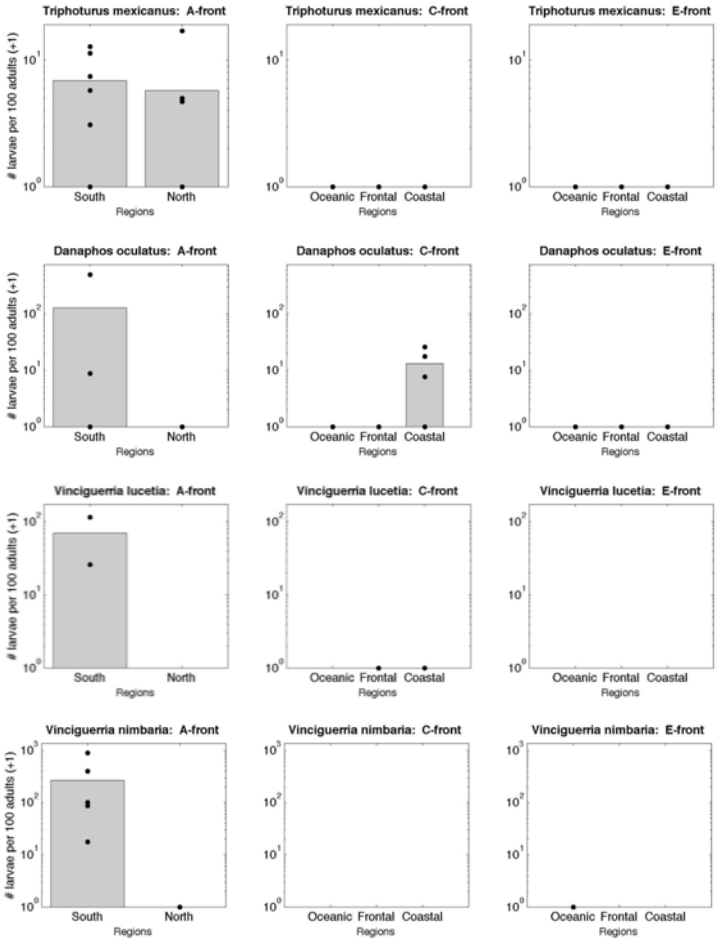

Group III. Offshore Spawners

This group is classified by peak spawning at the Oceanic regions of the two eddy-associated fronts, and includes the migratory fish *Ceratoscopelus townsendi* and the non-migratory *Tactostoma macropus* and *Nannobrachium regale*. This group is represented by both Subtropical-Transition Zone species (*C. townsendi, N. regale* and a Subarctic/Transition Zone species (*T. macropus)*. *C. townsendi* larval:adult ratio was also elevated at the frontal region of the E-front.

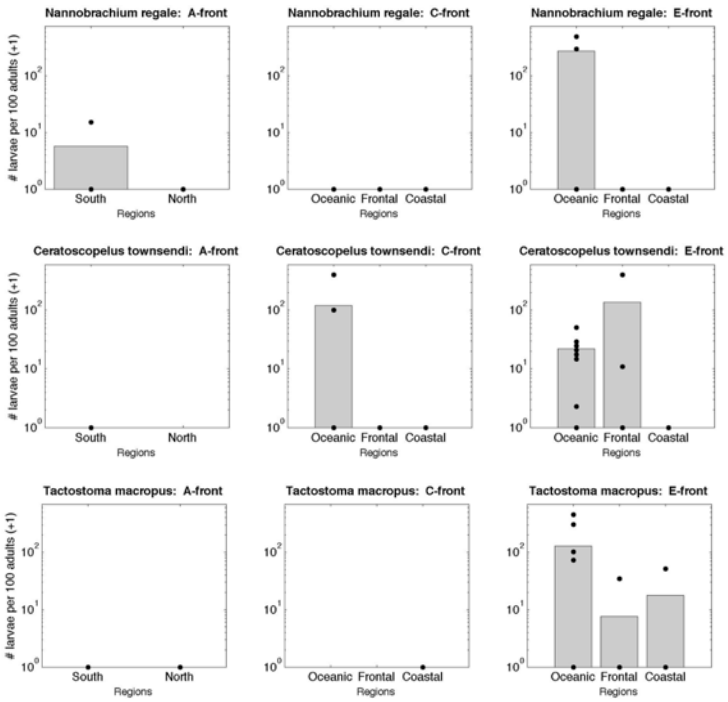

Group IV. Cold-water spawners

The single species in this group exhibited elevated larval:adult density in both the coastal (C-front, E-front) and frontal (E-front) regions. *Leuroglossus stilbius* has a Subarctic-Transition Zone distribution.

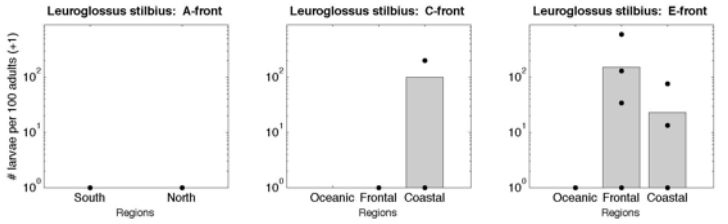

Group V. Dispersed spawners.
Species in this group exhibited elevated reproductive potential at both sides of fronts. The group is diverse in migratory behavior, including the migrators *Lipologus ochotensis*, *Tarlentonbeania crenularis*, and *Diogenichthys atlanticus* and the non-migrators *Chauliodus macouni*, *Protomyctophum crockeri*, and *Melamphaes lugubris*, as well as in biogeographic province (Subarctic-Transition Zone species include *L. ochotensis*, *T. crenularis*, *C. macouni*, *P. crockeri* and Subtropical species include *M. lugubris* and *D. atlanticus*).

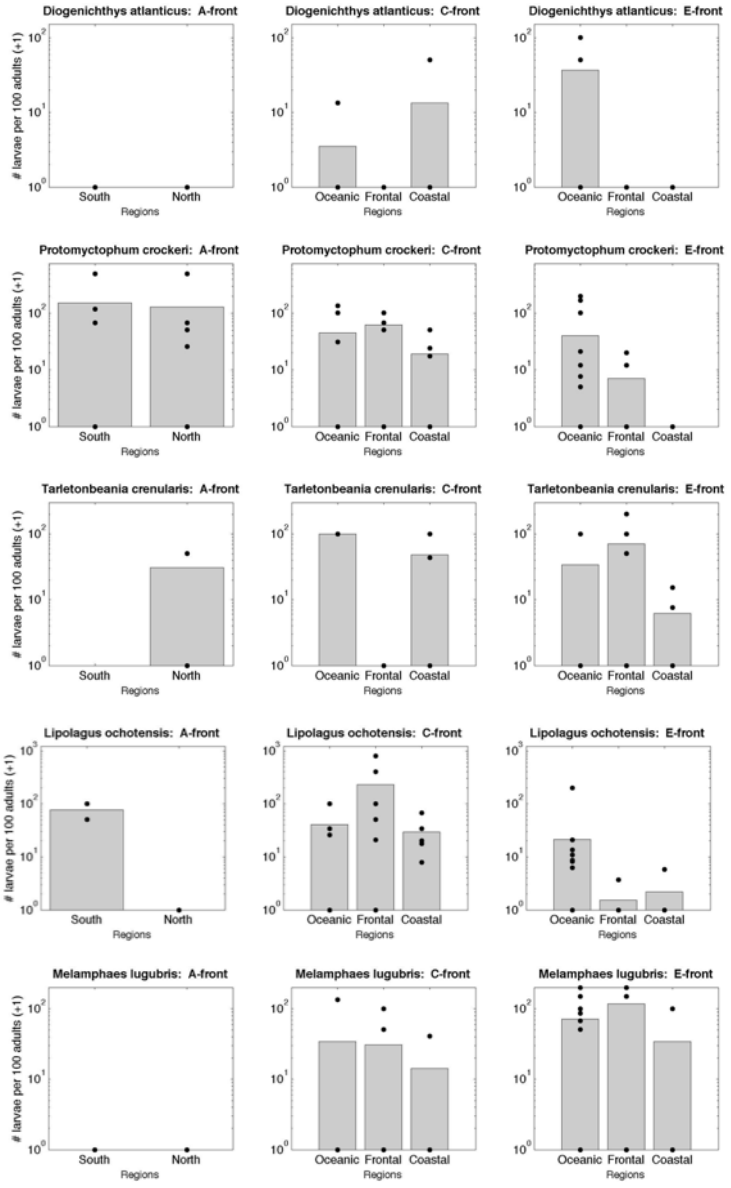

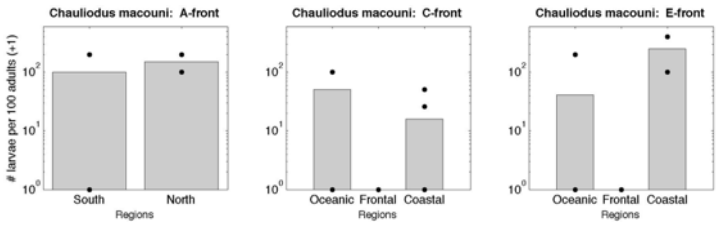
Chauliodus macouni: A-front
Chauliodus macouni: C-front
Chauliodus macouni: E-front
larvae per 100 adults (+1)
South
North
Oceanic
Frontal
Coastal
Regions

4.11 References

Angel MV (1989) Vertical profiles of pelagic communities in the vicinity of the Azores Front and their implications to deep ocean ecology. Prog Oceanogr 22:1–46

Backus RH, Craddock JE, Haedrich RL, Shores DL (1969) Mesopelagic fishes and thermal fronts in the western Sargasso Sea. Mar Biol 3:87–106

Bakun A (2006) Fronts and eddies as key structures in the habitat of marine fish larvae: opportunity, adaptive response and competitive advantage. Sci Mar 70S2:105–122

Beamish R, Leask K, Ivanov O, Balanov A, Orlov A, Sinclair B (1999) The ecology, distribution, and abundance of midwater fishes of the Subarctic Pacific gyres. Prog Oceanogr 43:399–442

Bednaršek N, Ohman M (2015) Changes in pteropod distributions and shell dissolution across a frontal system in the California Current System. Mar Ecol Prog Ser 523:93–103

Bertrand A, Bard F-X, Josse E (2002) Tuna food habits related to the micronekton distribution in French Polynesia. Mar Biol 140:1023–1037

Bograd SJ, Lynn RJ (2003) Long-term variability in the Southern California Current System. Deep Sea Res Part II Top Stud Oceanogr 50:2355–2370

Bower AS, Rossby HT, Lillibridge JL (1985) The Gulf Stream—Barrier or Blender? J Phys Oceanogr 15:24–32

Bowlin N (2015) Ontogenetic changes in the distribution and abundance of early life history stages of mesopelagic fishes off California (Dissertation)

Brodeur R, Yamamura O (2005) Micronekton of the North Pacific. Sidney, BC Canada

Brzezinski MA, Krause JW, Bundy RM, Barbeau KA, Franks P, Goericke R, Landry MR, Stukel MR (2015) Enhanced silica ballasting from iron stress sustains carbon export in a frontal zone within the California Current. J Geophys Res Ocean:n/a–n/a

Checkley DM, Barth JA (2009) Patterns and processes in the California Current System. Prog Oceanogr 83:49–64

Chekalyuk AM, Landry MR, Goericke R, Taylor AG, Hafez MA (2012) Laser fluorescence analysis of phytoplankton across a frontal zone in the California

Current ecosystem. J Plankton Res 34:761–777

Chereskin TK, Niiler PP (1994) Circulation in the Ensenada Front—September 1988. Deep Sea Res Part I Oceanogr Res Pap 41:1251–1287

Currie R, Boden BP, Kampa EM (1969) An investigation on sonic-scattering layers: the R.R.S. “Discovery” SOND cruise, 1965. J Mar Biol Assoc UK 49:489–514

Davison PC, Checkley DM, Koslow JA, Barlow J (2013) Carbon export mediated by mesopelagic fishes in the northeast Pacific Ocean. Prog Oceanogr 116:14–30

Davison P, Lara-Lopez A, Anthony Koslow J (2015) Mesopelagic fish biomass in the southern California current ecosystem. Deep Sea Res Part II Top Stud Oceanogr 112:129–142

Doniol-Valcroze T, Berteaux D, Larouche P, Sears R (2007) Influence of thermal fronts on habitat selection by four rorqual whale species in the Gulf of St. Lawrence. Mar Ecol Prog Ser 335:207–216

Field JC, Phillips A, Baltz K, Walker WA (2007) Range expansion and trophic interactions of the jumbo squid, Dosidicus gigas, in the California Current. CalCOFI Reports 48:131–146

Frost B, McCrone L (1979) Vertical distribution, diel vertical migration, and abundance of some mesopelagic fishes in the eastern subarctic Pacific ocean in summer. Fish Bull 76:751–770

Gartner J V, Brunswick N (1991) Marine BiOlOgy Life histories of three species of lanternfishes (Pisces : Myctophidae) from the eastern Gulf of Mexico. 27:21–27

Haury LR, Venrick EL, Fey CL, McGowan J (1993) The Ensenada Front: July 1985. CalCOFI Reports 34:69–88

Hoefer CJ (2000) Marine bird attraction to thermal fronts in the California Current System. Condor 102:423

Hood RR, Abbott MR, Huyer A, Kosro PM (1990) Surface patterns in temperature, flow, phytoplankton biomass, and species composition in the coastal transition zone of northern California. J Geophys Res 95:18081–18094

Hsieh CH, Kim HJ, Watson W, Lorenzo E Di, Sugihara G (2009) Climate-driven changes in abundance and distribution of larvae of oceanic fishes in the southern

California region. Glob Chang Biol 15:2137–2152

Hsieh CH, Reiss C, Watson W, Allen MJ, Hunter JR, Lea RN, Rosenblatt RH, Smith PE, Sugihara G (2005) A comparison of long-term trends and variability in populations of larvae of exploited and unexploited fishes in the Southern California region: A community approach. Prog Oceanogr 67:160–185

Irigoien X, Klevjer TA, Røstad A, Martinez U, Boyra G, Acuña JL, Bode A, Echevarria F, Gonzalez-Gordillo JI, Hernandez-Leon S, Agusti S, Aksnes DL, Duarte CM, Kaartvedt S (2014) Large mesopelagic fishes biomass and trophic efficiency in the open ocean. Nat Commun 5

John H (2001) Cross-front hydrography and fish larval distribution at the Angola–Benguela Frontal Zone. J Mar Syst 28:91–111

Kahru M, DiLorenzo E, Manzano-Sarabia M, Mitchell BG (2012) Spatial and temporal statistics of sea surface temperature and chlorophyll fronts in the California Current. J Plankton Res 34:749–760

Koslow J, Goericke R, Lara-Lopez A, Watson W (2011) Impact of declining intermediate-water oxygen on deepwater fishes in the California Current. Mar Ecol Prog Ser 436:207–218

Koslow JA, Goericke R, Watson W (2013) Fish assemblages in the Southern California Current: relationships with climate, 1951-2008. Fish Oceanogr 22:207–219

Krause JW, Brzezinski MA, Goericke R, Landry MR, Ohman MD, Stukel MR, Taylor AG (2015) Variability in diatom contributions to biomass, organic matter, production and export across a frontal gradient in the California Current Ecosystem. Jounral Geophys Res Ocean 120:1–16

Landry MR, Ohman MD, Goericke R, Stukel MR, Barbeau, K.A.Bundy R, Kahru M (2012) Pelagic community responses to a deep-water front in the California Current Ecosystem: overview of the A-front study. J Plankton Res 34:739–748

Landry MR, Ohman MD, Goericke R, Stukel MR, Tsyrklevich K (2009) Lagrangian studies of phytoplankton growth and grazing relationships in a coastal upwelling ecosystem off Southern California. Prog Oceanogr 83:208–216

Lara-Lopez AL, Davison P, Koslow JA (2012) Abundance and community composition of micronekton across a front off Southern California. J Plankton Res 34:828–848

Moku M, Tsuda A, Kawaguchi K (2003) Spawning season and migration of the myctophid fish Diaphus theta in the western North Pacific. Ichthyol Res 50:52–58

Moser H (1996) The early stages of fishes in the California Current region.

Moser G, Smith P (1993) Larval fish assemblages of the California Current region and their horizontal and vertical distributions across a front. Bull Mar Sci 53:645–691

Moser H, Smith P, Eber L (1987) Larval Fish Assemblages in the California Current Region, 1954-1960, a Period of Dynamic Environmental Change. CalCOFI Reports 18:97–127

Netburn AN, Koslow JA (2015) Dissolved oxygen as a constraint on daytime deep scattering layer depth in the southern California current ecosystem. Deep Sea Res Part I Oceanogr Res Pap 104:149–158

Ohman MD, Barbeau K, Franks PJS, Landry MR, Miller AJ (2013) Ecological Transitions in a Coastal Upwelling Ecosystem. Oceanography 26:162–173

Ohman MD, Powell JR, Picheral M, Jensen DW (2012) Mesozooplankton and particulate matter responses to a deep-water frontal system in the southern California Current System. J Plankton Res 34:815–827

Olson DB, Backus RH (1985) The concentrating of organisms at fronts: a cold-water fish and a warm-core Gulf Stream ring. J Mar Res 343:113–137

Oozeki Y, Hu F, Kubota H, Sugisaki H, Kimura R (2004) Newly designed quantitative frame trawl for sampling larval and juvenile pelagic fish. Fish Sci 70:223–232

Pauly D, Trites AW, Capuli E, Christensen V (1998) Diet composition and trophic levels of marine mammals. ICES J Mar Sci 55:467–481

Polovina JJ, Howell E, Kobayashi DR, Seki MP (2001) The transition zone chlorophyll front, a dynamic global feature defining migration and forage habitat for marine resources. Prog Oceanogr 49:469–483

Potier M, Marsac F, Cherel Y, Lucas V, Sabatie R, Maury O, Menard F (2007) Forage fauna in the diet of three large pelagic fishes (lancetfish, swordfish and yellowfin tuna) in the western equatorial Indian Ocean. Fish Res 83:60–72

Powell JR, Ohman MD (2012) Use of glider-class acoustic Doppler profilers for estimating zooplankton biomass. J Plankton Res 34:563–568

Powell JR, Ohman MD (2015) Covariability of zooplankton gradients with glider-detected density fronts in the Southern California Current System. Deep Res Part II Top Stud Oceanogr 112:79–90

Sassa C, Kawaguchi K (2004) Distribution patterns of larval myctophid fish assemblages in the subtropical – tropical waters of the western North Pacific. :267–282

Sournia A (1994) Pelagic biogeography and fronts. Prog Oceanogr 34:109–120

Steinberg DK, Cope JS, Wilson SE, Kobari T (2008) A comparison of mesopelagic mesozooplankton community structure in the subtropical and subarctic North Pacific Ocean. Deep Res Part II Top Stud Oceanogr 55:1615–1635

Steinberg DK, Mooy BAS Van, Buesseler KO, Boyd PW, Kobari T, Karl DM (2008) Bacterial vs. zooplankton control of sinking particle flux in the ocean's twilight zone. Limnol Oceanogr 53:1327–1338

Strub PT, James C (2000) Altimeter-derived variability of surface velocities in the California Current System: 2. Seasonal circulation and eddy statistics. Deep Res Part II Top Stud Oceanogr 47:831–870

Sydeman WJ, García-Reyes M, Schoeman DS, Rykaczewski RR, Thompson SA, Black BA, Bograd SJ (2014) Climate change. Climate change and wind intensification in coastal upwelling ecosystems. Science (80-) 345:77–80

Taylor AG, Goericke R, Landry MR, Selph KE, Wick DA, Roadman MJ (2012) Sharp gradients in phytoplankton community structure across a frontal zone in the California Current Ecosystem. J Plankton Res 34:778–789

Thompson DR, Furness RW, Monteiro LR (1998) Seabirds as biomonitors of mercury inputs to epipelagic and mesopelagic marine food chains. Sci Total Environ 213:299–305

Tont SA (1975) Deep scattering layers: patterns. CalCOFI Reports 18:112–117

Verneil A de, Franks PJS (2015) A pseudo-Lagrangianmethod for remapping ocean biogeochemical tracer data: Calculation of net Chl-a growth rates. J Geophys Res Ocean 120:4962–4979

Watanabe H, Moku M, Kawaguchi K, Ishimaru K, Ohno A (1999) Diel vertical migration of myctophid fishes (Family Myctophidae) in the transitional waters of the western North Pacific. Fish Oceanogr 8:115–127

CHAPTER 5

SUMMARY AND CONCLUSIONS

5.1 Summary

Given the numerous human impacts on mesopelagic fishes, such as global climate change, fishing, and plastic pollution (Ramirez-Llodra et al. 2011), there is an urgent need to develop and implement management strategies in the open ocean (Mengerink et al. 2014) in order to conserve critical processes such as carbon transport and sufficient forage availability to their predators (Robison 2009). Management mechanisms such as ecosystem-based management (Field & Francis 2006), pelagic marine protected areas (Game et al. 2009, Maxwell et al. 2014), and marine spatial management (Mengerink et al. 2014) could potentially address conservation needs in the deep sea. However, any management approach requires baseline data, a functional understanding of key processes that structure biotic communities, and ongoing monitoring to gauge its effectiveness.

Through my dissertation research, I had a rare opportunity to investigate how an assemblage of abundant unexploited marine fishes respond to natural environmental variability. Even in the absence of commercial exploitation of this diverse assemblage of fishes, I have identified some potential vulnerabilities of these animals to environmental changes, with implications for the future of the California Current Ecosystem. I have demonstrated that under increasingly hypoxic conditions, mesopelagic fish vertical distributions may shift shallower in the water column (Chapter 2), possibly to avoid suppressed metabolism in more hypoxic water (Chapter 3). I have further demonstrated the capacity of epipelagic fronts to restructure assemblages of adult vertically migratory mesopelagic fishes, and fish larvae, as well as to alter the population growth potential of these animals (Chapter 4).

In Chapter 2, I investigated the response of the deep scattering layer (DSL) depth to variations in midwater dissolved oxygen concentration, irradiance, and temperature. I found that the depth of the lower DSL boundary correlates most strongly with dissolved oxygen concentration. The upper boundary depth correlates best with irradiance and temperature. Based on the linear regressions of oxygen with DSL boundary depths, I predicted that both the upper and lower boundaries will shoal if the ocean deoxygenation trend continues, with the upper boundary shoaling at a faster rate than the lower boundary. These results suggest that the mesopelagic fish assemblage could lose volume of its preferred habitat in a deoxygenating ocean, providing a potential mechanism to explain the decline in mesopelagic ichthyoplankton abundance that has been found to accompany deoxygenation in the CCE over the last several decades (Koslow et al. 2011).

In Chapter 3, I investigated a physiological mechanism that could lead to the observed relationship between midwater oxygen concentrations and changing densities of mesopelagic fishes, as inferred from the larval fish studies in Koslow et al. (2011). I measured aerobic and anaerobic enzyme activities in white muscle tissue from diverse fishes living across a range of oxygen conditions. I did not observe a shift to increased reliance on anaerobic metabolism as I expected, but instead found a general reduction in maximum activities of both aerobic and anaerobic enzymes with declining oxygen concentrations for the combined assemblage (although the relationship was statistically significant for only two of seven families studied). This result suggests that fish may undergo metabolic suppression in more hypoxic conditions, potentially decreasing their fitness under ocean deoxygenation.

The focus of my fourth chapter shifted to a different kind of variability in the ocean, oceanic fronts. I sampled fish at three different frontal systems in the southern CCE, and found that the compositions of vertically migratory and larval mesopelagic fishes are altered across different fronts, while the assemblage of non-migratory fishes was not measurably affected. I used the ratio of larvae to adults as an index of population growth potential, and found that population growth potential is similarly altered across fronts for migratory species though not for non-migratory species. The magnitude of the observed patterns was generally proportional to the stability and persistence of each frontal system. If the pattern of increased frontal frequency (Kahru et al. 2012) continues, there could be changes in reproductive activity, assemblage composition, and distributions of mesopelagic fishes throughout the region.

The results of my dissertation research suggest that the mesopelagic community is quite responsive to selected environmental changes. Two of my chapters demonstrate that oxygen is a primary variable of the environment that affects distributions and individual fitness of fishes living in the already hypoxic mesopelagic waters of the CCE. In my fourth chapter, I found that the presence of epipelagic fronts affects assemblage composition and population growth potential of mesopelagic fishes.

5.2 Future Work

My dissertation results contribute significantly to the understanding of mesopelagic fish responses to environmental variability, yet elicit a number of related questions:

How do mesopelagic fishes respond to extreme hypoxic events?

My sampling times and locations were constrained by collaborative research cruise schedules and locales. I was able to effectively study changes in fish distributions and physiological responses to natural oxygen variability within the system, but I was not able to conduct targeted sampling during specific events, such as the onset of extreme hypoxia. Species that are abundant near the continental shelf (e.g., *Stenobrachius leucopsarus*) - where there are large fluctuations in deep oxygen concentrations - may be particularly vulnerable (or alternatively, particularly resilient) to such events. Adaptive sampling in response to specific hypoxia events would aid in answering the questions, that all pertain to the timescale and mechanisms of response to hypoxic events:

- Does the DSL shift in the vertical or horizontal direction to avoid an influx of hypoxic waters?
- Do assemblage composition and densities change in response to such an influx?
- Do anaerobic and/or aerobic metabolic enzyme activities change with influxes of hypoxic waters?

Autonomous tools such as moorings and gliders have been equipped with dissolved oxygen sensors to detect transitions in the oxygen environment (e.g., Ohman et al. 2013), and could be use to guide adaptive sampling of the mesopelagic community. The ideal measurements to study the responses of these fishes to an extreme hypoxic event are ship-based bioacoustic surveys accompanied by direct collection of specimens to evaluate assemblage composition (e.g., Lara-Lopez et al. 2012) and physiological (e.g., Seibel et al. 2014) responses. In the absence of ship availability, and for long-term studies on DSL response, echosounders of the appropriate frequencies to resolve

midwater fishes could be installed on or nearby moorings to collect concurrent measurements of oxygen changes and DSL depths. Surveying the mesopelagic fish community during and following stressful hypoxic events will contribute to identifying key vulnerabilities and the timescales of response and recovery.

How are mesopelagic fish distributions and physiology affected over gradients in dissolved oxygen concentrations greater than those in the southern California Current Ecosystem? Are responses to oxygen variability similar in all OMZ regions or do different regional assemblages have distinctive responses?

In Chapter 2, I predicted changes to DSL boundaries using simple linear regression based on a relatively narrow range of midwater oxygen concentrations. I was also limited to studying physiological responses within this same dissolved oxygen range (Chapter 3). Similar sampling across other OMZ regions (e.g., Eastern Tropical Pacific, Peru-Chile Current, northern Indian Ocean) would address the following questions:

- Is there a depth above which other variables (e.g., irradiance or temperature) surpass oxygen in limiting the upper boundary of the DSL?
- Where OMZs are very shallow, are fish better adapted to living within hypoxic waters? How do the responses of single species vary across their ranges?
- Are responses gradual and linear, or are there tipping points?

Through comparisons across different systems, we can identify which taxa are likely to adapt to deoxygenation and which may not, as well as what the assemblage-level response of CCE fishes may be if the oxygen environment changes to more closely

resembles that of shallower OMZ regions (e.g., conditions off the Pacific coast of Mexico).

Can myctophids and other mesopelagic fishes produce ethanol as a metabolic end-product?

I did not detect Alcohol Dehydrogenase activity for any of the fishes that I studied in Chapter 3, despite one published suggestion (Torres et al. 2012) that it may be present, and it remains unclear whether mesopelagic fishes can utilize an ethanol-production pathway. Studies must be conducted to directly measure ethanol-production in live animals living under extreme hypoxia to resolve this question. If there are mesopelagic fishes capable of respiring anaerobically without accumulating toxins within their tissues, this has major implications for their resiliency in a deoxygenating ocean.

What are the processes and timescales that lead to changes in assemblage composition and population growth potential across fronts?

I have found that migratory mesopelagic fish assemblages and population growth potential can be altered at fronts, and that the persistence and stability of a front affect the magnitude of these responses. However, questions remain as to the timescales and mechanisms that lead to these results. The number, magnitude, and duration of fronts may vary with upwelling intensity and other factors expected to be affected by climate change, with differential effects on the mesopelagic fish community. It would be enlightening to study fish assemblages throughout the progression of formation and

decay of a front or eddy. Changes to density, growth, reproduction, and feeding are all likely to vary with frontal intensity.

Are effects of fronts related to oxygen variability across these systems?

In Chapter 4, I did not specifically test a mechanism to explain why the fronts alter composition and population growth potential. Oxygen is the only environmental variable for which cross-frontal gradients at depths below 200 m are greater than at the surface, and dissolved oxygen concentration is a good candidate for further study in relation to frontal discontinuities. A future study could combine the methods used throughout my dissertation to investigate whether the DSL boundaries and metabolic enzyme activities that respond to regional oxygen gradients are also affected by frontal gradients, and whether these metrics respond similarly at the relatively small spatial scale of fronts.

Predator-prey interactions

Predators: A primary motivation for improving understanding of mesopelagic fish assemblages is because they seem to be important forage fish. It is known that a diverse group of predators, including fish, cephalopods, mammals, and seabirds feed on mesopelagic fishes, however it is not known how important this component of the diet is. Specific questions to be answered include:

- Are any species of mesopelagic fish essential prey for predators?
- Are predator densities or distributions correlated with densities or distributions of mesopelagic species?

- Do predators forage disproportionately at fronts?

Both stomach content and stable isotope analyses would inform understanding of the relative importance of mesopelagic fishes as prey to their predators. Predator tracking with tags, drones, and direct observations can provide information on where they are feeding, and could be associated with mesopelagic fish distributions. Ecosystem modelling can be used to track the theoretical energy transfer through mesopelagic fishes and to test the effects of altered mesopelagic fish densities predatory densities and distributions.

***Prey*:** Additionally, the distributions of mesopelagic fishes in relation to both DSLs and to frontal systems is likely related to the distributions of their prey resources. Acoustic and trawl data on zooplankton densities, assemblage compositions, and distributions, as well as direct dietary analyses of these fishes, will further inform our understanding of why mesopelagic fishes are distributed as they are.

Novel technologies

There are inherent limitations to the tools that are available for studying mesopelagic fauna. Trawls underestimate biomass by an order of magnitude, and likely undersample larger and faster individuals. Acoustic backscattering is highly sensitive to taxa, life stage, size, and material properties of an animal, complicating interpretation of echograms, particularly where assemblages are diverse. For example, siphonophores are undersampled by nets (Smith-Beasley 1992), but may contribute disproportionally to DSLs because of their high acoustic reflectance. Sampling with high resolution video on ROVs or manned and unmanned submersibles is more effective at sampling some taxa

(e.g., gelatinous organisms with weak or no escape responses; Robison 2004), and could be used to complement studies on deep scattering layer compositions, improving our understanding of taxonomically-specific responses to oxygen variability, fronts, and other environmental disturbances.

The measurements of enzyme activity are subject to a high degree of uncertainty. Captured fish undergo stress while in the trawl net, and it can take several hours from their capture time until they are frozen, during which time enzymes may degrade. This creates a challenge when attempting to detect relatively subtle differences in enzyme activities within and between species. In addition, enzyme activity is commonly measured with saturating levels of substrates, which may not always be applicable in situ. In situ respirometers have recently been developed, capable of measuring oxygen concentrations of individual live organisms in the deep sea without subjecting them to the stress of capture in a trawl net (Drazen & Yeh 2012). These systems provide high-precision measurements of respiration and the environment that may allow for detection of low magnitude effects on metabolism.

5.3 Conclusions

In this dissertation I have shown that ocean deoxygenation and oceanic fronts alter distributions, metabolism, and population growth potential of dominant species of mesopelagic fishes. Continued monitoring of this assemblage in the CCE will aid understanding and predictions of how this assemblage responds to oxygen and other variability over time. Repeated sampling at frontal systems during their formation and dissipation will inform understanding of the mechanisms that lead to changes in the

assemblage and population growth potential at frontal gradients, as well as the lasting impacts of these alterations. With advances in both autonomous and ship-based technologies, novel tools are available to study this assemblage, and I anticipate exciting and perhaps unexpected answers to the questions posed here to be answered in the coming years.

5.4 References

Drazen JC, Yeh J (2012) Respiration of four species of deep-sea demersal fishes measured in situ in the eastern North Pacific. Deep Sea Res Part I Oceanogr Res Pap 60:1–6

Field J, Francis R (2006) Considering ecosystem-based fisheries management in the California Current. Mar Policy 30:552–569

Game ET, Grantham HS, Hobday AJ, Pressey RL, Lombard AT, Beckley LE, Gjerde K, Bustamante R, Possingham HP, Richardson AJ (2009) Pelagic protected areas: the missing dimension in ocean conservation. Trends Ecol Evol 24:360–369

Koslow J, Goericke R, Lara-Lopez A, Watson W (2011) Impact of declining intermediate-water oxygen on deepwater fishes in the California Current. Mar Ecol Prog Ser 436:207–218

Lara-Lopez AL, Davison P, Koslow JA (2012) Abundance and community composition of micronekton across a front off Southern California. J Plankton Res 34:828–848

Maxwell S, Ban N, Morgan L (2014) Pragmatic approaches for effective management of pelagic marine protected areas. Endanger Species Res 26:59–74

Mengerink KJ, Dover CL Van, Ardron J, Baker M, Escobar-Briones E, Gjerde K, Koslow JA, Ramirez-Llodra E, Lara-Lopez A, Squires D, Sutton T, Sweetman AK, Levin L a (2014) A call for deep-ocean stewardship. Science 344:696–8

Ohman MD, Rudnick DL, Chekalyuk A, Davis RE, Feely RA, Kahru M, Kim H-J, Landry MR, Martz TR, Sabine CL, Send U (2013) Autonomous ocean measurements in the California Current Ecosystem. Oceanogaraphy 26:18–25

Ramirez-Llodra E, Tyler PA, Baker MC, Bergstad OA, Clark MR, Escobar E, Levin LA, Menot L, Rowden AA, Smith CR, Dover CL Van (2011) Man and the last great wilderness: human impact on the deep sea (P Roopnarine, Ed.). PLoS One 6:e22588

Robison B (2004) Deep pelagic biology. J Exp Mar Bio Ecol 300:253–272

Robison BH (2009) Conservation of deep pelagic biodiversity. Conserv Biol 23:847–58

Seibel BA, Hafker NS, Trubenbach K, Zhang J, Tessier SN, Portner H-O, Rosa R, Storey KB (2014) Metabolic suppression during protracted exposure to hypoxia in the jumbo squid, Dosidicus gigas, living in an oxygen minimum zone. J Exp Biol

217:2555–2568

Smith-Beasley L (1992) A study of the vertical distribution of upper mesopelagic animals in the Monterey Submarine Canyon, California

Torres JJ, Grigsby MD, Clarke ME (2012) Aerobic and anaerobic metabolism in oxygen minimum layer fishes: the role of alcohol dehydrogenase. J Exp Biol 215:1905–14